Molecular enantiodiscrimination by NMR spectroscopy in chiral oriented systems: Concept, tools, and applications

Christie Aroulanda, Philippe Lesot

Molecular Enantiodiscrimination by NMR Spectroscopy in Chiral Oriented Systems: Concept, Tools and Applications

Christie Aroulanda and Philippe Lesot*

RMN en Milieu Orienté, ICMMO, UMR CNRS 8182, Université Paris-Saclay, Bâtiment 410, 15, rue du Doyen Georges Poitou, F-91405 Orsay cedex, France.

This article is dedicated to Prof. Aharon Loewenstein (Technion Institute of Technology of Haifa) for his contribution to anisotropic NMR spectroscopy.

Abstract

The study of enantiodiscriminations in relation to various facets of enantiomorphism (chirality/prochirality) and/or molecular symmetry is an exciting area of modern organic chemistry, and an ongoing challenge for NMR spectroscopists who have developed many useful analytical approaches to solve stereochemical problems. Among them, the anisotropic NMR using chiral aligning solvents has provided a set of new and original tools by making accessible all intramolecular, order-dependent NMR interactions (anisotropic interactions), such as residual chemical shift anisotropy (RCSA), residual dipolar coupling (RDC), and residual quadrupolar coupling (RQC) for spin $I > ½$, while preserving high spectral resolution. The force of NMR in enantiopure, oriented solvents lies on its ability to orient differently in average on the NMR timescale enantiomers of chiral molecules and enantiotopic elements of prochiral ones, leading distinct NMR spectra or signals to be detected. In this compendium mainly written for all chemists playing with (pro)chirality, we overview various key aspects of NMR in weakly aligning chiral solvents as the lyotropic liquid crystals (LLCs), in particular those developed in France to study (pro)chiral compounds in relation with chemists needs: study of enantiopurity of mixture, stereochemistry, natural isotopic fractionation, as well as molecular conformation and configuration. Key representative examples covering the diversity of enantiomorphism concept, and the main and most recent applications illustrating the analytical potential of this NMR in polypeptide-based chiral liquid crystals (CLCs) are examined. The latest analytical strategies developed to determine in-solution conformational distribution of flexibles solutes using NMR in polypeptide-based aligned solvents are also proposed.

KEYWORDS
Chirality, Conformational distribution, Dynamics, Enantiotopicity, NMR spectroscopy, Oriented solvents, PBLG, Stereochemistry

Corresponding authors: philippe.lesot@universite-paris-saclay.fr

ORCID numbers : - Christie Aroulanda: 0000-0001-8019-2097
- Philippe Lesot: 0000-0002-5811-7530

I. INTRODUCTION

Nuclear Magnetic Resonance (NMR) spectroscopy nowadays plays a central place in various analytical domains of the modern organic chemistry involving chirality, from the enantiopurity determination to the three-dimensional (3D) structure elucidation through the intra-molecular distribution of isotopes **[1]**.

From the point of view of stereochemistry and the enantiomorphism concept, the study of molecular chirality/ isotopic chirality / prochirality (see **Figure 1**) is an ongoing challenge for NMR spectroscopists who have developed many useful approaches to solve many chemist's analytical problems **[2]**.

Among them, the anisotropic NMR spectroscopy using orientantionally oriented chiral environments has provided a set of new original tools by making accessible all order-dependent intramolecular, residual anisotropic NMR interactions, such as residual chemical shift anisotropy (RCSA), residual dipolar coupling (RDC), and residual quadrupolar coupling (RQC) for spin $I > ½$, while preserving high spectral resolution **[3]**. The origin of the term "residual" is associated with the idea that any solute interacting with a mesomorphic oriented media is both aligned (inside the magnetic field of spectrometer, $\mathbf{B_0}$) and mobile. This combination leads to anisotropic interactions whose the magnitude is reduced by a factor ranging from 10^{-5} to 10^{-1} (depending of type of liquid crystals used), with respect to the values that would be observed in a crystalline solid by solid-state NMR (SS NMR) (see **Figure 1a**) ».

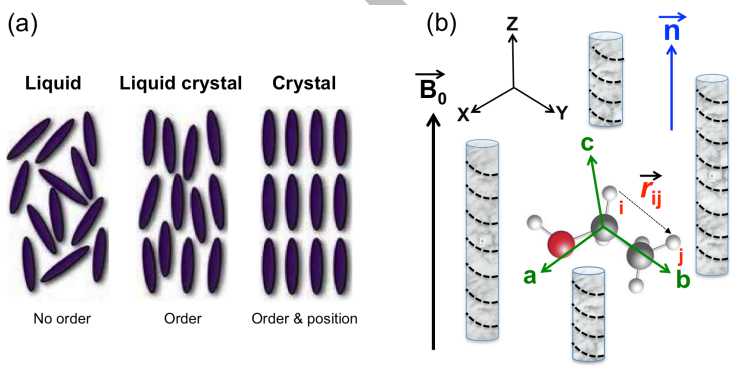

Figure 1 *(a) Schematic description of the molecular orientational order in an isotropic liquid (no order), in a liquid crystal (order) and in a crystalline solid (order and position). (b) Example of an (arbitrary) reference axis system (a, b and c axes) attached to a molecule oriented in a helical-polymer based chiral nematic system. The molecular order parameters and atomic coordinates will be described in accordance with this axis system.* ***Figure partially adapted from Refs. [4] with permission.***

The original analytical potential of NMR in enantiopure (non-racemic) oriented solvents lies on its ability to orient differently in average on the NMR timescale both enantiomers of chiral molecules and enantiotopic elements of prochiral solutes, thus leading to distinct NMR spectra or signals to be detected **[4, 5, 6]**.

In the frame of this special issue, "*Chirality in France*", we overview in this compendium (mainly written for chemists working with molecular (pro)chiral objects) various key aspects of NMR in weakly aligning chiral solvents based on organic lyotropic liquid crystals (LLCs), and in particular the methodologies developed at

Orsay (University of Paris-Sud/Paris-Saclay) to study chiral and prochiral compounds in relation with the needs of chemists. Various analytical aspects based on the enantiorecognition phenomena in relation to molecular symmetry as the enantiopurity determination of mixtures, the stereochemistry analysis, the determination of the natural isotopic fractionation in prochiral molecules, as well as the determination of the molecular configuration and conformation of analytes will be examined. Herein, we will discuss the most representative applications illustrating the original potential of this NMR tool, in particular when using polypeptide-based chiral LLCs as enantiodiscriminating anisotropic systems. A special attention will be also paid to the problem of the conformational analysis in weakly orienting environments.

1.1 | Enantiomorphism concept and NMR spectroscopy

Nature is highly enantioselective by producing paramount families of natural chiral molecules (as carbohydrates or amino-acids) with a given *D* or *L* stereochemistry. In contrast, chemists involved in asymmetric syntheses are able to make new compounds while controlling the stereochemistry of their molecular target. Enantiomorphism covers both the concept of chirality and prochirality, associated respectively with enantiomers of chiral compounds or enantiotopic elements in prochiral molecules **[2]**.

Enantiomers of a chiral molecule are mirror images objects of each other by a plane of symmetry, but are not superimposable. Majority of chiral molecules possess a stereogenic center (as an asymmetric tetrahedral carbon atom, for instance), but it is not a prerequisite as observed in cases of axial chirality or atropoisomerism. Prochiral compounds are simply defined as any molecule that can be transformed into a chiral one by a single isotopic substitution. Chirality can therefore originate from isotopic substitution around a stereogenic center or not, and called isotopic chirality (see **Figure 2**) **[2, 5]**.

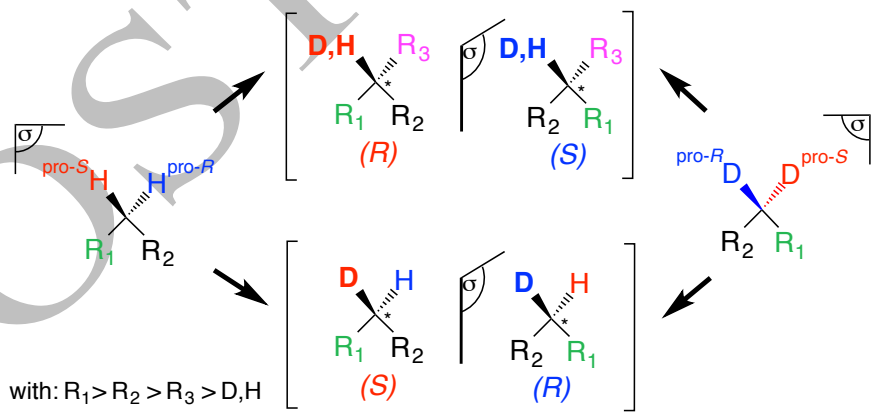

Figure 2 *Examples of R/S-enantiomeric pairs of a model C_1-symmetry chiral molecule ("classical" chirality and "(D/H) isotopic" chirality) with a single stereogenic center (tetrahedral carbon atom) deriving from their deuterated or hydrogenated prochiral precursors and characterized by methylene enantiotopic directions, pro-R/pro-S.*

Enantiotopic elements in prochiral compounds are atoms, groups of atoms or internuclear directions exclusively exchangeable by a plane of symmetry (C_s symmetry), or an improper symmetry axis (S_4 symmetry). Often, prochiral molecules possess a prostereogenic center, as in case of a CH_2 group in C_{2v}-symmetry molecules **[2, 5]**.

1.2 | Limits of classical enantiodiscriminating NMR approaches routinely used

NMR tools in isotropic liquids have been initially developed for the determination of the enantiomeric excess (*ee* in %) of mixtures of chiral compounds. The approaches employed in routine require the use of an enantiopure chiral partner reacting or interacting with the chiral analyte. Basically, three classes of enantiopure agents can be used: i) the chiral derivatizing agents (CDAs) able to form covalent bonds with enantiomers and convert them into stable diastereoisomers; ii) the chiral lanthanide-induced shift reagents (CLSRs) such as chiral lanthanide complexes (based on europium or ytterbium central cation), able to coordinate differently both enantiomers and create diastereoisomeric complexes; and iii) the chiral solvating agents (CSAs) including chiral cyclodextrines **[7, 8, 9, 10]**.

While CDAs prequisite a preliminary chemical transformation prior to the analysis, CLSRs and CSAs can be used *in situ* in the NMR sample. If tools involving CLSRs and CSA are rather easy to setup, they require however an enantiopure agent that must be carefully selected according to the (specific) chemical functionalities (hydroxyl group, carboxylic acid, amine, …) of the investigated chiral compound. With the exception of cyclodextrines (chiral macrocycles), these agents are often rarely suitable for apolar chiral compounds **[9, 10]**.

1.3 | Molecular order, chirality and NMR consequences

First, introduced by Saupe and Englert in 1963 **[11]**, NMR spectroscopy in liquid crystals is a fascinating analytical tool combining the advantages of the SS NMR (detection of anisotropic NMR interactions) and NMR performed in conventional liquids (acquisition of high-resolution spectra)
[12, 13, 14]. The detection of intramolecular anisotropic NMR interactions originates from the partial alignment (orientational ordering) of molecules in LC (analyte and solvent) with the static magnetic field, $\mathbf{B_0}$ of the spectrometer**,** while averaging out of most intermolecular anisotropic interactions.

The orientational behavior of an oriented molecule (solute or solvent) can be described by its orientational-conformational probability function **[12, 13, 14, 15]**. In practice, for a rigid molecular structure or a given conformation in a flexible compound, the dependence of NMR interactions on the molecular orientation, which affects the NMR spectra, can be described to a good approximation by a second-rank tensor, denoted also Saupe order matrix, which is much easier to work with. At the maximum, in a nematic uniaxial solvent, the molecular orientation can be described by five non-zero independent order parameters, S_{aa}, $S_{bb} - S_{cc}$, S_{ab}, S_{ac} and S_{bc}, where a, b and c refer to the axes of a molecular-fixed reference frame (see **Figure 1b**). Actually, this number can change depending on two key factors, accounting for the symmetry of the solute interacting within its solvent: i) the point group symmetry of the analyte, ii) the nature of the mesophase used, namely achiral or chiral. According to these two criteria, **Table 1** lists the number of independent order parameters needed to suitably describe the orientational behaviour of an oriented rigid molecule (chiral, prochiral, achiral), or a flexible one in a given

molecular conformation **[16]**. A special attention will be paid to molecules of symmetry C_s, C_{2v}, S_4 and D_{2d} as discussed in **Section V**.

From the NMR point of view, the existence of a molecular alignment leads to the detection of all intramolecular anisotropic NMR interactions (RCSA, RDC, RQC) which are no longer reduced to zero due to fast and random (Brownian) molecular motions. These order-dependent interactions will be described briefly below. In this sense, NMR spectra of a given nucleus recorded in anisotropic media are much more analytically informative than those recorded in isotropic ones.

Contrarily to solid phase, and even if analytes are uniformely oriented with respect to the magnetic field axis, they still continue to rotate and diffuse as in liquids, thus generally leading to high-resolution NMR spectra with full width at half-maximum (FWHM) of lines equal to 1 to 5 Hz.

1.4 | Advantages of NMR in chiral oriented environments

Isotropic and anisotropic NMR spectroscopies alone are basically blind to the chirality concept. In both cases, revealing the molecular enantiomorphism is only possible if a chiral (enantiopure) additional component or a non-racemic environment (seen as an enantio-stimulus) is used, and can create diastereomorphous interactions at the origin of the enantiodiscrimination mechanisms. This second approach was first explored by Snyder et *al,* in 1968, using a strongly orienting cholesteric-type mesophase and ^{1}H NMR **[17]**.

Phenomenologically, the distinct interactions between the *R*- and *S*-isomers and the enantiopure (non-racemic) molecules of the chiral liquid crystal (CLC) results in different average *R*- and *S*-orientations with respect to the $\mathbf{B_0}$ (Z axis). These molecular orientations can be described using two Saupe's order matrices, $\{S^S_{\alpha\beta}\}$ and $\{S^R_{\alpha\beta}\}$, whose elements can be expressed as **[5, 12, 13, 15]**:

$$S^{S\text{ or }R}_{\alpha\beta} = \frac{1}{2}\langle 3\cos\theta^{S\text{ or }R}_{\alpha_Z}\cos\theta^{S\text{ or }R}_{\beta_Z} - \delta_{\alpha\beta}\rangle \qquad (\mathbf{1})$$

where δ is the Kronecker function ($\delta_{\alpha\beta}$=1 if $\alpha = \beta$ and $\delta_{\alpha\beta}$=0 for $\alpha \neq \beta$). From the matrix elements of $S^{S\text{ or }R}_{\alpha\beta}$, we can derive any local order parameters, $S^{S\text{ or }R}_{ij}$, associated with any internuclear direction ij (vector r_{ij}) expressed in the molecular reference axis system (RAS) initially defined, $(a, b, c)^{S\text{ or }R}$, on the basis of the so-called director cosines following **Eq. 2 [5]**:

$$S^{S\text{ or }R}_{ij} = \sum_{\alpha\beta=a,b,c}\cos\theta^{S\text{ or }R}_{\alpha_{ij}}\cos\theta^{S\text{ or }R}_{\beta_{ij}}S^{S\text{ or }R}_{\alpha\beta} \qquad (\mathbf{2})$$

All anisotropic NMR interactions (tensorial properties) are related to these order parameters. Note finally that $S^{S\text{ or }R}_{ij}$ can be also described as a function of the angle between the internuclear vector, $r_{ij,}$ and the axis of the magnetic field $\mathbf{B_0}$, $\theta^{B_0}_{ij}$, for each enantiomer, namely **[4, 5, 6]**:

$$S^{S\text{ or }R}_{ij} = \langle\frac{3\cos^2(\theta^{B_0}_{ij})^{S\text{ or }R}-1}{2}\rangle, \qquad (\mathbf{3})$$

where <···> refers to an ensemble average. According to the $\theta_{ij}^{B_0}$ value [0°, 90°], relative to the so-called "magic angle", θ_m, the trigonometric term is positive ($\theta_{ij}^{B_0} < \theta_m$), negative ($\theta_{ij}^{B_0} > \theta_m$), or null ($\theta_{ij}^{B_0} = \theta_m = 54.7°$).

Table 1. Number of order parameters the Saupe matrix for non-flexible molecules of different point group symmetries dissolved in an achiral and chiral uniaxial mesophase and location of the a, b, c axes

	Non-chiral mesophase			**Chiral mesophase**		
Molecular point group symmetry	**Effective molecular point group**	**Indep. order parameters** (Saupe elements)	**Location of a, b, c axes**	**Effective molecular point group**	**Indep. order parameters** (Saupe elements)	**Location of a, b, c axes**
C_1, C_i	$\boldsymbol{C_1}$, $\boldsymbol{C_i}$	S_{aa}, $S_{bb} - S_{cc}$ S_{ac}, S_{ab}, S_{bc}	not special	$\boldsymbol{C_1}$	S_{aa}, S_{bb} - S_{cc} S_{ac}, S_{ab}, S_{bc}	not special
C_s [a]	$\boldsymbol{C_s}$	S_{ab}, $S_{bb} - S_{cc}$ S_{bc}	a ⊥ to the plane	$\boldsymbol{C_1}$	S_{aa}, $S_{bb} - S_{cc}$ S_{ac}, S_{ab}, S_{bc}	not special
C_2, C_{2h}	$\boldsymbol{C_2}$, $\boldsymbol{C_{2h}}$	S_{ab}, S_{bb} - S_{cc} S_{bc}	a // to the 2-fold axis, b ⊥ to the mirror plane	$\boldsymbol{C_2}$	S_{ab}, S_{bb} - S_{cc} S_{bc}	a // to to the 2-fold axis
C_{2v} [a]	$\boldsymbol{C_{2v}}$	S_{aa}, S_{bb} - S_{cc}	a // to the 2-fold axis, b ⊥ to the mirror plane	$\boldsymbol{C_2}$	S_{ab}, S_{bb} - S_{cc} S_{bc}	a // to the 2-fold axis
S_4 [a]	$\boldsymbol{S_4}$	S_{aa}	a // p-fold axis or intersection of mirror planes	$\boldsymbol{C_2}$	S_{ab}, S_{bb} - S_{cc}	a // to the 2-fold axis
D_2, D_{2h}	$\boldsymbol{D_2}$, $\boldsymbol{D_{2h}}$	S_{aa} S_{bb} - S_{cc}	a,b,c // to the 2-fold axes	$\boldsymbol{D_2}$	S_{aa}, S_{bb}-S_{cc}	a,b,c // to 2-fold axes
D_{2d} [a]	$\boldsymbol{D_{2d}}$	S_{aa}	a // p-fold axis or intersection of mirror planes	$\boldsymbol{D_2}$	S_{aa}, S_{bb} - S_{cc}	a,b,c // to 2-fold axes
C_n, C_{nv}, C_{nh}, D_n, D_{nh}, D_{nd}, (with n = 3, 4, 6), S_6, C_∞, $C_{\infty v}$, $C_{\infty h}$, $D_{\infty h}$	C_n, C_{nv}, C_{nh}, D_n, D_{nh}, D_{nd}, (with n = 3, 4, 6), S_6, C_∞, $C_{\infty v}$, $C_{\infty h}$, $D_{\infty h}$	S_{aa}	a // p-fold axis or intersection of mirror planes	C_n or D_n (with n > 3)	S_{aa}	// n-fold axis

[a] Compounds with these point groups have a lower effective symmetry and a change in the location of PAS of the order matrix.

In addition to the possibility to spectrally discriminate enantiomers, NMR in CLCs offers two other analytical advantages. The first one is to provide new tools to discriminate diastereoisomers, but also diastereotopic directions, not always differentiated in isotropic liquids. The second, and much more important, is its ability to spectrally differentiate enantiotopic elements (as atoms, groups of atoms, or internuclear directions) in prochiral molecules, whereas there are very few isotropic NMR approaches able to do so. In this review, the concept of spectral enantiodiscrimination covers both the differentiation of enantiotopic elements within a single molecular (prochiral) object or that of enantiomers, which can be formally considered as the discrimination of enantiomeric elements but involving two molecular (chiral) objects.

II. NMR TOOLS VERSUS MAGNETICALLY ACTIVE NUCLEUS

Any anisotropic NMR interaction and its associated observable noted, $\langle Obs \rangle^{A\ or\ B}$, can be simply described as the product of a constant, K^{NMR}, associated to a given NMR interaction, and a local or molecular of parameter, that we will note $S_{ij}^{A\ or\ B}$. This description applies to the case of enantiomers (*A, B* = *R* or *S* stereodescriptors) or enantiotopic elements (*A, B* = pro-*R* or pro-S stereodescriptors), so we can write:

$$\langle Obs \rangle^{A \text{ or } B} = K^{\mathrm{NMR}} \times \langle S_{ij}^{A\ or\ B} \rangle, \qquad (4)$$

assuming safely that K^{NMR} is identical for both enantiomers or enantiotopic elements.

As seen, the magnitude of $\langle Obs \rangle^{A \text{ or } B}$ both depends on the magnitude of K^{NMR} and $S^{A \text{ or } B}$, and subsequently on: i) the degree of alignment of the CLC used, strong ($S = 10^{-2}$ to 10^{-3}) or weak ($S = 10^{-3}$ to 10^{-6}), ii) the magnitude of the factor K^{NMR} in regards of the spectral features of nucleus considered, *e.g.* its gyromagnetic ratio, γ, and its spin number *I*. Among the detectable nuclei in almost all organic molecules (CHNO), a particular attention can be paid to ^{1}H (99 % abundant, I = ½), the ^{13}C nuclei (1 % abundant, I = ½), and the ^{2}H nuclei (0.0155 % abundant, I = 1, a small nuclear quadrupolar moment, QM). Quadrupolar nuclei as ^{17}O or ^{14}N can be theoretically used but are analytically less interesting in anisotropic NMR due to their inherent quadrupolar properties (spin I = 5/2 and 1, respectively, and large QM values) reducing drastically their T_1, T_2 relaxation times **[18]**.

In terms of spectral enantiodiscrimination efficiency, the difference of between *R* and *S* NMR observables, ΔObs, depends only on the magnitude of K^{NMR}. Considering only ^{1}H, ^{13}C, and ^{2}H nuclei, and based on numerous empirical observations, three important observables useful in practice can be retained, and can be roughly classified in terms of both enantio-efficiency and experimental feasibility/ease as follows: ^{2}H-RQCs >> ^{13}C-RCSAs > (^{13}C-^{1}H)-RDCs. Obviously, other observables such geminal (^{1}H-^{1}H)-RDCs in methyl group can provide good opportunities to reveal spectral enantiodiscriminations. All these interactions can be observed at natural abundance level (^{1}H-^{1}H: 99.97 %; ^{13}C: 1.08 %; ^{13}C-^{1}H: 1.069 %; ^{2}H: 0.0155 % with routine NMR spectrometers, but their analytical potentialities depend also to further factors such as, the amount of the analyte available, its MW, its chemical nature and its structural complexity **[6, 18, 19, 20]**.

2.1 | Recording "routine" nuclei

Hydrogen NMR. Hydrogen nuclei can be exploited for discriminating enantiomeric or enantiotopic direction using differences in (^{1}H-^{1}H)-RDCs of enantiomers. In this case, each pair of interacting nuclei, $^{1}H_i$ and $^{1}H_j$, produces distinct D_{HH} defined in Hz as **[4, 5]**:

$$D_{^{1}\mathrm{H}_i^{1}\mathrm{H}_j}^{A \text{ or } B} = -k_{\mathrm{HH}} \times \langle \frac{S_{\mathrm{HH}}^{A \text{ or } B}}{r_{ij}^{3}} \rangle, \qquad (5)$$

with:

$$k_{\mathrm{HH}} = \left(\frac{\mu_0}{4\pi}\right)\left(\frac{\mathrm{h}\gamma_{\mathrm{H}}\gamma_{\mathrm{H}}}{4\pi^2}\right) = 120.09\ \mathrm{kHz.A^{-3}}.$$

In this equation, r_{ij} is the internuclear distance between two interacting nuclei (i and j), γ_H is the gyromagnetic ratio of ^{1}H and μ_0 is the magnetic permeability of free space.

As a consequence of **Eq. 5**, the D_{HH} values can be positive, null or negative. This new term adds to the scalar coupling, J_{HH}, leading to total spin-spin coupling, T_{HH}, with: $T_{HH} = J_{HH} + 2D_{HH}$, for a classical AX spin system or $T_{HH} = 3D_{HH}$ for a spin system constituted by two and three equivalent (homotopic) nuclei, A_2 or A_3. An example of ^{1}H-^{1}H spectral differentiation (AX spin system) is shown in **Figure 3b**. D_{HH} can be positive, null (magic angle) or negative, and consequently T_{HH} can be positive or negative as well as null when $J_{HH} = -D_{HH}/2$.

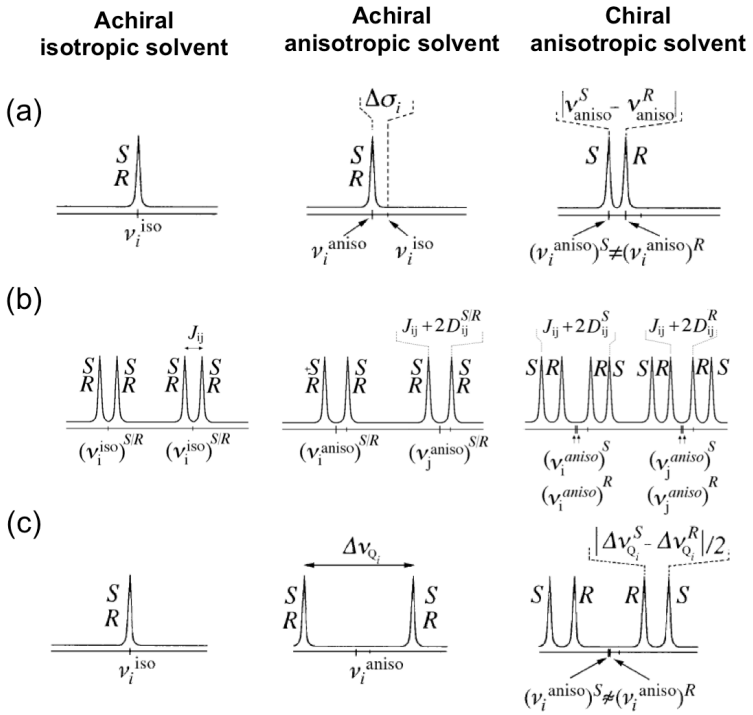

Figure 3 *Schematic principle of the spectral enantiodiscrimination in CLCs based on an absolute difference of: (a) (^{13}C)-RCSA ($|\nu_i^{aniso} - \nu_i^{iso}|$), (b) (^{1}H-^{1}H)-RDC (AX spin) with $|D_{ij}| > |J_{ij}|$ and (c) (^{2}H)-RQC (spin I = 1), expected in (left) achiral liquids, (middle) in ALCs and (right) in CLCs. The various 1D signals are not plotted to scale, and the S and R assignments are arbitrary.* ***Figure partially adapted from Refs. [4] and [6] with permission.***

Carbon-13 NMR. Naturally abundant at 1.07 % relative to Hydrogen, ^{13}C nuclei can be also efficiency used to discriminate enantiomers on the basis of a difference of anisotropic contribution to the electronic shielding, $\sigma_{\mathrm{i}}^{\mathrm{aniso}\,A\ \mathrm{or}\ B}$ that depends of $S_{\alpha\beta}$ parameter. Thus, for an enantiomeric/enantiotopic pair, their respective resonance frequencies (in Hz), $\nu_{^{13}\mathrm{C_i}}^{A}$ and $\nu_{^{13}\mathrm{C_i}}^{B}$, can be written as **[19, 20]**:

$$\nu_{^{13}\mathrm{C_i}}^{A\ \mathrm{or}\ B} = \frac{\gamma B_0}{2\pi}\left(1 - \sigma_{\mathrm{C}}^{\mathrm{iso}} - \sigma_{\mathrm{C}i}^{\mathrm{aniso}\,A\ \mathrm{or}\ B}\right), \qquad \textbf{(6)}$$

where $\sigma^{iso}_{^{13}C_i}$ is the isotropic contribution to the electronic shielding.

As a dilute spin (1 % with respect to ^{1}H) removing any ^{13}C-^{13}C interactions, this type of discrimination is simply observed when hydrogen nuclei are decoupled (^{13}C-{^{1}H}) leading to simple NMR spectra consisting of sum of independent ^{13}C resonances. Largest discriminations are genrally obtained with sp and sp^2 carbon atoms. An example of spectral ^{13}C differentiation (A spin system) in a CLC is shown in **Figure 3a**.

When no ^{1}H decoupling is applied, enantiodiscrimination is possible on the basis of a difference of (^{13}C-^{1}H)-RDCs according to **Eq. 7 [19, 20]**:

$$D^{A\text{ or }B}_{^{13}C_i^1H_j} = -k_{CH}\langle\frac{S^{A\text{ or }B}_{CH}}{r^3_{CH}}\rangle, \qquad (7)$$

with $k_{CH} = 30.09$ kHz.A^3. As for ^{1}H, D_{CH} adds to J_{CH} ($T_{CH} = J_{CH} + 2D_{CH}$). Note here that direct scalar coupling, $^1J_{CH}$, is always positive. As seen from **Eqs. 5** and **7**, the magnitude of k_{ij} that depend on the gyromagnetic ratio of isotopes involved can vary by one or two orders of magnitude. A few examples of k_{ij} values associated with interacting homo- and hetero-nuclear pairs (and their sign) can be found in Ref. **4**.

Deuterium NMR. Anisotropic ^{2}H spectra are dominated by the quadrupolar interaction resulting to from the interaction between the electric quadrupole moment of ^{2}H (Q) and the electric field gradient (EFG) along the C-D bond, with a good approximation. In practice, and as for the two other anisotropic interactions described above, we have access to the ^{2}H residual quadrupolar couplings, ^{2}H-RQCs, of molecules (isotopically enriched or normal), that corresponds to the distance (or quadrupolar splitting) between both components of a ^{2}H quadrupolar doublet (^{2}H-QD). As second isotope of ^{1}H, deuterium nuclei are naturally present in any hydrogenated molecules, with a very a low relative abundance of 1.55 x 10^{-2} % (respect to ^{1}H) namely about 100 less than for ^{13}C). This drawback is compensated by three analytical advantages **[6, 21, 22, 23]**: i) a small Q_D value leading to high-resolution ^{2}H-{^{1}H} NMR spectra, ii) a distribution of anisotropic ^{2}H signals on only two components ($2I$ peaks with $I = 1$), named a deuterium quadrupolar doublet (^{2}H-QD), leading to acceptable signal-to-noise ratio (SNR), iii) a very high sensitivity of the ^{2}H quadrupolar interaction relative to a difference of local ordering.

For an enantiomeric/enantiotopic pair *(R/S* or *pro-R/pro-S)*, the splittings (in Hz) between each component of a given ^{2}H-QD, $\Delta\nu_{Q\,^2H_i}^{A\text{ or }B}$, for given deuterium site, i, can be written as **[21, 22, 23]**:

$$\Delta\nu_{Q\,^2H_i}^{A\text{ or }B} = \frac{3}{2}QCC_{CD} \times S_{CD}^{A\text{ or }B} \qquad (8)$$

with

$$QCC_{CD} = (e^2Q_{D_i}q_{C\text{-}D_i})/h \text{ and } S_{CD}^{A\text{ or }B} = \frac{1}{2}\langle 3\cos^2\theta_{CD}^{A\text{ or }B} - 1\rangle.$$

A priori, the ^{2}H quadrupolar coupling constant, denoted QCC_{CD}, is assumed to be identical for two enantiomers or enantiotopic sites. The magnitude of this term depends on the ^{13}C hybridization state ($QCC_{C\text{-}Di} \approx 170 \pm 5$ kHz, 185 ± 5 kHz and 210 ± 5 kHz, for sp^3, sp^2 and sp carbons, respectively) and $S_{CD}^{A\text{ or }B}$ is the order parameter of the C-D_i axis (actually the electric field gradient along C-D) relative to $\mathbf{B_0}$. A schematic example of spectral ^{2}H

differentiation (a single deuteron) in a CLC is shown in **Figure 3c**. Here again, the $\Delta\nu_Q{}^{A\text{ or }B}$ value can be positive, negative or null (rare). As we will discuss below, this interaction is particularly well adapted to visualize monodeuterated enantio-isotopomers associated with enantiotopic directions of CH_2 groups in prochiral molecules (see **Figure 1**).

2.2 | Playing with "exotic" nuclei

In practice, any magnetically active, naturally abundant nuclei present in a molecule, such as ^{19}F, ^{31}P, ^{10}B, …, are possible nuclear probes to separate the signals of enantiomers or enantiotopic elements **[24, 25, 26, 27, 28]**. In particular, the CF_3 groups are excellent probes for a spectral differentiation (two triplets observed on ^{19}F-{^1H} spectra) on basis of (^{19}F-^{19}F)-RDCs difference (see below). For monofluorinated or organophosphored chiral compounds, enantiodiscriminations are expected on the basis of a difference of ^{19}F-RCSAs or ^{31}P-RCSAs, respectively, assuming that protons are decoupled **[26, 27, 28]**.

2.3 | Spectral analysis by 2D NMR tools

The wealth of information content of anisotropic interactions combined to the doubling of signals in CLCs has a "cost" in terms of spectral complexity that can be overcome by using 2D NMR experiments. Adapted to specificities of oriented NMR as in case of spin-1 nuclei, various types of homo or heteronuclear NMR experiments have been designed to accelerate the analysis of ½- and 1-spin nuclei spectra, and even both. For the former, most interesting experiments are based on a "*J*-resolved" type scheme in which only the homo- or heteronuclear coupling interaction evolves during the t_1 dimension, combined with a selective excitation (concept of SERF NMR) to reduce the amount of spectral information or to select one of both enantiomers. In the second case, the several 2D experiments referred to under the generic name of "QUOSY" (QUadrupole Ordered SpectroscopY) have been proposed.

2D experiments involving spins-½ nuclei Due to long-range (^1H-^1H)-RDCs or (^1H-^{13}C)-RDCs, ^1H 1D spectra as well as the proton-coupled ^{13}C 1D spectra can be complex to analyse mainly due to their weakly resolved spectral patterns at each inequivalent site **[29]**. In practice, ^1H-COSY-type 2D experiments can provide help for simplifying the analysis of chiral molecules **[30]**, including or not selective conditions (excitation of a given ^1H site) (see **Figure 4**) **[31]**. Better is the possibility to separate the homo- or heteronuclear spin-spin total couplings and the chemical shifts on both spectral dimensions using 2D experiments based on ^1H or ^{13}C "*J*-resolved"-type schemes or other schemes as ^1H *J*-HSQC-BIRD correlation sequence (see **Figure 4**) for which only the coupling interaction evolves during the t_1 dimension **[32]**. Associated with a selective excitation of nuclear site of interest, further spectral simplifications (family of homo or heteronuclear G-SERF experiments) are obtained (see **Figure 4**) **[33, 34, 35, 36, 37]**.

2D experiments involving spin-1 nuclei. ^{2}H quadrupolar interaction has been initially and extensively exploited with deuterated chiral analytes. However, as the isotopic enrichment is not always easy to perform (generally considered as time-consuming by chemists), and does not guarantee a spectral discrimination on the enriched site(s), either, it becomes preferable to detect ^{2}H nuclei at the natural abundance level, despite its low abundance level **[21, 22]**.

As any dilute spin (like ^{13}C spins), the detection of ^{2}H-^{2}H couplings (J and D) at natural abundance is not possible yet, and so the proton-decoupled, anisotropic natural abundance deuterium (ANAD-{^{1}H}) spectra correspond to the sum of independent ^{2}H-QDs associated with all monodeuterated diastereo-isotopomers and/or enantio-isotopomers of the mixture. Consequently, the ANAD 1D spectra in weakly orienting CLC can become overcrowded even for rather structurally-simple chiral molecules, because: i) the small range of ^{2}H-RQCs (generally below 1000 Hz) compared to the range of $\delta^{aniso}(^{2}H)$; ii) the detection of 2n ^{2}H-QDs (for a molecule of n inequivalent hydrogen site) if all sites are differentiated in CLC.

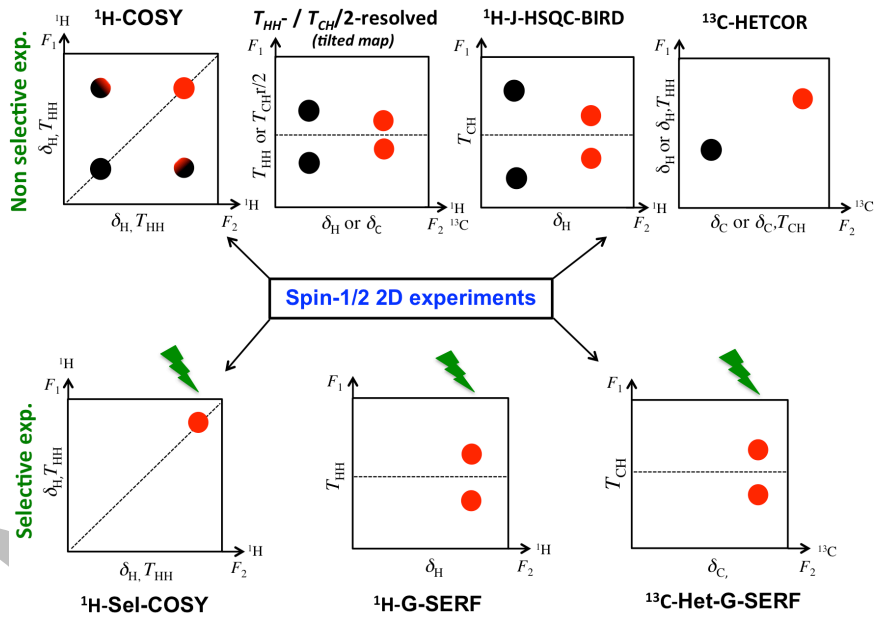

Figure 4 *A schematic description of the main homo- and heteronuclear (^{1}H-^{1}H or ^{13}C-^{1}H pairs) experiments used for simplifying the analysis of anisotropic spin-1/2 spectra (^{1}H/^{13}C) without (top) and with selective excitation (bottom).*

To facilitate the analysis of overcrowded ANAD spectra, several types of 2D/3D-NMR experiments (homo- and heteronuclear QUOSY) have been designed **[38, 39, 40, 41, 42, 43, 44, 45]** as schematically depicted in **Figure 5**. The common aim of all QUOSY's is to correlate the two components of each ^{2}H-QD and assign them on the basis of their anisotropic chemical shift, considering that $\delta(^{2}H)^{aniso} \approx \delta(^{2}H)^{iso} \approx \delta(^{1}H)^{iso}$. In this class of (autocorrelation) experiments, $\delta(^{2}H)^{aniso}$'s and $\Delta\nu_{Q}(^{2}H)$'s can evolve in both t_1 and t_2 dimensions (Q-COSY-type) or be refocused during t_1 (Q-resolved or δ-resolved experiments). Excitation of double quantum coherence deuterium (spin I = 1) is also possible (Q-DQ type), but needs an optimization of a delay, not required for other

experiment). The most useful experiments are the *Q*-COSY 2D and *Q*-resolved 2D experiments (and their phased variants) for which a tilt procedure (post acquisition procedure) can be also applied on 2D spectra removes the ^{2}H-QDs in F_2 dimension, and so the F_2 projection formally resembles the isotropic NAD NMR spectra **[38, 40]**. All QUOSY 2D experiments using the "Fz" extension possess a « Z-filter » block (specifically designed for spins I = 1) within the pulse sequence to obtain phased ^{2}H 2D spectra. Homonuclear 3D experiments (as 3D *Q*-DQ) **[41, 42]** were also designed, as well as heteronuclear versions of QUOSYs experiments. These latter correlate ^{13}C and ^{2}H nuclei either in deuterated molecules ("CDCOM" experiment: Carbon-Deuterium Correlation in Oriented Media) **[40]** or at natural abundance level ("NASDAC" experiment: Natural Abundance Spectroscopy Deuterium And Carbon) **[45]**. Obviously, all ^{2}H 2D experiments design for recording anisotropic ^{2}H spectra at natural abundance can be applied to study poly- or perdeuterated solutes, as well.

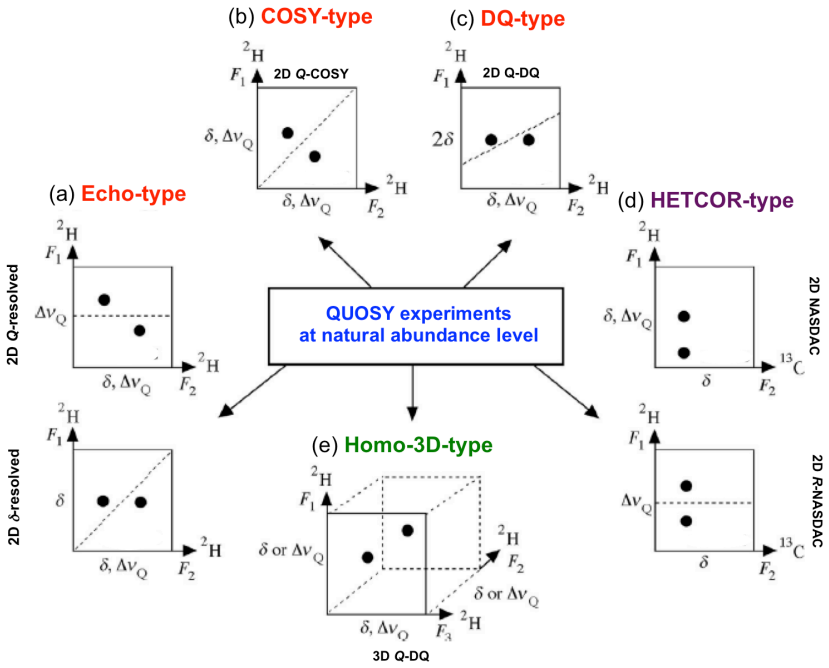

Figure 5 *Schematic description of homo- and hetero-nuclear ^{2}H-QUOSY 2D/3D experiments: (a) echo-type schemes (Q-resolved sequences and δ-resolved), (b) COSY-type scheme (Q-COSY), (c) double quantum-type scheme (Q-DQ), (d) Heteronuclear HETCOR-type sequence (CDCOM or NASDAC or 2D Refocussed-NASDAC) and (e) homonuclear 3D-type sequence (3D Q-DQ).* ***Figure adapted from Ref. [23] with permission.***

To experimentally fight the inherent low sensibility of ANAD 2D NMR, the use of higher magnetic fields (> 9.4 T) and selective ^{2}H probes (standard probe or better, a cryogenic probe **[46]** is a simple way to increase the sensitivity of NAD 1D/2D experiments. Besides to reduce the experimental time (T_{exp}) of ANAD QUOSY nD experiments that required a large number of scans for each t_1 transient, a new type of data acquisition in the direction dimension t_1 as the non unform sampling (NUS) approaches combined with an adapted reconstruction such as the covariance (Cov) method or compressed sensing (CS) processing can be applied **[47, 48, 49]**.

III. ENANTIODISCRIMINATING LYOTROPIC MESOPHASES

In addition to the early historical liquid-crystalline systems known as "thermotropics" which strongly align any analytes **[11, 12, 13, 14]**, it exists another type of organosoluble (or hydrosoluble) weakly orienting systems named “lyotropic liquid crystals” (LLC). These latter phases are made up of molecular components that do not possess intrinsic mesogenic properties as in case of thermotropics. Achiral or chiral LLCs are often formed by long molecules (rod-like shaped objects) such as polymers, that mixed with suitable (organic) solvent under appropriate conditions (concentration, temperature and pressure) lead a uniform/homogeneous oriented medium in the magnetic field of the NMR spectrometer **[50, 51]**.

3.1 | Polypeptide-based organosoluble polymers

Despite, the paradigm shift associated with NMR in CLCs as innovating approach for enantiodiscrimination purposes proposed from 1967 **[17]**, the analytical complexity of ^{1}H spectra recorded in thermotropic (cholesteric) systems (strongly orienting solvents) has greatly reduced its attractivity of this tool, and only a few reports exist **[52, 53]**. In fact, a revolutionary development came with the use of weakly-ordering chiral ordering agents (lyotropic system) consisting of polypeptide polymers dissolved in conventional organic solvents **[54]**, concomitantly with the development water-compatible dilute liquid crystalline media developed for the structure elucidation of biomolecules **[55]**.

Neat polypeptide. Among organo-compatible, weakly aligning enantiodiscriminating mesophases, a special attention has been paid to rod-like systems made of α-helicoidally chiral polymers. In this family of LLC, where $\text{Length}^{poly} >> \text{Diameter}^{poly}$, the stereogenic center can be present in the central backbone (as polypeptidic polymers with achiral side chains), on the flexible side chain (as polyacetylenic or poly(arylisocyanide) polymers) or simultaneously on both these structural elements (polypeptides bearing a chiral side chain) (see **Figure 6**).

So far, the most investigated homopolypeptide polymer as enantiodiscriminating CLCs and implied in many applications (in particular at Orsay) is made of poly-γ-benzyl-*L*-glutamate (PBLG) whose AC is of *L*-type, and a vast literature exists on its physical properties **[56, 57, 58, 59**]. However, other polypeptide polymers, such as poly-ε-carbobenzyloxy-*L*-lysine (PCBLL) **[60, 61]**, poly-γ-ethyl-*L*-glutamate (PELG) **[60, 61, 62]**, can provide robust enantiodiscriminating lyotropic systems. Obviously, the enantiomers of these polymers (PBDG, PCBDL, ...) are also enantiodiscriminating systems, but with inverted results in terms or enantio-orientation.

Over the last decade, new and original variants of enantiodiscriminating polypeptide-based polymers have been reported such as helicoidally chiral systems made of: i) poly-β-phenethyl-*L*-aspartate (PPLA) **[63]**, ii) poly-β-benzyl-*L*-aspartate (PBLA) **[64]**, iii) poly-γ-*p*-biphenylmethyl-*L*-glutamate (PBPMLG) **[65]**, iv) poly-γ-(*S*)-2-methylbutyl-*L*-glutamate (PSMBLG) **[66]**. The idea related to the use of PSMBLG is to reinforce the enantiorecognition efficiency and increase spectral enantio-separations by adding a second asymmetric center in

the side chain **[66]**. Finally, we can also mention the design of a polypeptide co-polymer (a polymer bearing two types of sidechain) made phenethyl and benzylpolyaspartate **[67]**.

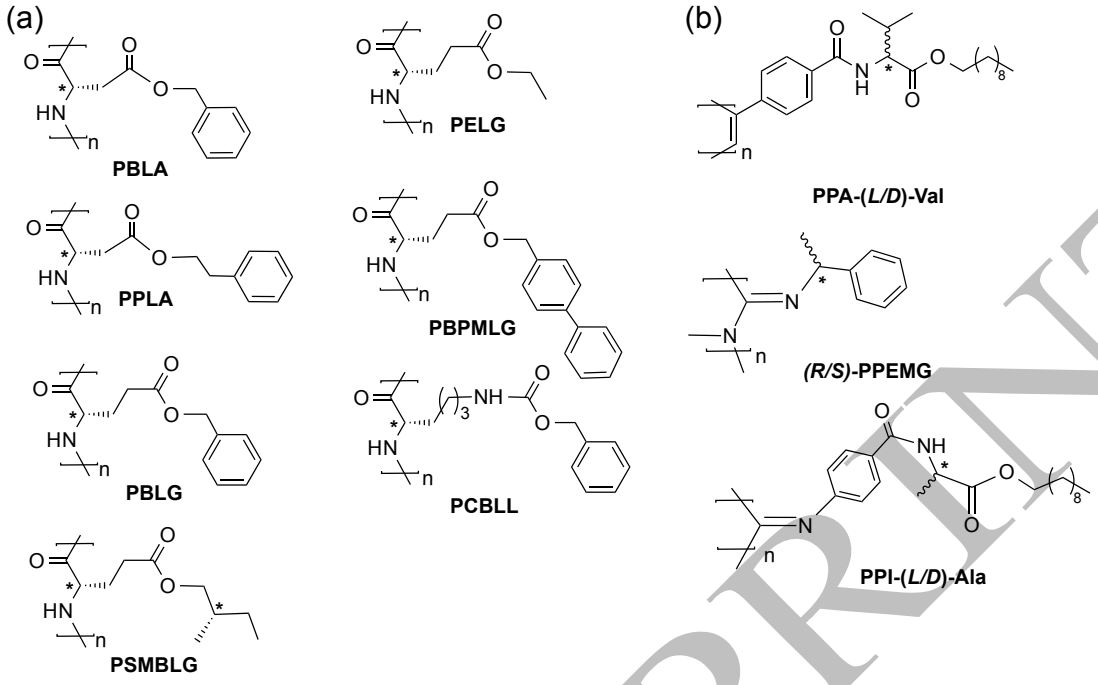

Figure 6 *(a) Some examples of structures of homopolypeptide-based helical polymers with a L-configuration for the repeating unit (PBLA, PPLA, PBLG, PSMBLG, PELG, PBPMLG, PCBLL). (b) Other examples of non-polypeptide helical polymers: (L/D)-Val-based PLA, (R/S)-PPEMG, (L/D)-Ala-based PPI. In these polymers, the stereogenic center is only located on the sidechain.*

Mixture of polypeptides with opposite absolute configuration. Contrarily to organic solutions of a single polypeptide, mixtures prepared by mixing equal amounts by weight of polypeptides (with close degree of polymerization (DP)) of same nature but with opposite absolute configuration (*e.g* PBLG and its enantiomer PBDG) lead to achiral liquid crystals (ALCs) where enantiodiscrimination phenomenon is inactive. In these achiral mesophases, noted « PBG », both enantiomers exchange rapidly, between the *L*- and *D*- helical vicinities of each polypeptide on the NMR time scale. This result in identical average magnetic interactions for enantiomers, and no difference on their NMR spectra is therefore expected **[68, 69]**.

From analytical viewpoint, the comparison of NMR spectra recorded in the chiral mesophases (PBLG or PBDG) and the achiral mesophase (PBG) obtained by compensation is interesting for several reasons: i) the simplification of spectra by reduction of the number of resonances, ii) an help for the identification of ^{2}H signals, iii) the checking whether the doubling of spectra (signals) originates from an enantiorecognition effect in the CLC, or is related to another (dynamic) phenomena (exchange), iv) the determination of relative sign of ^{2}H-RQC for a given site. For instance, recording ^{2}H spectra in PBG can be very useful for assigning the ^{2}H-QD associated with diastereotopic positions in methylene groups of chiral molecules, both in isotopically enriched solutes or at natural abundance level (see below).

Mixture of chemically different polypeptides. When chemically compatible, the mixture of two polypeptides (of same family) with different types of side chains, such as PBLG and PCBLL (same AC), may lead to uniform a new monophasic oriented system, allowing the discrimination of both enantiomers and enantiotopic directions in prochiral molecules. Interestingly in such mixed systems, the magnitude of anisotropic observables and enantiodiscriminations can be adjusted by varying the relative proportion of the two polypeptides in the mixture **[70, 71]**. These enantiodiscriminating media can therefore be proposed as an alternative to single-polypeptide mesophases for stereochemical applications. Note finally that, whatever their polymeric ratio used, the mixture of two polypeptides of chemically different compensated by the same mixture of their respective enantiomers leads to an achiral orientationally ordered environment **[71]**.

3.2 | Polymeric-based LLCs optimisation

The enantiorecognition efficiency and analytical potential of polypeptide systems, and notably PBLG, have been intensively explored and studied for various practical reasons: i) PBLG is soluble in a large range of organic co-solvents, ii) preparation of samples is a rather simple and alignment of polymeric mesophase with the $\mathbf{B_0}$ field is rapid (< 60 s), iii) the possibility to play with the concentrations of phase components (analyte, polymer, co-solvent), iv) and last but not least, their commercial availability. Playing with all these advantages, PBLG-based mesophases revealed to be able to discriminate enantiomers of almost all classes of organic chiral molecules, but also various aspects of enantiomorphism, such as chirality by virtue of the isotopic H/D substitution, or the enantiotopy in prochiral molecules (see below).

Concentration and temperature. Compared to thermotropic liquid crystals, organic LLCs are much more "flexible" systems because they can accommodate a large amount of many types of organosoluble solute, while maintaining their liquid-crystalline properties on rather large range of temperatures (depending of the co-solvent). Also, the degree of alignment of LLC, and in turn the magnitude of anisotropic interactions, can be controlled by adjusting the amount of polymer relative to the co-solvent in the phase or modifying the degree of polymerisation (DP) of polypeptide **[72]**.

Polarity of organic co-solvent and additives. One of the most remarkable interest of PBLG-based oriented matrices is their ability to form LLCs with various organic co-solvents, ranging from polar (DMF, TMU, NMP, pyridine, ...) to weakly polar (toluene, benzene, 1,1,2,2-tetrachloroethane, CH_2Cl_2, $CHCl_3$, …). This large variety of co-solvents allows an optimal optimisation of the phase toward the nature of the analyte studied (polar, apolar, neutral, charged), but also the possibility to optimize the chiral environment in terms of enantiodiscriminations **[72]**. Thus, the replacement of low polar solvent by higher polar one can significantly enhance the enantiodiscrimination properties of the phase, as shown in case of chiral amines **[73]** or fatty acids **[74, 75]**. In practice, the multi-parameters choice of co-solvent is never trivial whilst a wrong choice can affect the quality of discrimination **[72, 74]**.

The main limitation of PBLG and more generally of all homopolypeptide-based CLCs is their difficulty to dissolve highly polar analytes, and their inability to dissolved water-compatible molecules. This drawback can be overcome by adding a small proportion (1% w/w) of polar additives, such as DMSO, in order to (slightly) increase the amount of solute in solution in the mesophase **[76]**. Another more drastic option is to record their NMR spectra in β-peptide-based helical systems in the presence of water **[77]** or using non-peptide other water-compatible phases (see **Section 3.4**).

3.3 | Alternatives to polymeric chiral systems

From 2010, various new chiral mesophases made of helically chiral polymers have been synthesised and described as enantiodiscriminating oriented media (see **Figure 6b**). Without being exhaustive, we can mention the oriented chiral systems some of them, made of: i) poly(guanidine), poly(arylisocyanide), poly(arylacetylene) containing chiral side chains, poly(isocyanopeptide) **[78, 79, 80, 81, 82, 83]**. Another interesting source of weakly oriented media can be found with compressed or stretched polymer gels. The analytical potential of both these equivalent concepts for introducing anisotropy in the sample have been demonstrated from the mid-2000's by various groups **[84, 85, 86]**.

3.4 | Hydrosoluble chiral environments

Amphiphilic chiral systems. Historically, the first descriptions of spectral enantiodiscriminations of small chiral molecules (*L*/*D*-alanine) in water-based chiral LLCs was reported by Tracey *et al*. who used enantiopure sodium decyl-2-sulfate as an interesting model membrane system in 1975 **[87]**, and then the potassium *N*-dodecanoyl-*L*-alaninate based system in 1984 **[88, 89]**. More recently enantiodiscriminating phases made of glucopon (a mixture mainly composed of alkyl (octyl and decyl) α- and β-mono- and diglucosides)/ hexanol/ buffered water **[89]**, as well as alanine-based surfactant solutions **[90]** were described. The main drawback of these aligning media is the complexity of their preparation and/or their ability to orient uniformly in the magnetic field, and as a result, the number of efficient and very robust systems proposed remains rather limited.

When ignoring any enantiodiscriminations issues, a large variety of water-based mesophases have been mainly explored and used to elucidate the 3D structure of large water-soluble biomolecules, such as proteins, based on the analysis of anisotropic interactions such as RDCs, in particular following the first work of Bax's group using hydrosoluble dilute liquid-crystalline media **[91]**. In this field, we can mention the use of bicelles, micelles, bacteriophages, non-ionic dilute liquid crystalline media, polyacrylamide-based gel, collagen-based gels, DNA LLCs **[55, 92, 93, 94, 95, 96]**. Interestingly, the review by Prestegard *et al*. provides a useful overview of the main LLCs for biomolecules and their use as ordered media **[95]**.

Polynucleotide systems (DNA). Another type of helically chiral polymers (rod-like molecules) can be found with aqueous solution of polynucleotide systems as deoxyribonucleic acid (**DNA**) strands (a double helix) as first demonstrated in 2009 **[97]**. At suitable concentration, DNA/water systems can form cholesteric phases **[98]** that initially used to measure RDCs in biomolecules **[97**]. In practice, only chiral LLCs made of short DNA-fragments (150–300 base pairs) has shown interesting enantiodiscrimination potentialities when combined with ^{2}H NMR of isotopically enriched molecules (as chiral amino acids) **[99]**. Clearly, those DNA-based systems may therefore provide convenient oriented media for chirality NMR studies, but here again, compared to polypeptides LLCs, their preparation (control of pH, ionic balance, sample homogeneity, …) is more difficult, and requires the fragmentation of (sonication step by microwave) of commercially available material **[99]**.

3.5 | Amount of analyte and limits of detection

The sensitivity of NMR experiments depends on many parameters. We can mainly mention: i) the strength of the magnetic field ($\mathbf{B_0}$), the type of probe (cryogenic probe or not, direct or inverse probe, selective or broadband), ii) the spectral characteristics of the detected nuclei (spin number, gyromagnetic ratio and relaxation times), iii) and the spin density present in the sample. This last criterion is directly related to the abundance level of nucleus as well as the mass (m) of analyte available in the sample (5-mm o.d. tube), the molecular weight (MW) and the symmetry of solute and the type of chiral mixtures analyzed, (enantiopure, scalemic or racemic). In anisotropic NMR, it exists another important parameter related to the ability of the (chiral or not) liquid-crystalline mesophases to dissolve or not a large amount of a given analyte.

Generally, thermotropic phases, oriented gel based media but also DNA-based system (and more generally amphilic systems) are not ideal solvents to dissolve a large amount of analyte (5-20 mg), limiting the use to ^{1}H and ^{13}C NMR as well as ^{2}H NMR for isotopically-enriched molecules. In this last case, few mg of solute are generally enough for a detection. LLCs made of chiral polymers (polypeptide or polyacetylenic) provides more flexibility, accepting larger amounts of solute (up to 100 - 120 mg) depending on the choice of the organic co-solvent used. Using anlytes with MW < 150 - 300 g/mol and sufficient long T_2, the detection of low abundant nuclei as ^{13}C is easy while the ^{2}H signals at natural abudance level is still possible with reasonable SNR (10 - 50) and experimental time (15 - 20 h). For smaller MWs, the analyte amount can be safely divided by a factor of two, at least.

Obviously, for a given m and MW, the combination of high magnetic fields with cryogenic selective probe boosts considerably the sensitivity of anisotropic NMR, reducing the experimental times while improving the (low) detection limit. However in all cases, the amount of analyte has to choose considering all parameters mentionned above and the type of applications required (dynamic experiments, measurement of anisotropic data, enantiomeric determination, isotopic studies, …).

IV. ILLUSTRATIVE EXAMPLES OF ENANTIODISCRIMINATIONS AND ENANTIOPURITY CONTROL

4.1 | Proton NMR

Due to their high isotopic abundance (99.985%), their γ and spin (I = 1/2), Hydrogen atoms are basic nuclear spies for revealing spectral enantiodiscriminations based on a difference of (^{1}H-^{1}H)-RDCs (see **Eq. 4**). However, even for small-size molecules, a dense homonuclear network made of (long and short range) ^{1}H-^{1}H residual dipolar interactions is obtained. This results in complex spectra, often poorly resolved, much more difficult to analyze than isotropic ^{1}H spectra as illustrated in **Figure 7** in the case of (±)-1,2-epoxypropane in PBLG phase **[29]**.

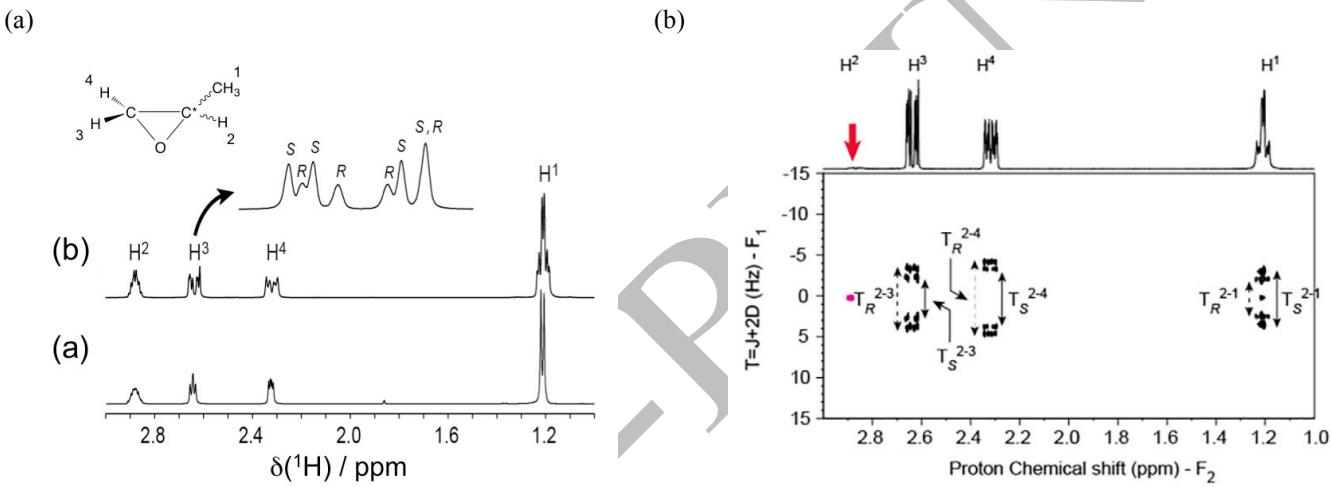

Figure 7 *(a) ^{1}H 1D spectrum (400.1 MHz) of (R)-1,2-epoxypropane (25% ee) recorded in (bottom) isotropic phase ($CDCl_3$) and (top) anisotropic chiral phase (PBLG/$CHCl_3$). An assignment of the lines belonging to each enantiomer is shown for the site H^3. (b) ^{1}H GSERF 2D experiment applied on the propylene oxide to edit the total couplings for each enantiomer.* ***Figure partially adapted from Ref. [29] with permission.***

Experimentally, there is no doubt that proton NMR is the most sensitive and fastest tool for routine use. However due to numerous dipolar ^{1}H-^{1}H couplings, anisotropic ^{1}H spectra usually became generally inextricable (even for small molecules), and hence very difficult to analyze by non-experts. Although they are more time consuming than ^{1}H NMR experiments, the analysis of ^{1}H coupled or decoupled ^{13}C/X NMR spectra remains more simple for two reasons: i) the ^{13}C/X-RCSA values, even larger than ^{1}H-RCSA, do not change significantly the overall chemical shifts profile on the analyzed spectra, and ii) the magnitudes of (X-^{1}H)-RDC are usually lower than their scalar couplings counterpart, keeping generally first-order type spectral patterns to analyze. Under these conditions, only slight perturbations compared with the conventional isotropic spectra are expected and generally observed, thus facilitating their interpretation.

Several homonuclear 2D NMR approaches (as the GSERF family) have been explored to improve the resolution of ^{1}H spectra of enantiomeric mixtures in CLCs, and to extract the structural information related to the numerous anisotropic interactions. Most of these methods rely on the ability of the NMR pulse sequences to

separate the evolution of chemical shifts and ^{1}H-^{1}H spin-spin coupling interactions for each enantiomer of a mixture as shown in **Figure 7b [29]** (see **Section 2.3** above).

To be complete, we can mention the latest methodological developments associated with the pure shift ^{1}H NMR experiments, first developed by Zanger **[100]**, that lead to ^{1}H decoupled ^{1}H NMR spectra where each inequivalent proton atom gives rise to a single line both in isotropic and anisotropic solvents **[29, 30]**. Although powerful, this technique is, however, not yet simple to be implemented as a routine NMR tool because: i) the optimisation of some specific experimental parameters remains challenging, ii) NMR sequence and adapted spectral reconstruction algorithms are not always compatible with NMR hardware and software, iii) this approach is not optimal with second order ^{1}H spin systems, as often observed in polypeptide-based liquid-crystalline solvents. As an alternative to this challenge, we can limit the effect of second-order on ^{1}H NMR spectral patterns using for instance LLCs with lower aligning power as done in **[101]**. By using low molecular weight PBLG, it has been shown that smaller RDCs were obtained and a better resolution on ^{1}H signals observed on the F_2-dimension of the ^{1}H-^{13}C HSQC experiments. Limitations of this approach are the commercial availability of such low-DP polypeptides, as well as the weaker stability of these mesophases.

4.2 | Carbon-13 NMR

^{13}C-{^{1}H} 1D NMR. The complexity of ^{1}H spectra in CLC mainly due to a dense network of ^{1}H-^{1}H scalar and dipolar couplings disappear when detecting "dilute" nuclei, namely weaky abundant as ^{13}C (1.1%) or even ^{2}H (0.015%) for which no coupling is simply detected. In this context, ^{13}C-{^{1}H} 1D NMR in CLCs rapidly emerged as an efficient alternative for chirality purposes, without any isotopic enrichment, and a wide collection of enantiomers were explored to be discriminated on the basis of ^{13}C-RCSA difference. Recording ^{13}C spectra at highest magnetic fields (see **Eq. 5**) becomes a fantastic advantage in terms of enantiodiscrimination magnitudes ($\Delta\nu^{A\text{ or }B}_{^{13}C_i} \propto$ strength of B_0) as well as sensitivity, leading robust determinations of *ee*'s calculating by peak deconvolution or even by peak integration. Depending on the magnitude of discriminations, it is easy to determine *ee*(^{13}C)'s within an error range of 2 - 5%.

Illustrative examples. This tool has been implied in the analysis of enantioselectivity of many and various asymmetric synthesis. Thus, we can mention: i) the double diastereoselection in [2+3] cycloaddition reactions of chiral oxazoline *N*-oxides and their application to the kinetic resolution of a racemic α,β-unsaturated δ-lactone **[102]**, ii) the intramolecular hydroamination catalysed by ate and neutral rare-earth complexes **[103]**, iii) the aza-Michael additions of *O*-benzylhydroxylamine to *N*-alkenoyloxazolidinones catalysed by samarium iodobinaphtholate **[104]**, iv) the monofluorination reactions on propargylic compounds (see **Figure 8a**) **[26]**, or v) the asymmetric reactions leading to chiral monophosphine oxides and boranes (see **Figure 8b**) **[105]**, vi) address the dynamic kinetic resolution of racemic α-chloro-β-ketoesters and α-chloro-β-ketophosphonates through ruthenium-mediated asymmetric hydrogenation **[106]**. Among other important results reported, this approach has

been also successively applied to discriminate enantiomers planar chirality of chiral as manganese/chromium tricarbonyl complexes ((η^6-arene)X(CO)$_3$ with X: Mn or Cr) obtained with new asymmetric reactions **[107, 108]** (see **Figure 9a**). Finally, the possibility to differentiate enantiomers of chiral molecules having heteronuclear asymmetric atoms as in case of chiral sulfoxides show the analytical versatility of this tool (see **Figure 9b**).

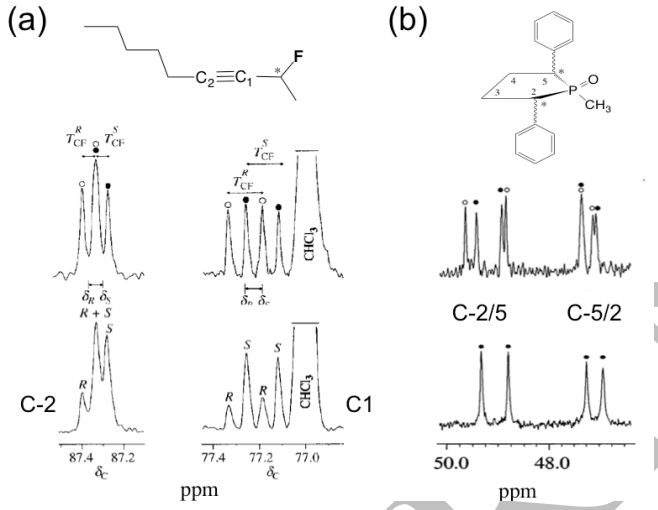

Figure 8 *(a) 100.3 MHz ^{13}C-{^{1}H} signals of the ethynyl carbon atoms (sp carbon) of 2-fluoro-3-nonyne in racemic (top) and enantioenriched (bottom) series in PBLG/CHCl$_3$. (b) signals of the 1-methyl-1-r-oxo-2-cis,5-trans-diphenyl-phospholane in PCBLL/CHCl$_3$. In these two xexamples, the chiral discrimination on the basis of a difference of ^{13}C-X total couplings (X = ^{19}F and ^{31}P, respectively)****. Figure adapted from Refs. [26] and [105] with permission.***

^{13}C-^{1}H couplings and heteronuclear correlation 2D experiments. Removing the ^{1}H decoupling, the one-bond (^{13}C-^{1}H)-RDCs (^{1}D$_{CH}$) are potential NMR observables for the chiral analysis (see **Eq. 4**). However, the presence of long-range (^{13}C-^{1}H)-RDCs combined with doubling of ^{13}C-^{1}H spectral patterns when the discrimination occurs can considerably complicate the spectral analysis at a given ^{13}C site. Nevertheless, for chiral analytes exhibiting isolated methyl groups, it may be advisable to examine the proton-coupled carbon-13 signals of these CH$_3$ sites. To illustrate this idea, we present in **Figure 10a** an expansion of the proton-coupled ^{13}C spectrum of methyl group of (±)-2-bromopropionic acid in PBLG. The expected (ideal) spectral pattern might be is the sum of two quadruplets dedoubled due to the direct T_{CH} coupling (with $^1T^R_{CH_3} \neq {}^1T^S_{CH_3}$) and the long-range coupling with the proton of stereogenic site (with $^2T^R_{CH-CH_3} \neq {}^2T^S_{CH-CH_3}$). At the temperature selected here, one enantiomer shows no long-range coupling ($^2T^R_{CH-CH_3} = 0$). Here the large separations between *R*- and *S*-resonances would allow a simple determination of *ee* in case of a scalemic mixture (0 < *ee*(%) < 100). **Figure 10b** reports another interesting example of ^{13}C enantiodiscrimination of an isolated methyl group bonded now on an asymmetry sulphur atom. In the case of this (±)-*S*-methyl-*S*-*p*-tolyl-*N*-tosylsulfoximine, the broadening of ^{13}C resonances observed (6 - 10 Hz) originates mainly from the long-range D$_{CH}$ with aromatic protons of the analyte.

Extraction of (^{13}C-^{1}H)-RDCs for each enantiomer can be simplified using heteronuclear correlation 2D experiments of ^{13}C-detected "resolved" type or ^{1}H-detected "HSQC" type (see **Figure 4**) **[32]**. In heteronuclear

resolved-type 2D experiments for which only the J_{CH}'s and D_{CH}'s evolve during the t_1-dimension (noted *T*-resolved or *J/D*-resolved experiments) lead to a full separation of $\delta(^{13}C)$'s and T_{CH} couplings on F_2 and F_1 dimensions, respectively, and so a better visualisation of enantiodiscriminations (see **Figure 11a**).

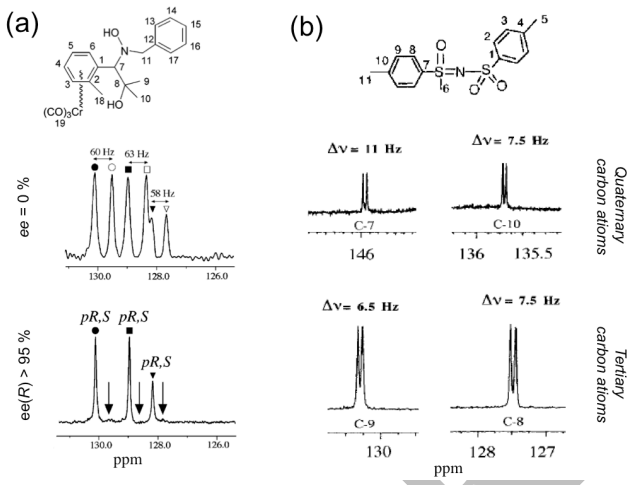

Figure 9 *(a) Comparison of three ^{13}C-{^1H} 1D signals of the N-(2-methyl-2-hydroxy-1-((2-methylphenyl)chromiumtricarbonyl) propyl)-N-benzyl-hydroxylamine, a chiral (η^6-arene) chromium tricarbonyl complex recorded in PBLG in racemic (top) and enantiopure series (bottom). (b) Four enantiodisciminated ^{13}C-{^1H} 1D signals of (±)-S-methyl-S-P-tolyl-N-tosylsulfoximine.* ***Figure partially adapted from Refs. [21] and [26] with permission.***

Elegant and efficient modification of this *T*-resolved experiment is to replace the 180° hard pulse by a band-selective 180° pulse in order to simplify the ^{13}C spectral pattern on a given site when enantiodifferentiation is difficult to identify and therfore quantify due to too many lines overlaps [**33**]. This experiment, called HetSERF, requires the calibration and optimisation of a shaped band-selective pulse, originally a REBURP-type pulse, easily implementable on routine NMR spectrometers through a dedicated "plug-and-play" module nowadays available on recent NMR softwares [**110**]. Those *J*-resolved-type experiments were, over the years, well integrated in the strategy of elucidation of molecules in order to univocally establish their 3D structure [**111**].

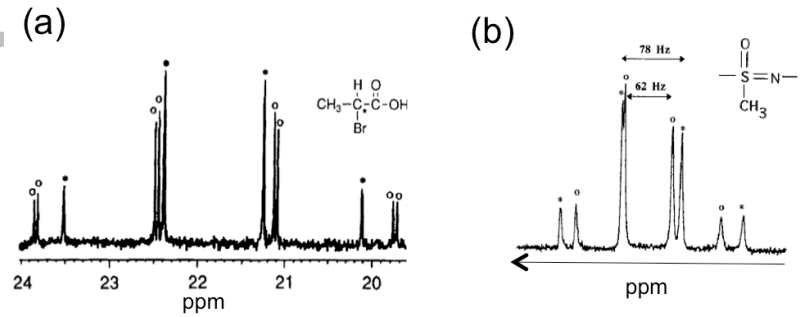

Figure 10 *Two typical examples of dedoublet quadruplets associated with the ^1H coupled ^{13}C signals (100.3 MHz) of a methyl group bonded to a stereogenic C or S atom, respectively: (a) of (±)-2-bromopropionic acid, (b) (±)-S-methyl-S-P-tolyl-N-tosylsulfoximine.* ***Figure partially adapted from Refs. [20] and [26] with permission.***

Alternative to these ^{13}C experiments is the used of ^{1}H-detected *J/D*-HSQC experiments where ^{1}H signals are now detected, thus offering a significant gain in sensitivity compared to the ^{13}C-detected sequences. **Figure 11b** shows an example of chiral analysis by ^{1}H-*J*-HSQC-BIRD experiments where the ^{13}C BIRD NMR module (inserted in the middle of the t_1 evolution period of ^{13}C-^{1}H 2D experiments) removes all long-range ^{13}C-^{1}H couplings (*J* and *D*) **[32]**. In the same family of sequence, we can also mentionned the CLIP/CLAP HSQC 2D experiments which allow the total couplings, $^{1}T_{CH}$, to be extracted with high resolution from the indirect dimension F_1 **[111]**.

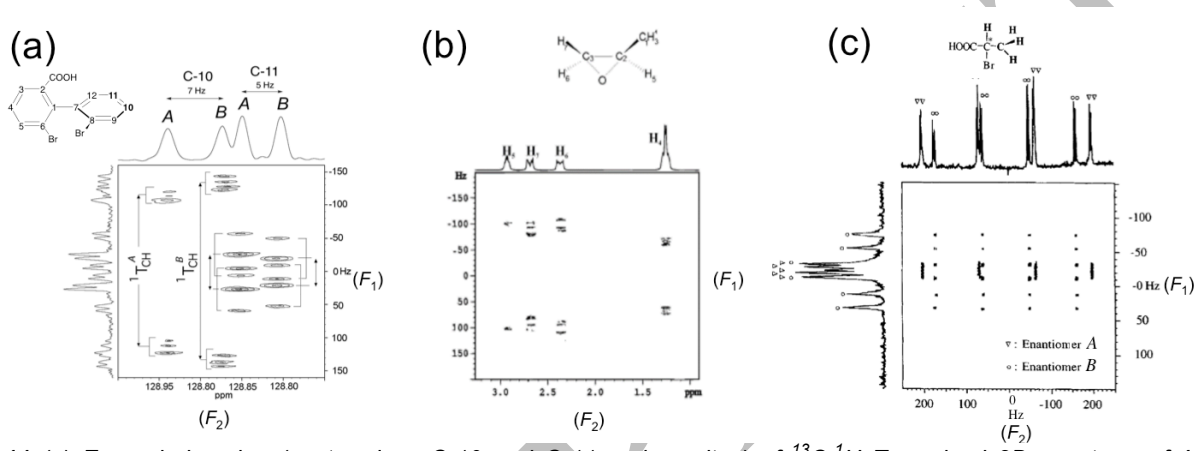

Figure 11 *(a) Expanded region (centered on C-10 and C-11 carbon sites) of ^{13}C-^{1}H T-resolved 2D spectrum of (±)-2,2'-dibromo-6-biphenylcarboxylic acid. (b) ^{1}H-J-HSQC-BIRD 2D spectrum of (±)-propylene oxide. (c) Zoom of the ^{1}H-^{13}C HETCOR 2D spectrum of (±)-2-bromopropionic acid located on the region of the methyl group. All spectra were recoded in the PBLG mesophase.* ***Figure adapted from Refs. [28], [32] and [109] with permission.***

Finally, in the world of heteronuclear ^{13}C-^{1}H experiments, the ^{13}C-detected "HETCOR" sequence without any ^{13}C and ^{1}H decoupling can provide interesting maps where two sets of spectral information are correlated while enantiodisciminations are simultaneously observed on a difference of T_{HH} (F_1) and T_{CH} (F_2) **[112]**. A nice example of such spectral situation is presented in **Figure 11c**.

4.3 | Deuterium NMR

1D/2D NMR on enriched molecules. Disregarding the high sensitivity of quadrupolar interaction to a difference of local order parameters, $S_{C\text{-}D}$ (see **Eq. 7**), the main advantage interests to use selectively deuterated chiral analytes are the simplicity of the spectral analysis due a limited number of deuterons and the absence of total *J/D* couplings ^{2}H-^{1}H (^{1}H decoupling).

The exploratory, systematic study of analytical potential of ^{2}H-{^{1}H} 1D NMR in polypeptide-based CLCs was initiated with the case of (±)-1-phenylethanol (PE) deuterated on the stereogenic center, **[54]**, an interesting model molecule featured by polar groups (OH able to form hydrogen bonds) and a strong shape anisotropy of substituent around the asymmetric carbon atom (see below) **[113]**. From this first result almost all classes of organic chiral compounds were tested, including the case of compounds chiral by virtue of the isotopic substitution, and enantiomers with a large variety of structures and functional groups, such as alcohol, amines,

carboxylic acids, esters, ethers, epoxides, tosylates, chlorides, bromides, …, and even cyclic hydrocarbons were successfully spectrally discriminated **[114, 115, 116, 117, 118, 118, 120]**. In majority of case, the method revealed to be efficient whatever the molecular structure: rigid, semi-rigid or flexible, with however significant variations in RQC difference ($|\Delta\Delta\nu_Q|$), which generally depends on the distance of deuterated site to the sterogenic center in more or less flexible compounds **[116]**.

Figure 12 presents four typical examples of ^{2}H-{^{1}H} 1D spectrum of monodeuterated flexible and rigid enantiomers with or without polar chemical functions or atoms, including the difficult case of enantiomers of chiral deuterofluoroalkanes with generic formula $C_mH_{2m+1}C^*D(F)C_nH_{2n+1}$ **[120]**. In this last example, the spectral enantiodifferences, although smaller, are observed both on a difference of ^{2}H-RQCs as well as on the total ^{2}H-^{19}F couplings, leading *in fine* to two dedoubled ^{2}H-QDs, (see **Figure 12d**). The analysis of these four selected examples illustrates the versatility of the method in terms of type of enantiomers that can be differentiated by the chiral polymer as well as the magnitude of ^{2}H enantiodiscriminations. Clearly, the deuteration position (on the stereogenic center or more or less far from it) is not necessarily crucial. However, the position can affect the quality of the enantiodiscriminations ($\Delta\Delta\nu_Q$), depending on the molecular dissymmetry "probed" at a given nuclear site (see below) **[116, 118]**.

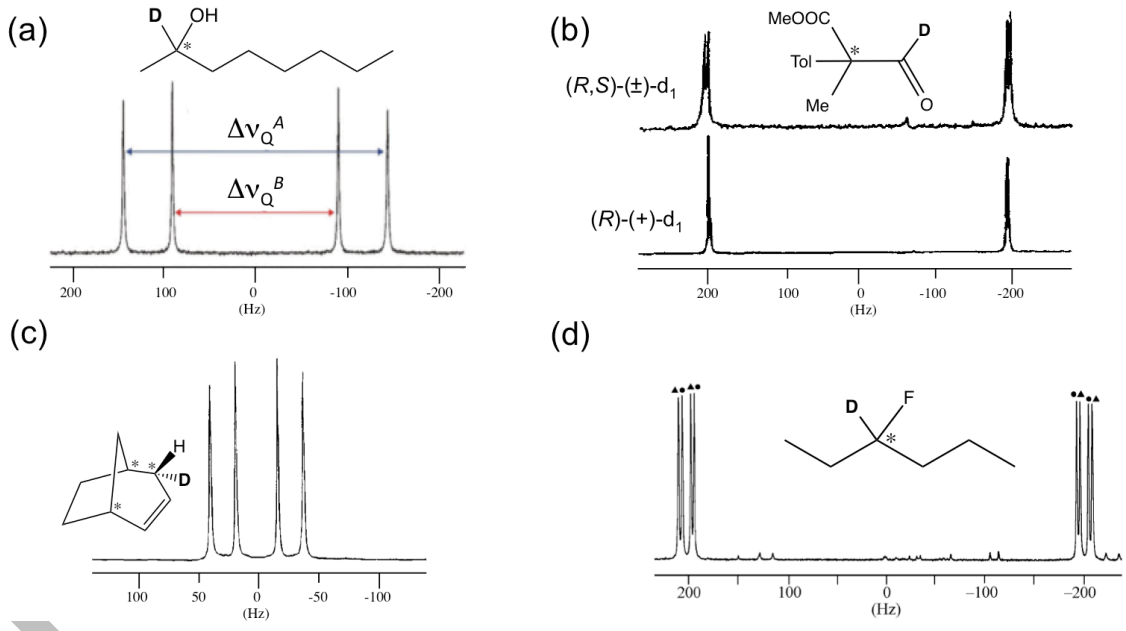

Figure 12** Four illustrative examples of monodeuterated chiral structures enantiodiscriminated by ^{2}H-{^{1}H} NMR (38.4 MHz): (a) (±)-2-deutero-octan-2-ol in PBLG/CH_2Cl_2, (b) (±)-*2-methyl-2-(4-methylbenzene)-3-oxo-3-deutero-propanoic acid, methyl ester, *(c) (±)-endo-4-deuterobicyclo[3.2.1]oct-2-ene and (d) (±)-3-deutero-3-fluorohexane. **Figure adapted from Refs. [114], [116], [118] and [120] with permission.

Exchangeable deuterons. Discrimination of deuterated chiral enatiomers prepared *in situ* by ^{2}H NMR in CLCs is possible in the case of compounds bearing a labile hydrogen (OH or NH) since their isotopic labelling can be achieved by a simple exchange in presence of MeOD or D_2O **[116, 118]**. First example was reported with NH group of amides and amines of drug candidates **[27]** at room temperature) for which the labile site was in a

slow exchange regime. The case of chiral alcohols is more generally difficult. Indeed, the labile deuterons in -OD are often in the fast exchange regime, from one enantiomer to the other, preventing their visualization except by slow down the exchange by decreasing the sample temperature. Thus at 260K the ^{2}H-{^{1}H} spectrum of (±)-[*O*-^{2}H]-1-phenylethanol in PBLG show two ^{2}H-QD, one for each isomer (see **Figure 13**) **[122]**. Although the linewidth, are large in this example, a robust measurement of *ee*(%) whether by a direct integration of the signals or by using lineshape deconvolution is possible. In practice, the H-D exchange procedures can be directly made in the NMR tube containing the anisotropic phase and the analyte by adding slowly small amounts of MeOD (or D_2O). As classical samples, the liquid-crystalline phase is then centrifuged in order to both achieve the H/D exchange process and homogneize the sample.

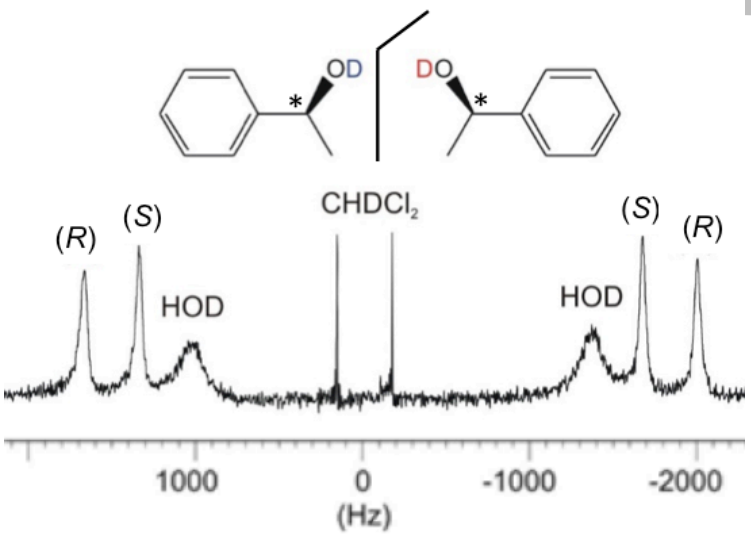

Figure 13 *Example of spectral enantiodiscrimination on (deuterated) hydroxyl group of (±)-[O-^{2}H]-1-phenylethanol in PBLG by ^{2}H-{^{1}H} NMR (61.4 MHz). Figure adapted from ref. **[121]** with permission.*

^{13}C-^{2}H correlation 2D experiments. As a consequence of the weak dispersion of $\delta(^{2}H)^{aniso}$'s (in Hz) due to the low $\gamma(^{2}H)$ value, the assignment of ^{2}H-QDs can be quickly problematic with the number of inequivalent deuterated sites. An interesting alternative consists into the acquisition of heteronuclear QUOSY experiments (CDCOM sequence (Carbon–Deuterium Correlation in Oriented Media) involving ^{2}H-^{13}C cross correlations and providing significant resolution enhancements in the direct domain (F_2) offered by the higher chemical shift dispersion of ^{13}C nuclei compared to ^{2}H **[40]**.

First successfully applied to analyse and assign ^{2}H-QDs of chiral compounds with polydeuterated alkyl chain **[40]**. For molecules with sp an sp^{2} hybridized carbon was also demonstrated the possibility to simultaneously correlate ^{2}H and ^{13}C enantiodiscrimination information both based on ^{2}H-RQC and ^{13}C-CSA differences **[123]**. This double information can be exploited with chiral and prochiral molecules as shown in **Figure 14** in the case of (±) - [1- ^{2}H]-1-octyn-3-ol and [$^{2}H_{11}$]-dibenzylmethanol, respectively.

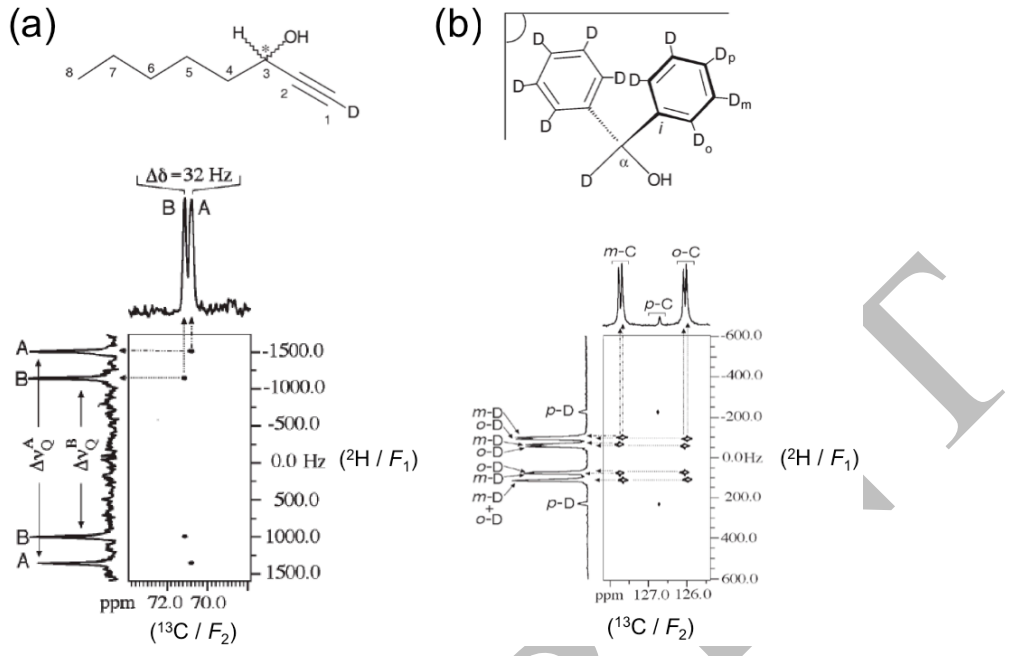

Figure 14 *Two CDCOM 2D maps recorded at 9.4 T (100.3 MHz (F_2) and 61.4 MHz (F_1)) showing the simultaneous enantiodiscrimination for both ^{13}C and ^{2}H: (a) (±)-[1-^{2}H]-1-octyn-3-ol (chiral molecule) and (b) [$^2H_{11}$]-diphenylmethanol (prochiral molecule), both recorded in the PBLG phase.* ***Figure adapted from Refs. [122] with permission.***

ANAD 2D NMR. Introduction of a deuterium probe in a target molecule without a real guarantee of success can be seen by organic chemists as a severe technical limitation of ^{2}H-NMR in CLCs applied. Ideal alternative avoiding any step of isotopic enrichment and opening this tool for a routine use, is obviously the detection of all natural monodeuterated isotopomers of a molecule. Achievement of high-field NMR spectrometers, the high quality of modern electronic or even NMR tubes as well as the possible use of cryogenic probe (not a prerequisite) made anisotropic natural abundance deuterium (ANAD) NMR an emerging tool for chiral analysis purposes, but also for other important applications (as isotope fractionation analysis or structure/configuration determination) as we will describe below.

First ANAD-{^{1}H} 1D NMR spectra of a chiral analyte recorded in PBLG phase (ternary mixture) were reported from 1998 using again (**±**)-PE as model analyte **[123]** before the development of arsenal of QUOSY 2D sequences designed to simply overcrowded ANAD spectra (see above) **[38]**. **Figure 15a** shows the NAD-{^{1}H} 1D-NMR spectrum of (±)-hept-3-yn-2-ol dissolved in PBLG/$CHCl_3$ and recorded at 14.1 T with a selective ^{2}H cryogenic probe, within 30 minutes **[42, 46]**. As seen the various position of two components of each QD as well as the overlapping peaks on the 1D spectrum makes the data analysis difficult. In contrast, the analysis *Q*-resolved-Fz 2D spectrum (after a tilting process) is direct, visualizing enantiodiscriminations (in F_1 dimension) for each inequivalent ^{2}H site (F_2 dimension) with a simple assignment of ^{2}H-QDs on the basis of their $\delta(^2H)$. Here the presence of four ^{2}H-QDs for the methylene group 6, indicating the discrimination of pair of enantio-isotopomers associated to both diastereotopic hydrogen sites of CH_2. The identification of ^{2}H-QDs for the

diastero-isotopomeric pair can be performed by recording the ANAD spectrum in the PBG achiral mesophase, thus eliminating the doubling of signal due to the enantiodiscrimination (see above).

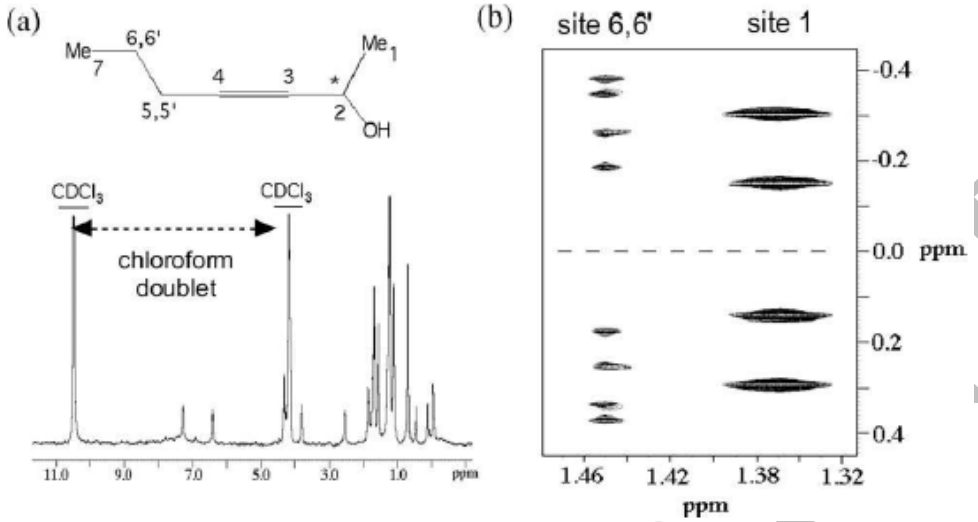

Figure 15** (a) Example of ANAD-{^{1}H} spectrum of (±)-hept-3-yn-2-ol in PBLG/$CHCl_3$. (b) Zoom on the tilted Q-resolved Fz 2D spectrum showing the discrimination on the group methyl 1 (two ^{2}H-QDs) and group methylene 6,6' (4 ^{2}H-QDs). **Figure partially adapted from Ref. [42] with permission.

Enantiopurity of small chiral blocks. One of the most major challenges in the synthesis of large-size bioactive substances as dolastatine-14 (a cyclic macromolecule with potential anticancer activities) is the control of enantiopurity of various small chiral precursors leading to the final molecular target. Similarly to ^{2}H NMR of deuterated analyte, NAD NMR in CLC is also a very adapted tool for the control *ee*'s of key chiral blocks **[124]**, and can play an important role because: i) chiral precursors have rather low MW (100-150 g/mol), ii) large amounts of analytes are available during the initial stages of a total synthesis, allowing preparation of anisotropic samples with rather large quantities, that can be even analysed using NMR spectrometers without cryogenic NMR probe.

A first illustrative example of the ANAD NMR in CLC can be found with the study of the enantioselectivity of the alkyne zipper reaction leading to hept-6-yn-2-ol from the hept-3-yn-2-ol, a possible chiral building block for preparing the dolatrienoic acid used to build the south fragment of dolastatine-14 (see **Figure 16a**) **[124]**. The analyses of the NAD signals of the methyl of precursor and those associated with one of the diastereotopic deuterons of the methylene group 3 for product, both in racemic and enantioenriched series, have established unambiguously that the reaction was a racemisation-free process (*ee* over 95%) (see **Figure 16b-e**). In another context, NAD 2D NMR in CLC was also successfully applied for controlling the enantiopurity of mono-methylated chiral fatty acids, prepared by a zinc-mediated cross-coupling, prior to be incorporated into the trehalose core preparation of an analogue of *Mycobacterium tuberculosis* tetra-*O*-acylated sulfolipid **[125]**.

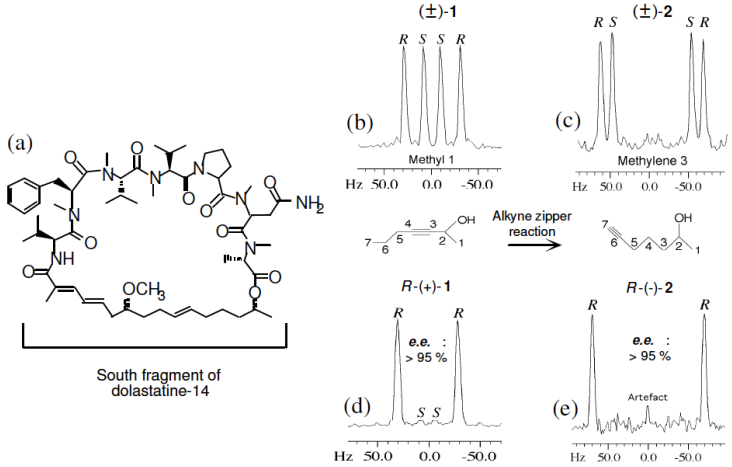

Figure 16. *(a) Structure of dolastatine-14. (b-e): 61.4 MHz NAD signals of (b and c) methyl group 1 of* ***1*** *and (d and e) one of two deuterons in methylene group 3 of* ***2*** *in racemic (top) and enriched series (bottom) in PBLG/$CHCl_3$.* ***Figure partially adapted from Refs. [124] with permission.***

From practical aspects, the detection of enantiodiscriminations on methyl groups (see also **Section 4.2**) is highly advantageous in terms of sensitivity and subsequently robustness of *ee* determination, because three equivalent monodeuterated isotopomers contribute to the ANAD signal. In case (±)-hept-6-yn-2-ol, the two methyl groups showed spectral differentiation, indicating that both sites are able to probe the chirality of the molecule despite the distance of the methyl group on the terminal alkyl chain. It can be noted, however, that this occurrence no longer exists for tridec-3-yn-2-ol recorded in PBLG/$CHCl_3$ since only the methyl group bonded to the stereogenic center shows a spectral separation. This situation illustrates the importance of position of probed ^2H site (in particular in linear flexible molecules) relative to the stereogenic center where the molecular asymmetry appears be seen as the strongest. Here the complex conformational dynamic of the methyl of the alkyl chain (8 consecutive cooperative rotors) with the averaged motion of three homotopic sites in each methyl) leads to a large molecular space explored with two effects: i) the reduction of ^2H-RQC value, ii) the absence of discrimination. This may be seen as a decorrelation effect between this methyl site and the asymmetric center, leading to a formal loss of the chirality memory at this specific site.

Apolar alkyl enantiodiscriminations. Very few routine isotropic NMR approaches are able to discriminate enantiomers of unsaturated and saturated chiral hydrocarbons. Indeed, the absence of highly reactive or polar functions generally prevents to form stable diastereisomers (derivatizing agent) or diastereomeric adducts (lanthanide shift reagent or solvating agent **[126]**. Although exotic NMR tools have been successfully applied for discriminating some specific allenics, olefinics or aromatic chiral hydrocarbons, the enantiodifferentiations observed on the basis of isotropic shifts, $\delta^{aniso}(^1H)$, does not guarantee a reliable enantiomeric purity determination. Besides enantiodiscriminations of highly flexible, apolar chiral alkyls, such as (±)-3-methylehexane (**MH**) (the simplest chiral molecule), has remained an NMR important challenge over decades.

In 2000, ANAD 2D NMR in the PBLG phase has proved to be able to discriminate enantiomer of 3-methylhexane (see **Figure 17**) and superior homologous, as 3-methylheptane or methyloctane, and a general tool

for efficiently analyzing all classes of chiral hydrocarbons: apolar (rigid and flexible) hydrocarbons, such as bicyclic and acyclic alkenes, alkanes, alkynes, aromatics, including the cases of chiral molecules with no stereogenic carbon, with large resonances **[21, 126]**. The effectiveness of this approach comes from efficient shape recognition mechanisms both involved in the orientation and enantiodiscrimination phenomena of the solute interacting with the chiral polymer. This first ^{2}H-RQC-based enantiodiscriminations observed of (±)-**MH** in PBLG was nicely confirmed recently by replacing in the polypeptide-based CLC by another helical polymer made of poly(arylacetylene) (see **Figure 17b**) where the stereogenic center is located on the side chain **[127]**.

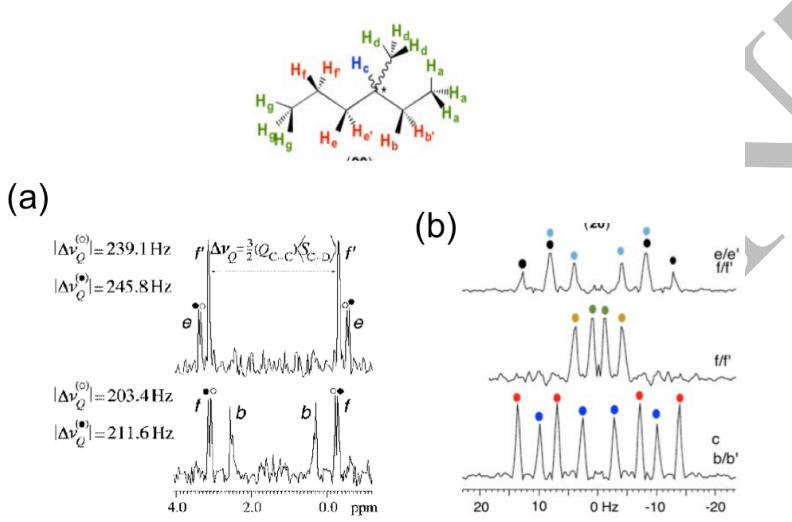

Figure 17 *^{2}H-RQC-based enantiodiscriminations observed with (±)-**MH** observed in (a) PBLG and (b) valine-derived polyacetylene (PLA) mesophases (NAD sub-spectra extracted from Q-COSY and Q-resolved Fz map, respectively.* ***Figure partially adapted from Refs. [126] and [127] with permission.***

^{2}H-X heteronuclear couplings at natural abundance. Considering their specific/particular properties, numerous chiral molecules having heteroatom as fluorine-19 in modern (medicinal) chemistry. *De facto*, when a chiral solute possesses other magnetically active heteroatoms such as fluorine-19 nuclei (natural abundance = 100%, I = 1/2), it becomes possible to detect ^{2}H-^{19}F isotopomers (1.55 10^{-2} % × 100 %), and then exploit the heteronuclear couplings, ^{2}H-X, in particular whether a ^{2}H cryogenic probe is used to boost the sensitivity. An example of analysis of coupling fine structures between ^{19}F and ^{2}H atoms at natural abundance level as well as the ^{2}H-QDs on the same ANAD QUOSY map is shown in **Figure 18a** in case of the (±)-2-(fluoromethyl)oxirane dissolved in PCBLL/DMF **[129]**. Thus, on this *Q*-COSY Fz map, recorded in around 5 hours with $m_{R\ or\ S}$ = 0.20 mmol of analyte, all deuterons coupled with the ^{19}F nucleus (methylene group 1,1') are characterized by ^{2}H-QDs which each component is dedoubled by the ^{2}H-^{19}F total coupling. This extra splitting appears parallel to the main diagonal of the map (dotted line) and allows a direct measurement of the total ^{2}H-^{19}F spin-spin couplings ($^{n}T_{DF}$ = $^{n}J_{DF}$ + 2$^{n}D_{DF}$). In this example that the two bonds (^{2}H-^{19}F)-RDCs are slightly different for each isomer whereas those between the ^{19}F nucleus and the deuteron in the stereogenic carbon atom (site 2) is null by compensation with scalar couplings ($^{3}J_{DF}$ = -2$^{3}D_{DF}$).

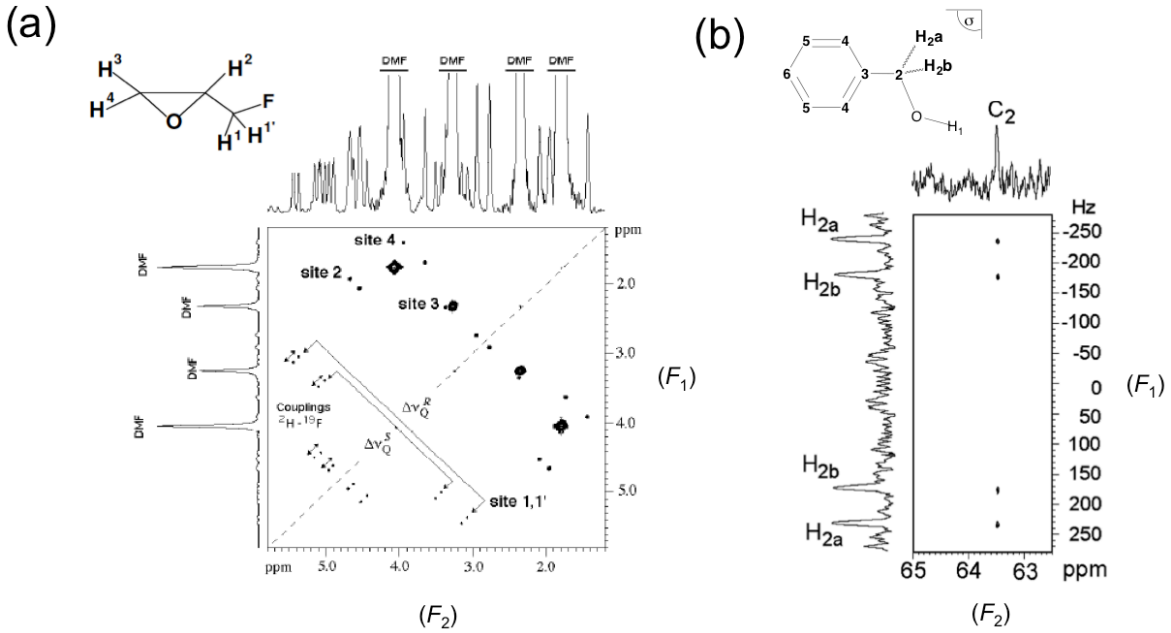

Figure 18 *(a) Two examples of ANAD QUOSY maps recorded in PBLG (Q-COSY Fz and Refocussed-NASDAC experiment) showing the detection of ^{2}H-X enantio-isotopomers where X is a fluorine-19 nucleus ((±)-2-(fluoromethyl)-oxirane) or a carbon-13 nucleus (benzyl alcohol). Note in (a) that the ^{2}H-^{19}F total couplings, T_{DF}, are slightly different for each enantiomer.* ***Figure adapted from Refs. [45] and [128] with permission.***

In the same spirit, but experimentally more difficult, it is possible to detect isotopomers containing both deuterium and carbon nuclei at their natural abundance level (1.55 10^{-2} % × 1.1 %) using NASDAC and *R*-NASDAC 2D experiments, (see above). This optimized version of the ^{2}H-^{13}C correlation 2D experiments (HECTOR type) are able to eliminate all ^{2}H-^{12}C and ^{1}H-^{13}C isotopomers, and so detected 1 molecule over about 600 000) **[45]**. A first example was reported in the case of isotopomer ^{2}H-^{13}C of a small prochiral molecule, the benzyl alcohol in PBLG. In **Figure 18b** is shown the differentiation of two ^{2}H-^{13}C enantio-isotopomers associated to the methylene group of benzyl alcohol. Finally, the comparison of the F_2 projection of anisotropic NASDAC 2D spectra and 1D ^{13}C-{^{1}H} 1D spectra allows to determine the ^{2}H to ^{13}C isotopic effect on $\delta(^{13}C)$, without deuteration of the analyte.

4.4 | Probing "Atypical chirality"

Chiral discrimination in CLCs is not limited to one type of chirality, such as compounds bearing four distinct substituents around an asymmetric atomic centre as carbon, sulphur or phosphorus atoms (see above), including the case of chirality by virtue of the isotopic (H/D, H/T, D/T, H/D/T) substitution. Indeed, the concept of chirality is larger and covers many kinds of enantiomorphisms without stereogenic center. Thus, atropoisomerism as well as the axial, planar or helical chirality are other important form of chirality, that could be defined as "atypical" or "exotic", even if the condition of nonsuperposability of their enantiomers remains true **[5]**.

Thus, first examples of enantioseparations of exotic chirality in polypeptide phases have been observed by ^{2}H-{^{1}H} NMR with monodeuterated chiral allenics that exhibits axial chirality of C_1 symmetry **[129]**. In this

case, two ^{2}H-QDs were detected (see **Figure 19a**). The spectral differentiation of enantiomers (*Λ* and *Δ*) of deuterated metallic complexes that are chiral by virtue of helical chirality has been reported in PBLG (see **Figure 19b) [130, 131]**.

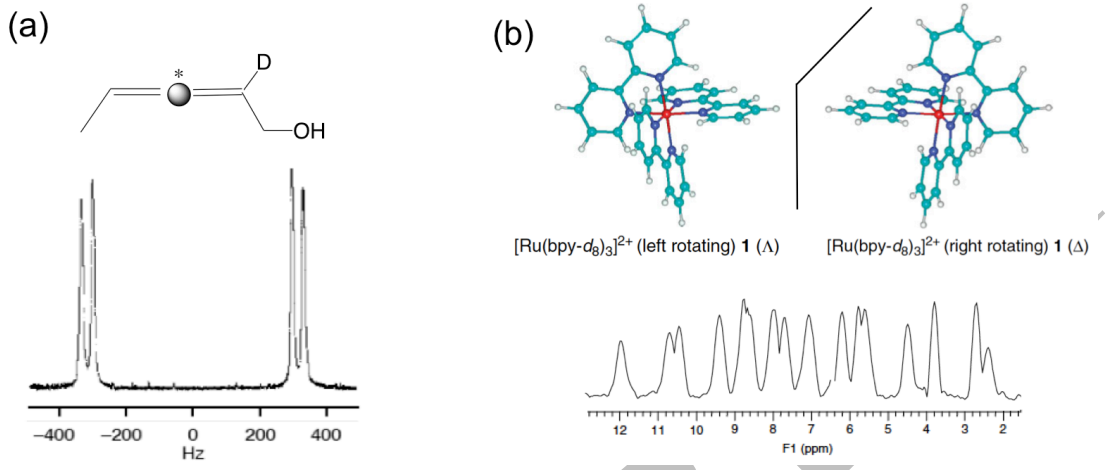

Figure 19 *Two examples of enantiodiscrimination involving "atypical chirality" revealed by ^{2}H-{^{1}H} NMR (61.4 and 46.0 MHz), on isotopically enriched molecules: (a) the (R/S)-2-deutero-2,3-pentadiene-1-ol, (b) the (Λ/Δ)-perdeuterated tris(diimine)ruthenium(II) complexe. The spectrum (b) corresponds to the F_1 projection of a Q-COSY 2D map. Both analytes are dissolved in a PBLG phase.* ***Figure adapted from Refs. [129] and [130] with permission.***

Another interesting examples of "exotic" chirality can be found with the family of cone-shaped (rigid) chiral compounds (cyclotriveratrylene or CTV) that also exhibit an axial chirality but of C_3 symmetry. In case of enantiomers of (±)-nonamethoxy-CTV (see **Figure 20a**), discriminations were obtained by ^{2}H-{^{1}H} NMR both on the diastereotopic sites of three homotopic methylene groups (hexadeuterated solute) (see **Figure 20b**) as well as on the three homotopic methyl groups (1, 2, 3) using NAD 2D NMR in PBLG at 14.1 T (see **Figure 20c**). Although nine deuterium sites contribute to the ANAD signal for each inequivalent methyl and each enantiomer,

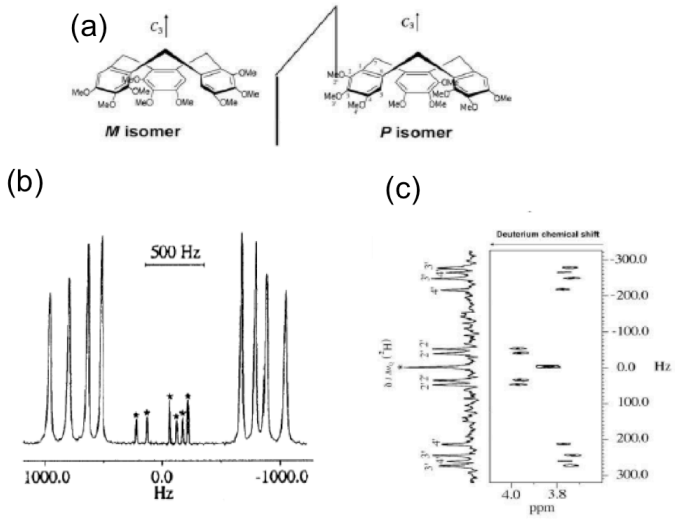

Figure 20 *^{2}H enantiodiscrimination of (±)-nonamethoxy-CTV observed on: (a) the dideuterated methylene goups located in the cone, (b) the methyl of methoxy- groups (tilted NAD Q-resolved Fz map), both recorded in PBLG/DMF (320 K).* ***Figure adapted from Ref. [132] with permission.***

this last result is remarkable considering the MW of the analyte. The smallest ^{2}H-differentiation observed on the methyl groups compared to the methylene junctions, originates mainly from an averaging effect due to their double rotation of hydrogen (deuterium) site (C-O and O-CH_3) and their positions located at periphery of the molecular cone.

Finally, the enantiorecognition phenomenon in case of "exotic chirality" was not only observed by ^{2}H-{^{1}H} or NAD -{^{1}H} NMR on the basis of ^{2}H-RQC differences, but also revealed by ^{13}C-{^{1}H} NMR on the basis of ^{13}C-RCSA differences (recorded at 9.4 T) as in the case of atroposiomers **[20, 21, 28]**. Thus, it has been demonstrated that enantiomers of chiral *ortho*-trisubstituted biphenyls (see **Figure 21a**), as well as binaphthyls (the 2,2-di-hydroxy-1,1-binaphthyl and 2,2-dimethyl-1,1-binaphthyl) (see **Figures 21b, 21c**). As seen enantiodifferences up to values of 17 Hz have been discrimination, but only affects its magnitude experimentally measured, allowing an easy measurement of possible *ee*. The intercomparison of the two last examples are interesting and shows the role of the hydroxyl group in the discrimination mechanisms, and finally on the magnitude to the spectral difference. Thus, it appears here that the replacement of a polar functional group (such as OH) by a nonpolar one (CH_3) does not avoid the mechanisms of enantodiscrimination.

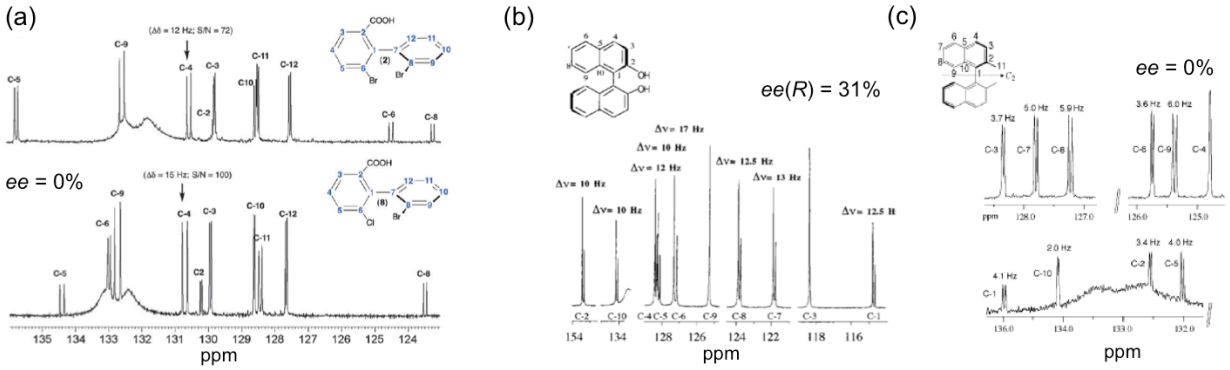

Figure 21 *Four examples of atypical chirality (atropoisomerism) revealed by ^{13}C-{^{1}H} NMR (100.3 MHz) in the PBLG mesophase.* ***Figure adapted from Refs. [20], [21] and [28] with permission.***

4.5 | Cryptochirality

In the world of stereochemistry, the concept of "cryptochirality" (meaning "hidden chirality") was introduced to define molecules which are chiral but do not have measurable optical rotation in the ordinarily accessible UV/Visible spectral range (800 ± 200 nm), even in neat form. The idea of cryptochiral compounds, better called as crypto-optically active compounds, was first introduced by Mislow and Bickart **[133]**. *De facto*, the determination of the absolute configuration of these cryptochiral compounds remains analytically extremely challenging. A typical example is found with the 5-ethyl-5-propylundecane (termed trivially as (*n*-butyl)ethyl(*n*-hexyl)(*n*-propyl)methane), a chiral saturated hydrocarbon with a central, stereogenic quaternary carbon atom and bearing similar substituents. Neither enantiomeric form has any observable optical rotation, as demonstrated by

Wynberg *et al.* some 35 years ago **[134]**. The underlying reason for the lack of optical rotation is the lack of heteroatom(s), π-electrons, or chromophores, as well as the very small difference between the four substituents on the asymmetric carbon atom or the specific electronic properties (mass distribution) of the chiral molecule **[135]**.

Excluding carbon isotopologues, the "smallest" cryptochiral compound possessing an all-carbon quaternary stereogenic center is the appropriately deuterated neopentane ($^2H_6$-**NP**): $C(CH_3)(CH_2D),(CHD_2)(CD_3)$ **[132, 136]**. It is the prototype of a crypto-optically active molecule that owes its chirality exclusively to an asymmetric distribution of the masses of the nuclei, whilst having virtually the same electron distribution as all-^{1}H-neopentane. As a matter of fact, within the commonly envoked Born-Oppenheimer (BO) approximation, $^2H_6$-**1** is electronically *achiral* and computations of its optical rotation would return a zero value **[137]**. The experimental assignment of the absolute configurations of the enantiomers of $^2H_6$-**NP** therefore poses a formidable challenge but was accomplished through matching of the experimentally determined Raman Optical Activity (ROA) spectra and Vibrational Circular Dichroism (VCD) with density functional theory (DFT) computations **[136, 137]**. From the NMR point of view, it should be noticed that the ^{2}H-{^{1}H} NMR in PBLG phase failed to discriminate the enantiomers $^2H_6$-**NP**, while: i) this tool allowed the determination of the *e.r.* of its deuterated ω-ene cyclopropanic precursor (axial chirality) (see **Figure 22a**), ii) the isotropic ^{2}H-{^{1}H} NMR confirmed the structure of $^2H_6$-**NP** (see **Figure 22b**) **[136]**. Clearly in the case of $^2H_6$-**NP**, the overall shape recognition mechanisms are of PBLG was insufficient to differentiate the extremely small topological differences between the mono-, di-, and trideuterated asymmetric methyl groups around the central, stereogenic carbon atom.

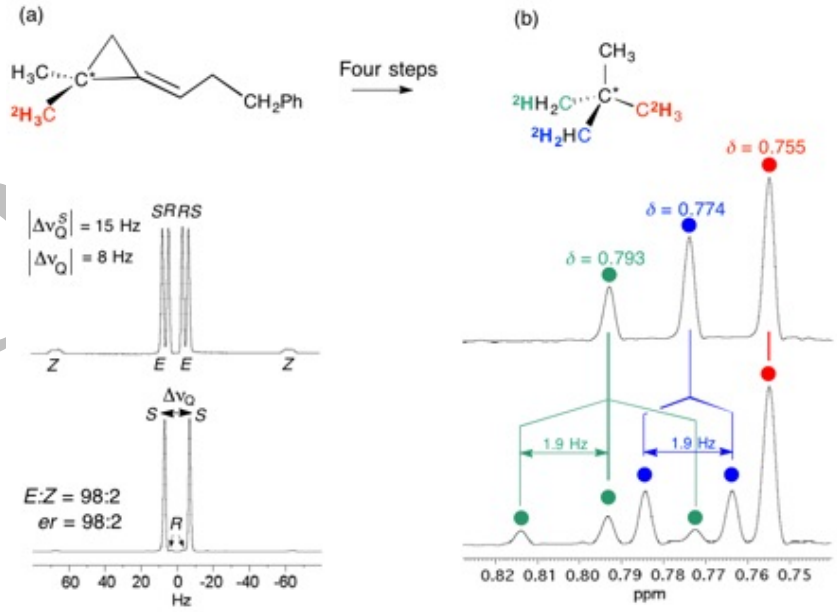

Figure 22 *(a) Determination of the enantiomeric ratio (e.r.) of cyclopropanic precursor of $^2H_6$-**NP** by ^{2}H-{^{1}H} NMR (14 T / cryogenic probe) in PBLG (upper panel: racemic series; lower panel: enantiomerically-enriched series). (b) ^{2}H assignment (δ and J) of $^2H_6$-NP recorded in pyridine. Note that the scalar coupling patterns associated with CDH_2 and CD_2H groups when ^{1}H decoupling is off (lower panel).* ***Figure adapted from Ref. [136] with permission.***

V. PROCHIRALITY AND ENANTIOTOPY

5.1 | Molecular objects of C_S, C_{2V}, D_{2d}, S_4 symmetry

Prochirality and enantiotopicity are two important concepts in chemistry and stereochemistry **[5]**. Simply defined, prochiral molecules are chemical substances that can be converted to chiral structures by a single chemical transformation **[51]**. Prochiral molecules possess enantiotopic elements (nuclei, groups of nuclei or internuclear directions) whose the corresponding stereodescriptors, pro-*R* and pro-*S*, are used to distinguish between them, according to the idea that promoting the pro-*R* element to higher priority than the pro-*S* element results in an *R* enantiomer, and *vice versa* **[5]**. The simplest case of enantiotopic elements is found with a pair of hydrogen atoms (in methylene groups) bonded to a prostereogenic atomic center and are exchangeable by a plane of symmetry (σ). This occurence can be observed on rigid prochiral structure of C_s-symmetry or molecule of C_s-symmetry in average in agreement of the Altmann's definition, as in case of diiodoferrocene (see below) **[138]**.

First experimental enantiotopic discriminations in polypeptide CLCs have been evidenced in 1994 by using ^{2}H-{^{1}H} NMR on C_s-symmetry deuterated analytes **[116]**. These first results have demonstrated that differentiation of (^{2}H/^{1}H) isotopic enantiomers of C_1-symmetry was a direct consequence of the differentiation of enantiotopic elements in the parent deuterated prochiral molecules of C_s-symmetry (see **Figure 1**). A practical consequence of this dependence is the possiblity to establish if enantiotopic directions in a prochiral molecule are discriminated or not by detecting the pair of monodeuterated enantio-isotopomers associated to the enantiotopic sites and check if their ANAD signal is discriminated or not **[139]**.

In 1998, the quantitative description (using anisotropic data) of the facial discrimination of ethanol in PBLG revealed that five order parameters are requested to describe correctly the orientational behavior of this C_S-symmetry prochiral molecule interacting with a chiral oriented environment, while only three parameters are needed in a non-chiral LC **[140]**. In fact, using group theory, it can be demonstrated that for rigid prochiral molecules, the spectral discrimination of enantotiopic elements in CLCs originates from the reduction of the effective molecular symmetry of solute when interacting with a chiral environment **[140]**. This effective symmetry reduction (as far as orientation is concerned) affects only four molecular improper point groups, namely the symmetries C_s, C_{2v}, S_4 and D_{2d}. The effect on this reduction (from ALCs to CLCs) on change of the effective molecular point group and the number of (non-zero) order parameters of the Saupe matrix are reported in **Table 1**. The change of effective molecular point group affects also the position and orientation of the principal axes system (PAS) of the Saupe ordering matrix, ongoing from achiral to chiral LC. Such changes are illustrated schematically in **Figure 23** for the four allowed symmetry groups.

While many prochiral molecules of C_s and C_{2v} symmetry exist and can be studied using ^{2}H NMR on isotopically normal or enriched material **[140, 141, 142]**, finding prochiral rigid compounds of D_{2d} and S_4 symmetries is more difficulty because these structures are rather scarce in nature but also in synthetic chemistry. Interestingly, ANAD 2D-NMR in PBLG has allowed the spectral discriminate the monodeuterated enantio-isotopomers of spiropentane (D_{2d}) **[5]** and two examples of S_4 structures, the 1,3,5,7-

tetramethylcyclooctatetraene (**TMCOT**) which exhibit no dynamic effect at RT and the icosane **[143]**. The enantio-isotopomeric discriminations observed demonstrate in turn the possibility to discriminate enantiotopic directions in the parent rigid prochiral compound with D_{2d} and S_4 symmetries, respectively.

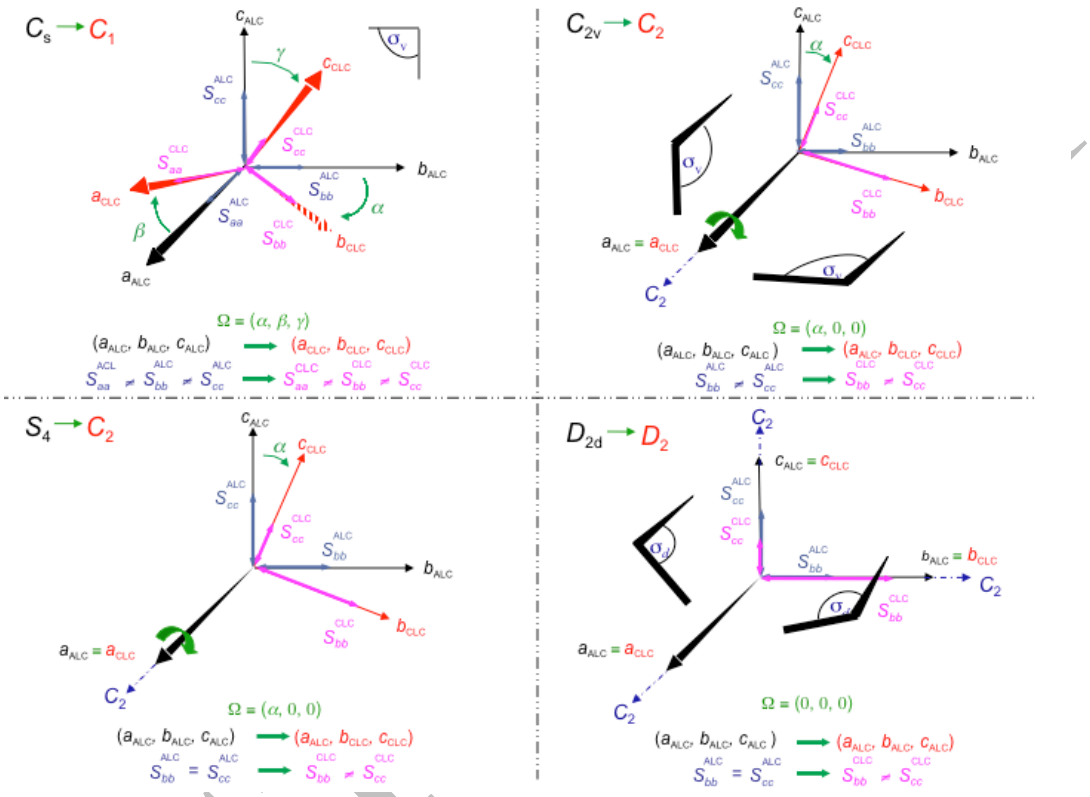

Figure 23. *Schematic representation of changes expected in the orientation and equivalence of the principal axes system (PAS) of the Saupe ordering tensor in the four allowed groups, ongoing from achiral to chiral LC. The variation of the length of the double arrows represents the change in the magnitude of the S_{ii}.* ***Figure from Ref. [5] with permission.***

Figure 24 presents four examples of the discrimination of enantio-isotopomers in a CLC using NAD NMR. All these experimental outcomes validated definitely the theoretical work showing that only the C_s, C_{2v}, S_4 and D_{2d} molecular structures undergo a reduction of their effective symmetry in a CLC, thus leading to the differenciation of their enantiopic elements. As a last illustrating example, we can mention the interesting case of 1,2-diiodoferrocene, a C_s-symmetry prochiral molecule in average (see **Figure 25**). Actually this molecule possesses both enantiotopic C-H directions (not bonded on the same carbon atom) as well as homotopic direction due to the fast rotation of the cyclopentadienyl ring around the axis joining its center and the Fe atom. As in case of ethanol, the enantiotopic C-H directions are expected to be oriented differently in average in a CLC, and so be spectrally discriminated. Experimentaly, this enantiodiscrimination has been clearly observed, as expected, by ANAD NMR in PBLG **[142]**. Note that this enantiotopic discrimination phenomenon in prochiral molecules have been also detected with other chiral oriented systems than those made of polypeptide. Thus we can mention, for instance, the case of oriented systems made polyacetylene **[128]** or polysaccharide gels **[143]**.

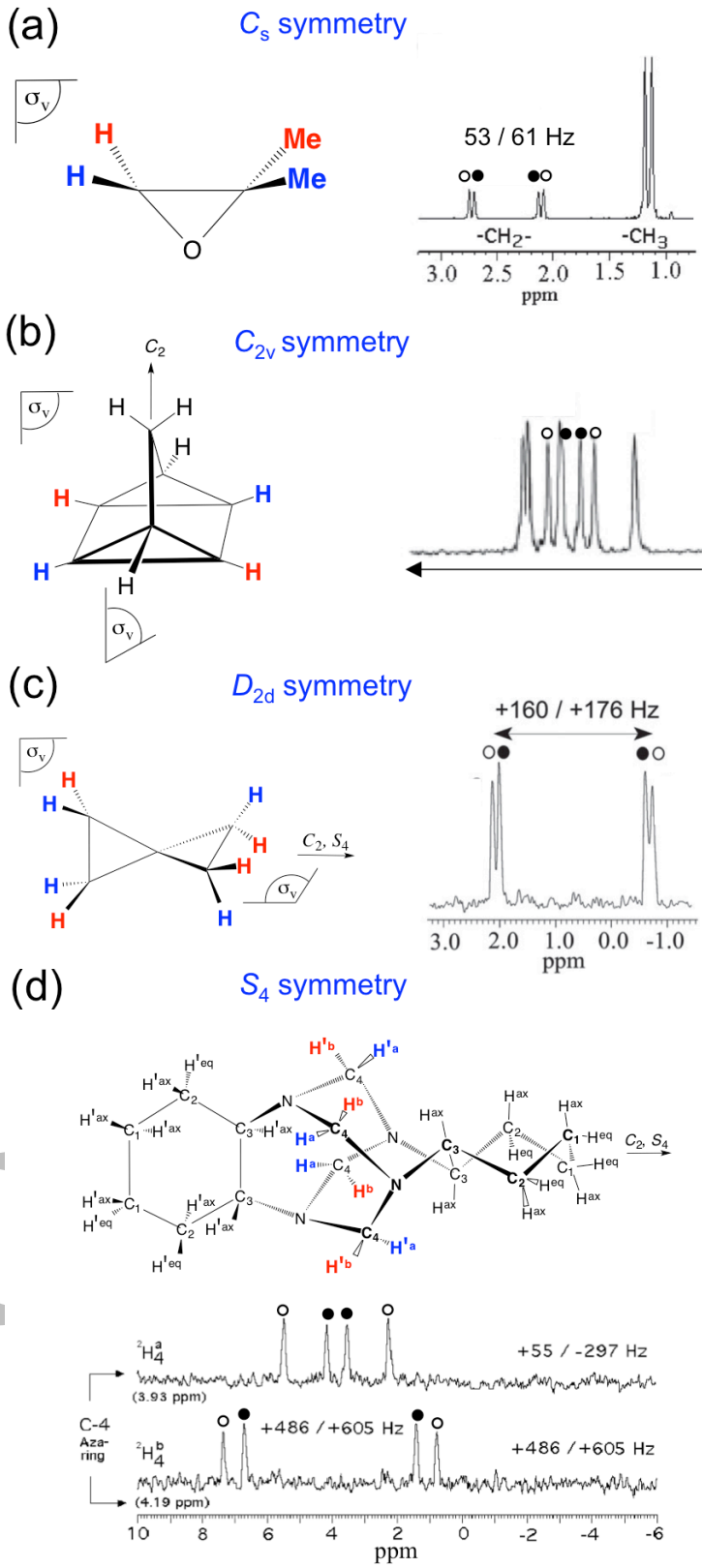

Figure 24 *Four typical examples of C_s, C_{2v}, D_{2d} and S_4 molecules possessing enantiotopic sites (red/blue) and their associated NAD-{^{1}H} enantiodiscriminated signal: (a) 1,1'-dimethyloxyrane (C_s), (b) quadricyclane (C_{2v}), (c) spiropentane (D_{2d}), (d) icosane (S_4). In each structure, the pairs of enantiotopic sites are shown with a red or blue color. In spectra, enantiopic signals are marked by an open or filled circle.* ***Figure from Refs. [5]*** *and* ***[144] with permission.***

Associated to the key concept of chemical desymmetrization of a prochiral molecule, it could imagine to establish a parallel between the enantiodiscrimination phenomena occuring in a prochiral solutes interacting with polypeptide fibers of polymeric CLC and the chemical desymmetrization of those same prochiral molecules to produce chiral entities with the help of homochiral ligands. Indeed the role of the polypeptide and the chiral ligand is rather similar in regard to the face recognition phenomenon. The final aim would be to find an empirical correlation between both phenomena (*ee versus* magnitude of enantiotopic discrimination) in order to possibly predict, from NMR measurements, the *ee* that could be obtained by desymmetrizing prochiral substrates **[141]**.

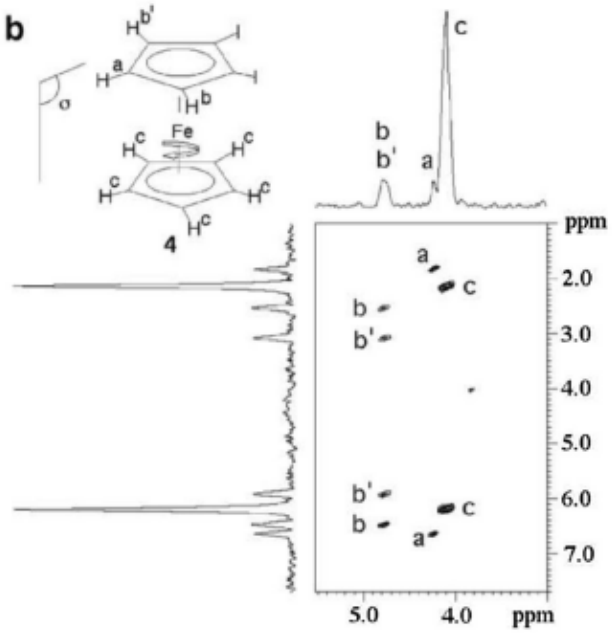

Figure 25 *Tilted Q-COSY Fz 2D spectrum of 1,2-diiodide ferrocene (C_s symmetry in average) recorded in PBLG and where enantiotopic sites (noted b and b') are spectrally discriminated. Figure adapted from Ref.* ***[142]*** *with permission.*

5.2 | Intriguing aspects of stereogenicity: the case of malononitrile

Malononitrile (**MLN**) is a typical example of rigid C_{2v}-symmetry compounds without any prostereogenic tetrahedral center (see **Figure 26a**). Strictly speaking, this particular molecular structure can be seen as non-prochiral, because it may be superimposed upon itselves by an overall rotation, thus producing a structure that is indistinguishable from the original. For chemists, this molecule could be defined as pro-prochiral, because a priori two steps would be need to convert **MLN** into a chiral structure. From NMR viewpoint, the two ^{1}H nuclei and two ^{13}C nuclei (in nitrile group) are isochronous.

From a stereochemical point of view, the one-bond ^{13}C-^{1}H directions in **MLN** are defined as homotopic and so cannot be differentiated even using a CLC. However, in this structure, the long-range $^{13}C^{\cdots\cdots}{}^{1}H$ (nonbonded) internuclear directions are enantiotopic, and so expected to be spectrally distinguished in a CLC. Theoretically, an AXY spin system (A = ^{13}C of nitrile group and X/Y = ^{1}H) is expected, but experimentally, a typical second-order spectral pattern (AXX' spin system with X/X' = ^{1}H and $\delta(X) \approx \delta(X')$) is observed for ^{13}C signals (C-2/C-3) of

nitrile group in the PBLG chiral phase. This pattern disappears in the PBG-based ALC as displayed in **Figure 26b [139]**. The transformation of the RAS (a, b, c) into the PAS (a', b', c') can be viewed as a simple rotation around the b axis with a tilting angle, α, of +14° between the initial and final planes (see **Figure 26a**).

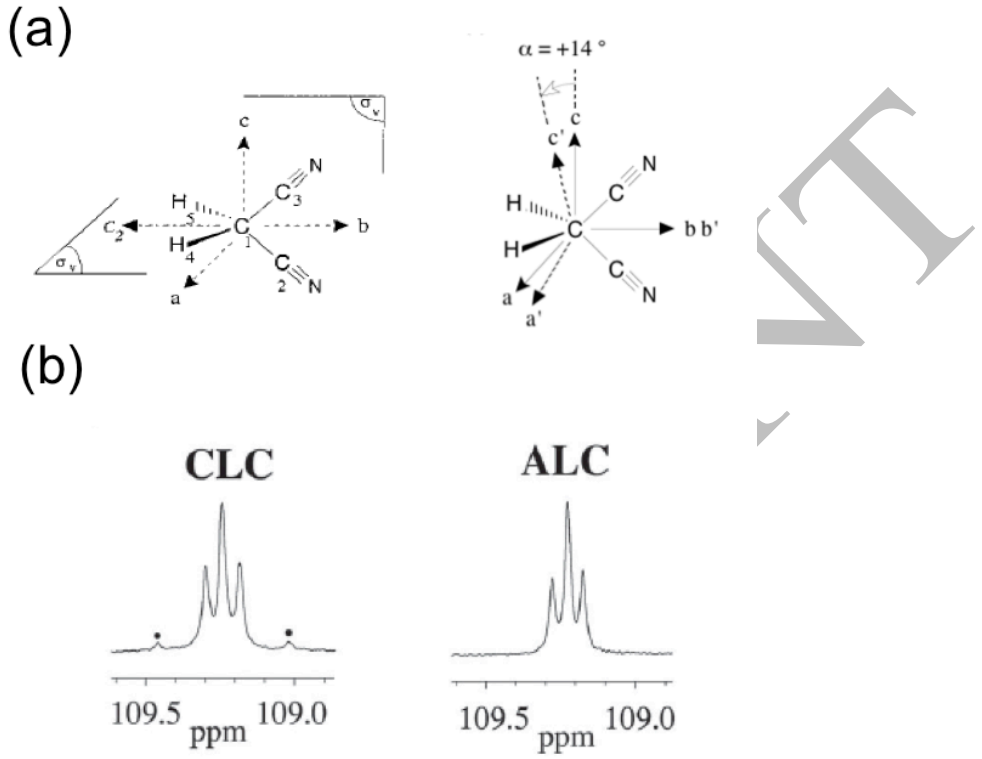

Figure 26 *(a) Structure of malononitrile and representation of the b'c' and a'b' planes relative to the initial bc and ab planes seen from the b axis. (b) 100.3 MHz ^{1}H-coupled ^{13}C NMR signal of the nitrile groups in PBLG/$CHCl_3$ (CLC) and PBG/$CHCl_3$ (ALC). Note the disappearing of external small peaks in the ALC.* ***Figure adapted from Ref. [139] with permission.***

From this experimental result, a more fundamental stereochemical issue about the definition of the concept of prochirality and enantiomorphism is raised here. Indeed, **MLN** can be regarded as a prochiral compound when interacting with the CLC, while for organic chemists (who generally define prochirality in terms of the practical possibility that an achiral molecule becomes chiral in the course of a single-step chemioselective chiral process), this molecule is not! Amazingly, the spectral differentiation in a CLC of enantiotopic directions in **MLN**, a C_{2v} symmetry molecule without a prostereogenic tetrahedral center has validated a stereochemical hypothesis made by Mislow and Raban in 1967 **[145]**. Indeed it had been speculated that "for molecules of the type "CXXYY"…, the two X groups as well as the Y groups are equivalent and cannot be distinguished in chiral or achiral circumstances. However, the relationships between X and Y groups are not all equivalent. The four X-Y relationships may be ordered into two enantiotopic sets of two equivalent relationships" The NMR result obtained with **MLN** validate also a more recent concept of stereogenicity defined by Fujita in 1990 who considers that "the compounds (CX_2Y_2) can be regarded as prochirals, since the four edges (X-Y) construct an enantiospheric $C_{2v}(C_1)$ orbit" **[146, 147, 148]**.

VI. (^{2}H/^{1}H) ISOTOPIC FRACTIONATION IN PROCHIRAL COMPOUNDS

6.1 | Analysis of Fatty acids and derivatives

Investigation of $(^2H/^1H)_i$ isotopic fractionation by isotropic ^{2}H-{^{1}H} 1D-NMR, namely the measurment of the intramolecular non-statistical site-specific distribution of deuterium and its analytical applications have been extensively explored and developped by Martin et and co-wokers from 1981 **[149]**. This tool, best known as SNIF-NMR® tool (site-specific natural isotopic fractionation), has proved to be an invaluable NMR approach for investigating the natural isotope ^{2}H profile in biosynthesized compounds of interest such as ethanol, fatty acids, vanilline or limonene for instance **[150]**.

In practice, the value of site-specific $(^2H/^1H)_i$ isotope ratios (expressed in ppm) measured by NMR under quantitative conditions ($T_R = 5 \times T_1$) is different from one hydrogenated site to another, and can be compared to the "Vienna Standard Means Ocean Water" (V-SMOW) value ($1.55\ 10^{-2}$%). This molecular isotopic information provides crucial data to understand the enzymatic processes/pathway leading to a given biomolecule (kinetic isotopic effects (KIEs) associated, source of hydrogen, ...) **[151, 152]**. It can be also exploited to identify the geographical origin and/or botanical source of analyte, and hence to fight against counterfeiting and adulteration of substances sold as "natural" (authenticity/traceability investigations).

Despite many practical applications, this approach has two drawbacks: i) it is not able to measure the $(^2H/^1H)_i$ isotopic ratios of enantiotopic sites in CH_2 groups of prochiral molecules due to the absence of external chiral stimuli, ii) its efficiency is basically limited by the small dispersion of $\delta(^2H)$'s expressed in Hz ($\gamma(^2H) = \gamma(^1H)/6.515$). In this context, quantitative ANAD NMR in CLC provides fruitful alternative enable to discriminate between enantio- or diastereo- isotopomers nuclei by exploiting the spectral distribution of ^{2}H-RQCs **[153]**.

First successful applications of this approach were experimentally pioneered in 2004 with the analysis of 1,1'-*bis*(phenylthio)hexane (**BPTH**), a fragment of the methyl linoleate (**ML**), a prochiral fatty acid methyl ester (FAMEs) defined as an essential unsaturated fatty acid (UFA) (see **Figure 27**). Indeed, the analysis of ANAD-{^{1}H} 2D spectrum of **BPTH** (recorded at 61.4 MHz) revealed the difference of intramolecular isotope ratios of enantiotopic hydrogen sites in each CH_2 groups with a proportion of (*R*)- enantio-isotopomers were higher than those of the (*S*)-enantio-isotopomers **[154, 155]**. Taking advantage of NMR spectrometers operating at higher field (92.1 MHz for ^{2}H) and equipped with a selective ^{2}H cryogenic probe, the method was then easily extended to study more complex prochiral FAMEs with longer chains, such as C-18 mono- or poly-unsaturated FAMEs as well as conjugated, unsaturated FAMEs (CUFAs), such as methyl oleate (**MO**), methyl linolenate (**MLn**), methyl vernoleate (**MV**), methyl eleostearate (**ME**), methyl punicate (**MP**) (see **Figure 27) [74, 156, 157]** and finally it also been tested on saturated fatty acids (SFA) **[75].**

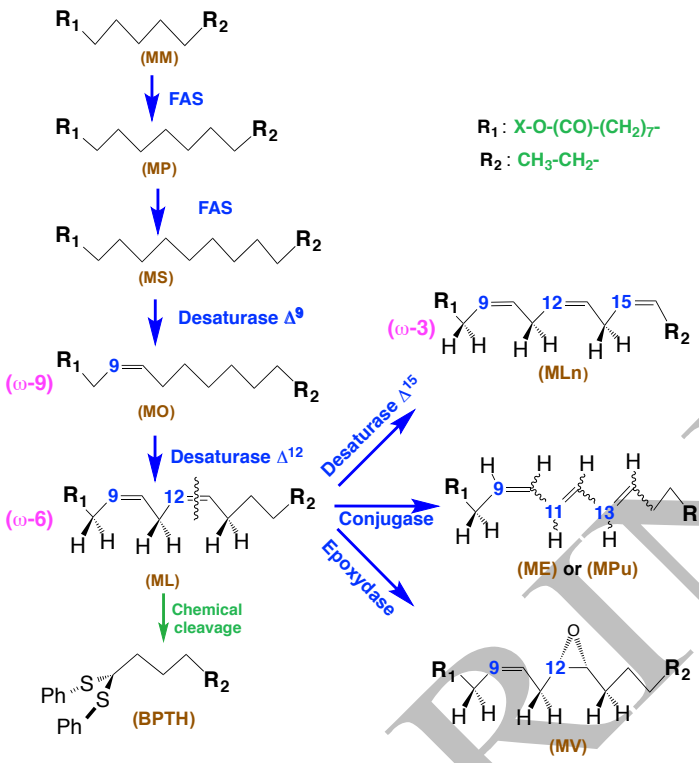

Figure 27 *Successive biotransformations of methyl myristate (MM) into longer SFAs (palmitate (MP) and stereate (MS)), then leading to various UFAs, (9Z)-MO, (9Z, 12Z)-ML, (9Z, 12Z, 15Z)-MLn, (9Z, 12R, 13S)-MV or two CUFAs, (9Z, 11E, 13E)-ME and (9Z, 11E, 13Z)-MPu (X is a methyl group). Except* ***MV****, the other FAMEs are prochiral of molecules* C_s*-symmetry.* ***Figure from ref. [154] with permission****.*

Actually, all the potential of the method was nicely illustrated in the case of ML oriented in the PBLG/pyridine phase in (see **Figure 28a**), because all inequivalent mono-deuterated enantio-isotopomers are spectrally detected in a single experiment, whereas isotropic ^{2}H 1D-NMR spectra resolve only 30% of inequivalent ^{2}H sites. As a new molecular isotopic information related to the discrimination of all (*R*/*S*)-enantio-isotopomers, it is possible to determine the bio enantio-isotopomeric excess, (*eie*) *(%)* for each CH_2 group, according to the equation **[157]**.

$$eie(\%) = \frac{\left|\left(^2\mathrm{H}/^1\mathrm{H}\right)_i^R - \left(^2\mathrm{H}/^1\mathrm{H}\right)_i^S\right|}{\left(^2\mathrm{H}/^1\mathrm{H}\right)_i^R + \left(^2\mathrm{H}/^1\mathrm{H}\right)_i^S} \times 100 \qquad (9)$$

From the *eie* values, it has been evidenced that at the odd-numbered CH_2 positions are larger than those measured at even-numbered CH_2 groups all along the chain (see **Figure 28b**). This observation was explained by the different incorporation mechanisms of hydrogens into the chain during the elongation of fatty acids via the fatty acid synthetase (FAS) enzyme **[158]**.

Interestingly, using chiral FAMES (as **MV**), the discrimination of diastereotopic positions in methylene groups allows the determination of the diastero-isotopomeric excesses, (DIEs) for each CH_2 group of the chiral molecule. Access to *eie* and *die* to key hydrogenated sites have enabled to answer two specific biochemical questions never solved previously: i) the stereoselectivity during the elongation (by FAS) and the desaturation

steps (by the Δ^9 and Δ^{12} desaturase) leading to the biosynthesis of the **ML** in *Fusarium Lateritium*, (a fungus species) **[158]**, ii) the possible difference of enzymatic bioconversion processes of **ML** to **MV** involved in the case *Euphorbia lagascae* and *Vernonia galamensis*, plants **[159]**.

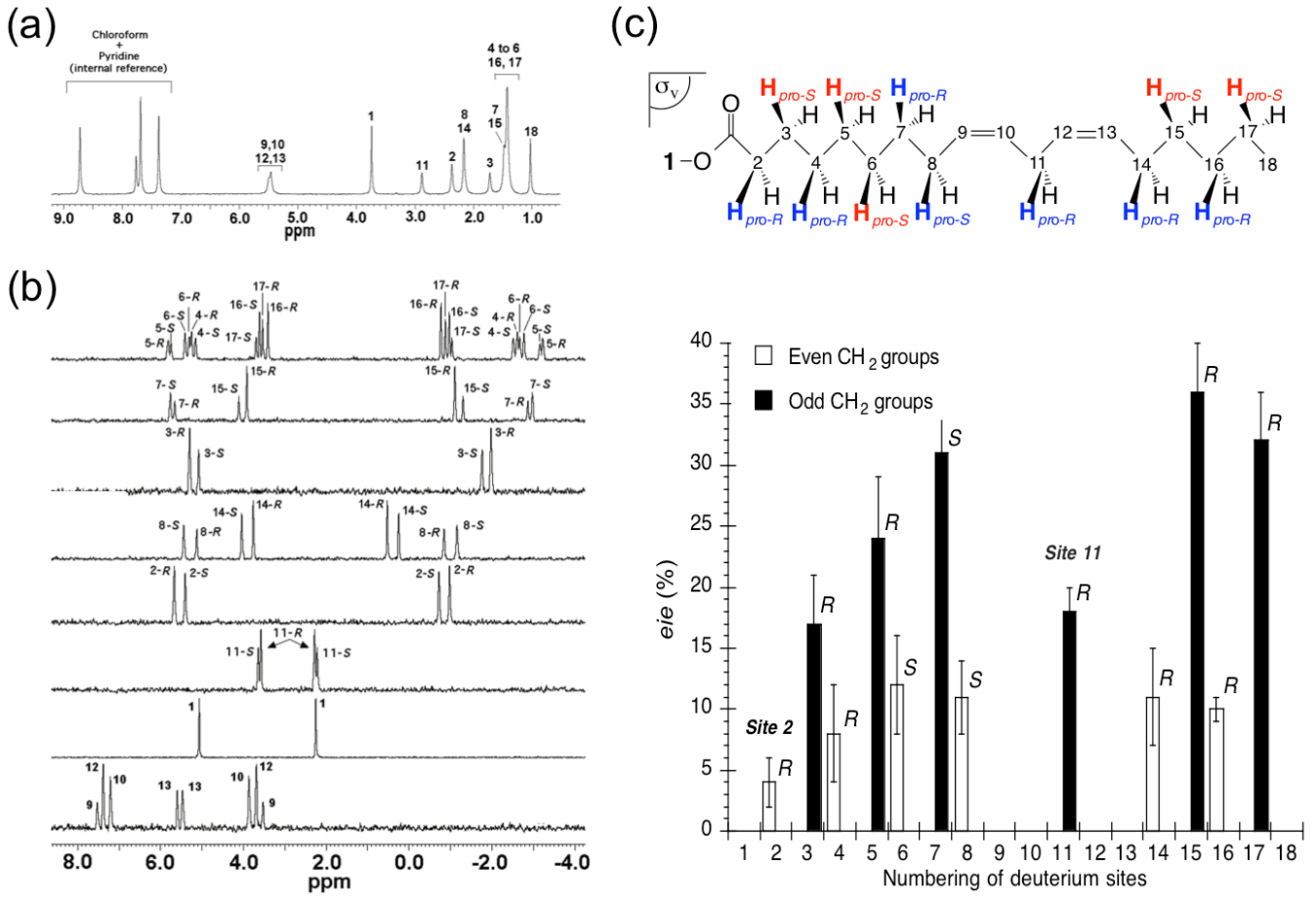

Figure 28 *(a) Isotropic ^2H 1D spectrum of methyl linoleate. (b) Series of NAD 1D sub-spectra of* ***ML*** *in PBLG/pyridine extracted from the anisotropic ^2H tilted Q-COSY Fz map. The ^2H-QD of methyl 18 is not shown. (c) Variation of eie(%) vs. the methylene groups.* ***Figure adapted from ref. [157] with permission.***

6.2 | The complex case of homogeneous triglycerides

In cells, FAs are actually stocked under the form of (homogenous or not) triglycerides (TGs) with various lengths and nature of flexible chain (C4 to C36), thus corresponding to the most complex class of lipids.

From a more stereochemical viewpoint, TGs defined as homogenous (three identical chains) are fantastic prochiral molecular structures containing both homotopic, enantiotopic and diastereotopic elements (atomic sites, groups or chains) **[160]**. In **Figure 29a** is detailed the various stereochemical relationships relationships of tributyrin (**TB**), a short-chain (4 carbon atoms) TG. In accordance with Altmann's definition **[138]**, homogeneous TGs are flexible molecules of C_s symmetry on average, containing: i) a plane of symmetry σ associated with two enantiotopic side chains for which hydrogen atoms in a given methylene group are diastereotopic, ii) a central chain (that is diastereotopic relative to the two side chains) but where hydrogen atoms in a given methylene

group are enantiotopic. Interesting diastereo- and enantiodisciminations was therefore expected when using ANAD NMR CLC, in comparison with NAD 1D NMR in achiral isotropic medium that only exhibits seven resonances corresponding to all the diastereotopic sites of the molecule (50% of the molecule's inequivalent ^{2}H sites).

Amazingly, the analysis of all ANAD 1D subspectra extracted from the *Q*-COSY Fz map of **TB** recorded in PBLG/Py indicates that 95% of the unequivalent ^{2}H sites (*i.e.* 19 ^{2}H-QDs out of 20) are spectrally discriminated (see **Figure 29c**). In other words, chiral ANAD NMR was able to discriminate between the two lateral enantiotopic chains, a and c, chains as well as the enantiotopic C-H directions in the central chain b, while the number of differentiated sites agrees with the theoretical number expected for a C_s-symmetry molecule. In this example, the enantio/diastereorecognition mechanisms were able to separate isotopomers. Such an ideal situation was however not meet for trimyristate (**TM**), another homogenous TG with longer chain (C-14), since

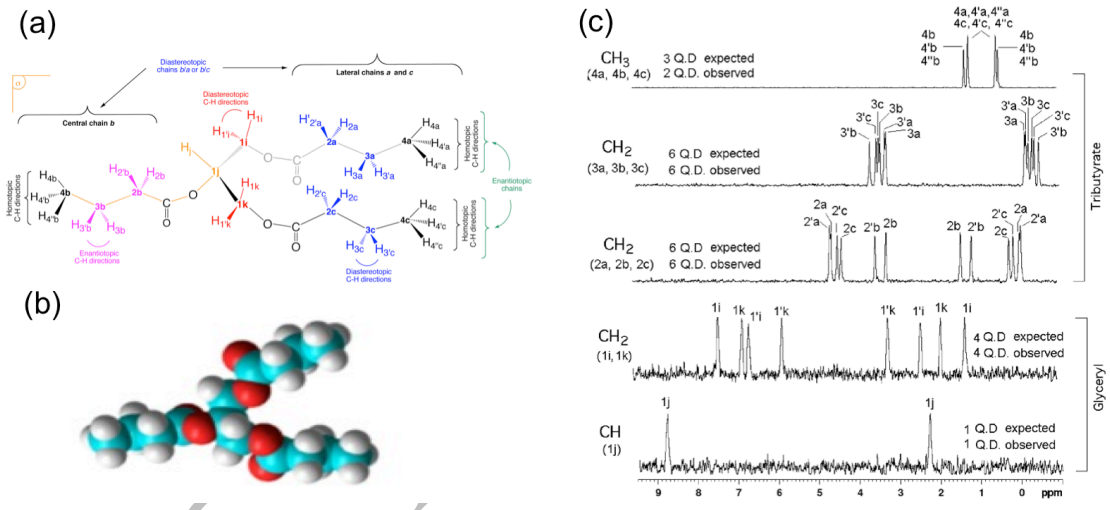

Figure 29 *Atomic numbering of TB along with the stereochemical relationships between the different hydrogenated sites of the glyceryl part (sites i, j, k) and methylene (2 and 3) and methyl (4) groups of the three acyl chains (a, b and c) of TB. (b) Computed 3D structure of the "all-trans" conformer of TB. (c) Series of 1D NAD subspectra extracted from the 92.1 MHz tilted Q-COSY Fz spectrum of TB in PBLG/Py. The assignment of ^{2}H-QDs in relation to the various diastero- and enantiotopic positions is arbitrary.* ***Figure from Ref. [160] with permission.***

in that case only about twenty ^{2}H-QDs out of the theoretically expected 80 were observed (no signal was detected for the glyceryl fragment sites). The divergences between experimental and theoretical (ideal) results have been very informative to understand the shape recognition phenomena involved in discrimination mechanisms differentiate the central chain from the two side chains. Thus, the results with **TM** have indicated that enantiorecognition mechanisms are no longer able to distinguish the side chains (a and c) from the central chain (b) as they did for **TB**. In other words, **TM** behaves more as a C_{3v}-symmetry molecule instead of a C_s-symmetry molecule on average. This situation occurs because the ratio ($V_{a,c}/V_b$) of the persistent molecular volume of the side chains ($V_{a,c}$) compared to the central chain (V_b) tends strongly towards unity. Here $V_{a,b,c}$ corresponds to the 3D space explored by the moving atoms of each chain **[160].**

VII. TOOLS FOR STRUCTURE DETERMINATION OF SMALL RIGID MOLECULES

7.1 The problem of *meso*/*threo* mixtures

The analysis of *meso*/*threo* mixtures is an interesting challenge. Indeed they can be difficult to study by isotropic NMR while the components are not always properly separated using a chiral stationary phase. Here again, NMR in oriented solvent, due to its ability to spectrally enantiodifferentiate groups of enantiotopic elements in *meso* isomers and couple of enantiomers of *threo* isomers, reveals to be a valuable tool for helping to describe quantitatively the mixture, allowing to determine diastreoisomeric and enantiomeric excesses (*de* and *ee*) and finally give unambiguous proof to evidence a reaction mechanism.

As an example, we can mention the study of the 3-*exo-trig* cyclisation of *anti*-(*E*)-benzyl-5-iodo-4-methylhex-2-enoate, induced by samarium diiodid and according with the assumed mechanisms shown in **Figure 30b [161]**. According to this mechanism, if the opening of intermediate B into A is slower than the reduction oif B into C, no racemisation is expected. In order to facilitate the study, a dideurated probe (-CD_2-) was chemically introduced without biasing the original composition through a $LiAlD_4$ reduction of the esters groups, while introducing a (non-zero) geminal ^{2}H-^{2}H couplings (dipolar) on each stereoisomer in an oriented solvent.

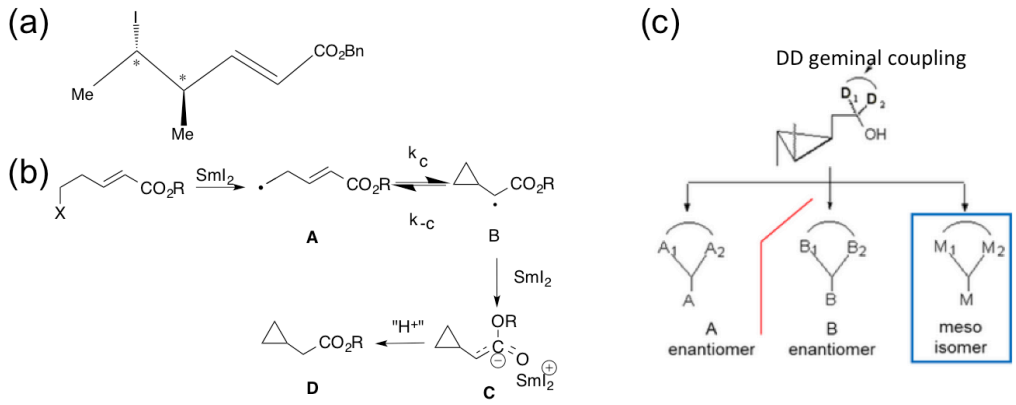

Figure 30 *(a) Structure of 'anti'-(E)-benzyl 5-iodo-4-methylhex-2-enoate. (b) Assumed mechanisms for the intramolecular cyclisation. (c) Structure of the meso (M) and active forms (A and B) of deuterated cyclopropanic derivatives. The enantiotopic deuterons in the meso are referred to as M1 and M2.* ***Figure adapted from Ref. [161] with permission.***

The principle of the analysis as schematically depicted in **Figure 31a** lies on the principle that the *meso* isomer in an ALC phase should to give a single ^{2}H-QD whose quadrupolar splitting is equal to the average of those two coupled ^{2}H-QDs expected in the CLC. Regarding the *threo* isomers, it exists a relationship between the diastereotopic deuterons and their ^{2}H-QDs, coupled to each other within each isomer **[160]**. The analytical strategy adopted was therefore to record the ^{2}H-COSY of deuterated mixture in ALC and CLC in order to exploit: i) the correlations between deuteron signals of the same isomer and ii) the relationship (in magnitude) existing between ^{2}H-QDs within the *meso* isomer on the one hand and the *threo* isomers on the other hand.

Finally, it was possible to fully individuate and assign the signals of each isomer. The deconvolution of the experimental ^{2}H spectrum for better accuracy in the determination of mixture composition leads to *de* = 35% ±

5% (*d*,*l*) and *ee* = 20% ± 5% (see **Figure 31c**). These results indicated a limited racemisation of the mixture during the chemical reaction, and therefore allowed to evidence that the opening of B into A with the reduction of B into C.

In the same framework, several homo- and heteronuclear 2D NMR approaches have been proposed to simplify the analysis of mixture of deuterated *meso*/*threo* compounds oriented in weakly ordering chiral liquid crystals **[44]**.

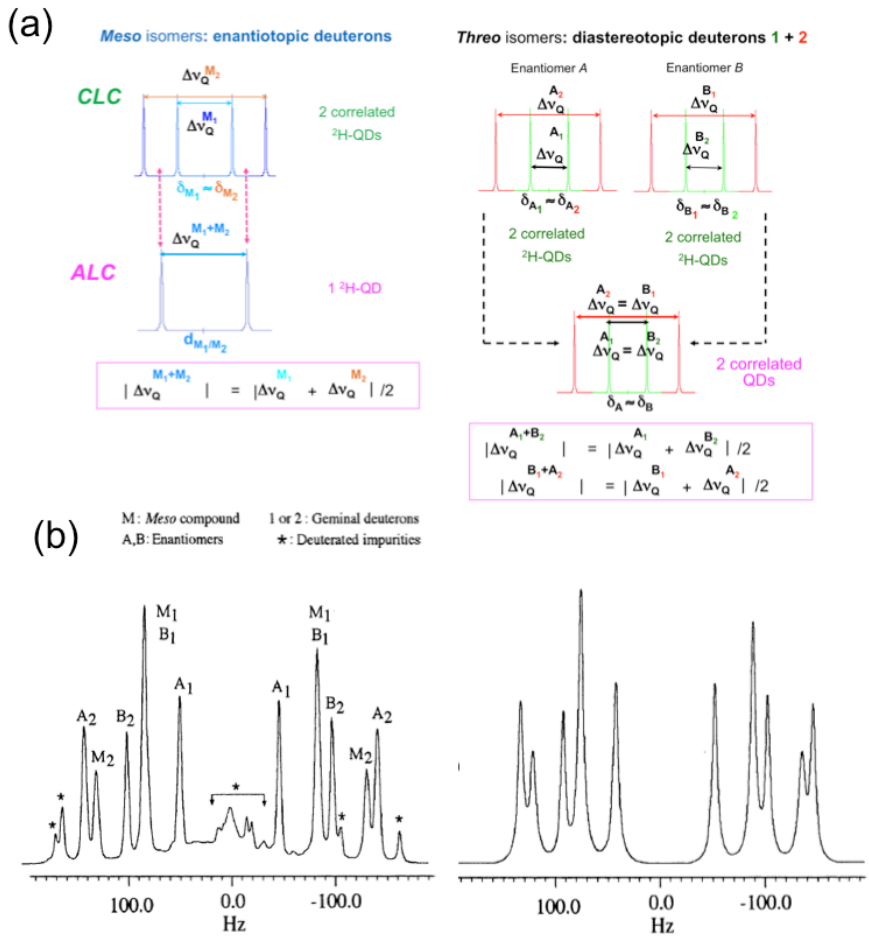

Figure 31** (a) Spectroscopic principle for grouping the ²H-QDs observed in a mixture made of dideuterated, meso-isomer and A,B enantiomeric pair in CLC and ALC. Coupling correlations are only observed between doublets originating from deuterons belonging to the same stereoisomer. (c) Experimental and deconvolution ²H-{¹H} spectra recorded in PBLG.* ***Figure adapted from Ref. [161] with permission.

7.2 | Structure elucidation using the Saupe matrix: a computational approach

Determination of the *cis*/*trans* isomerism. Anisotropic NMR is a valuable tool in determining easily and rapidly the relative configuration within a given molecular group. Indeed, as RDC between two nuclei, i and j, are related to orientation of the associated i-j bond, it is possible to evidence if two internuclear directions, ij, are parallel or not, meaning that their relative configuration is either *trans* or *cis*, for instance.

In other word, it is possible to distinguish between stereoisomers by exploiting the univocal relationship between the geometry of a (rigid) solute, its orientation into the aligned solvent and the observed NMR observables, namely here dipolar couplings as schematically depicted in **Figure 32**.

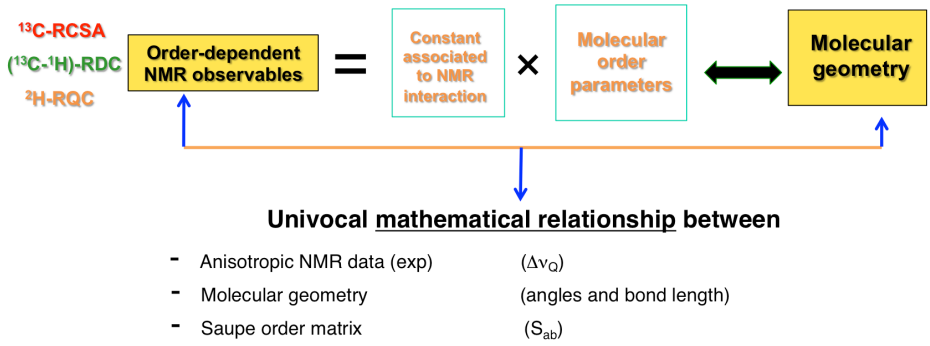

Figure 32 *(a) Schematic description of the univocal relationship between a set of experimental anisotropic observables, the molecular geometry and the molecular order parameters (alignment tensor).*

A first illustrative case was found with dihydropyridone (see **Figure 33b**) in 2003, whose *cis* and *trans* isomers were chromatographically separated into two different samples after their synthesis, without being possible to determine the configuration *cis*/*trans* by any standard anaytical method unambiguously **[162]**. Thus, in this example, it is expected that (^{13}C-^{1}H)-RDC couplings between internuclear pairs C6-H6 and C3-H3 are quite different in the *cis* isomer, unlike the *trans* isomer, due to a greater degree of collinearity of these C-H bonds in the *trans* isomer.

The sets of experimental ^{13}C-^{1}H and ^{1}H-^{1}H dipolar couplings observed for each sample were fitted towards the back-calculated dipolar from the Saupe order tensor and an optimized (semi-empirical method) for each stereoisomer. **Figure 33c** shows the correlation plot between both sets of data for each isomer. As seen, only experimental dipolar data extracted for a sample fit perfectly with the back-calculated dataset using the right geometry of the isomer present in the sample. In this study, an achiral aligned solvent could have been also used, but for a sake of facility within the preparation of the oriented samples, it was preferable to use an enantiopur polypeptide polymer, instead of a couple of enantiomers polypeptide leading to a racemic mixture **[162]**.

Case of prochiral molecules: the quadricyclane. Quadricyclane is a fully carbonated polycyclic prochiral molecule of C_{2v} symmetry that could be formed by photochemically induced [2 + 2] cyclisation of norbornadiene (**NBN**) (see **Figure 34a**) **[142]**. There have been numerous discussions about the geometry of the formed cycle 2-3-5-6, due to large contraints undergo by norbornadiene during the chemical transformation. Indeed, molecular mechanics method MM2 model predicts distances of 147.7 and 149.1 pm for the C2-C6 (C3-C5) and C2-C3 (C5-C6) bonds, respectively, while the semi-empirical PM3 model (or *ab initio* models) clearly foresees a lower σ-bond character leading to longer internuclear bonds (152.8 and 154.8 pm, respectively).

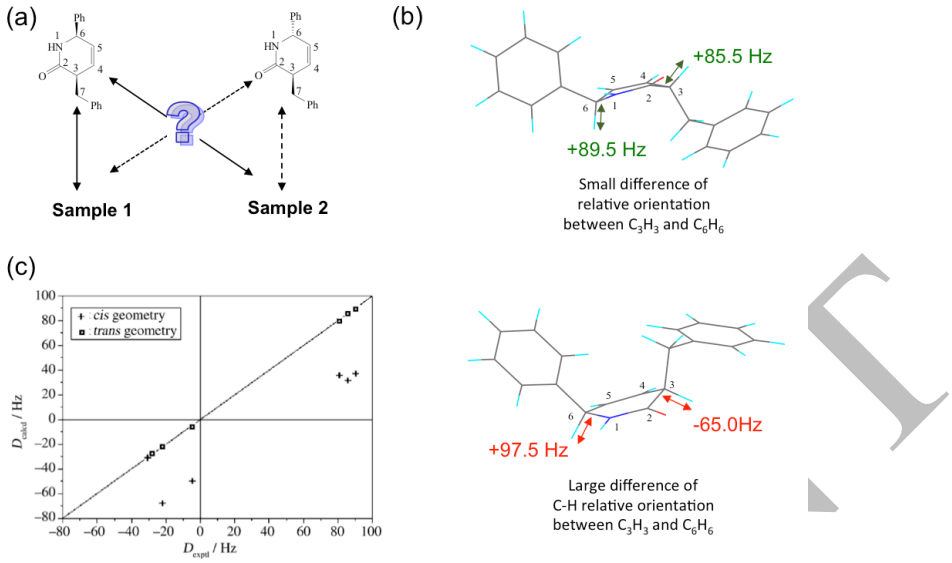

Figure 33 *(a) Structures of both isomers to be individuated. (b) Structures obtained by molecular modelling of the cis and trans compounds. (c) Correlation plot between experimental RDC ($D^{Exptl.}$ / $D^{Calc.}$), and the back-calculated RDC values, $D^{Calc.}$, for the two geometrical structures considered. The ideal results are obtained when points are aligned on the line $D^{Exptl.} = D^{Calc.}$.* ***Figure adapted from Ref. [162] with permission.***

Exploiting again the univocal relationship between the geometrical data for a rigid solute given, and its NMR observables (here, the ^{2}H-RQCs), through the iterative process presented in **Figure 34b**, it was possible to define the most adapted molecular modelling method for these types of highly-stressed cycle. Indeed, the fitting procedure using the MM2-based geometry was not satisfactory at all, as the relative differences (RD) between experimental and back-calculated data were larger than 30% and the quality of the iteration in terms of root mean square (RMS) value was too poor to be acceptable (RMS > 20 Hz). On the contrary geometries resulting from semi-empirical methods or *ab initio* calculations are good enough to satisfactorily reproduce experimental data within 10% and RMS < 3 Hz).

Contrarily to previous example, NMR analysis of quadricyclane in a CLC is advantageous for two reasons: i) the possibility to spectrally differenciate the enantiotopic pairs that allows, in turn, to overdetermine the system during the iterative process (4 experimental data to fit in the CLC instead of 3 parameters to fit in an ALC), ii) the unambiguous determination of ^{2}H-RQCs values associated to enantiotopic directions by comparison with ^{2}H-RQCs measured in the ALC.

Case of chiral molecules: the Fenchone. As in the case of quadricyclane, it is valuable to exploit the analytical consistency between NMR observables and Saupe parameters for a given molecular geometry in order to solve stereochemical challenges in case of chiral solutes. Besides, it arises the opportunity to determine the Saupe matrix of each enantiomer (in racemic/scalemic mixture) to compare them and then evaluate the ability of a CLC to discriminate enantiomers. For this purpose, the fenchone (**FCH**), a typical chiral, rigid molecule, has been investigated using ANAD NMR **[163]**. For this bicyclic compound up to 20 ^{2}H-QDs are expected to be observed for racemic/scalemic mixtures in the presence of a CLC if all ^{2}H enantio-isotopomers are discriminated (see **Figure 35a**).

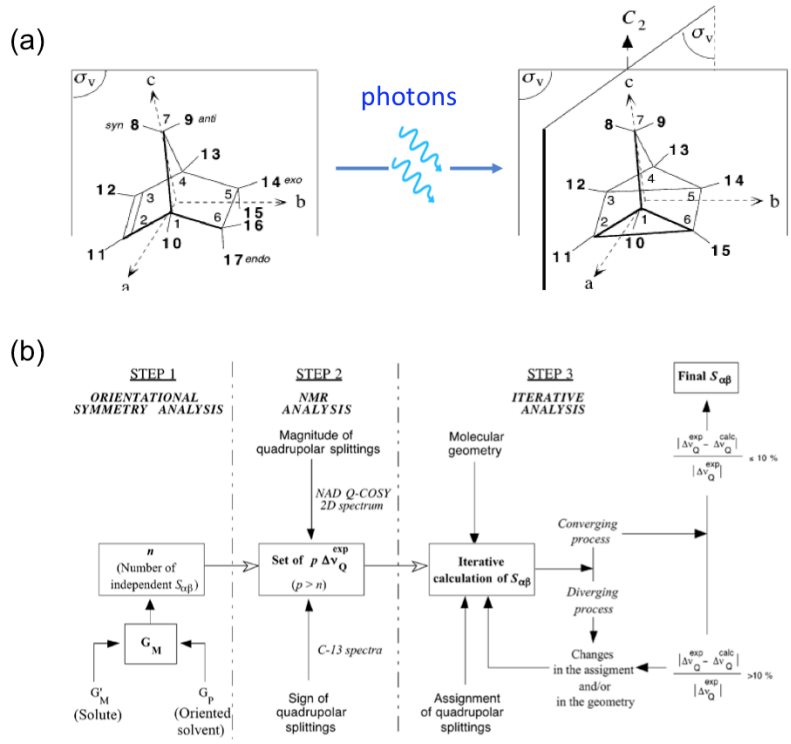

Figure 34 *(a) Structure of quadricyclane. (b) Flowchart showing the three-step analytical procedure adopted for the analysis of weakly ordered organic prochiral molecules through ANAD NMR.* ***Figure from Ref. [142] with permission.***

Experimentally, a single oriented sample containing a scalemic mixture of FCH (*ee* of 30% with (2*S*,5*R*)-(+)-**FCH** as the major enantiomer) has been prepared and analysed by proton decoupled NAD NMR. This strategy is advantageous for three reasons: i) the accuracy of the measurement of ^{2}H-RQC values (up to two orders of magnitude compared to (^{13}C-^{1}H)-RDCs), ii) the difference of amplitude of ^{2}H-QDs associated with the *ee* allowed easily to assign the signals belonging to the same stereoisomer, iii) the absence of bias in the determination of orientational order that can never be exluded when the analysis of two enantiomers is performed with two separated oriented samples containing a single isomer (as generally done when RDCs are used as anisotropic data).

In this example, 19 distinct ^{2}H RQCs (over 20) were extracted from the analysis of the NAD 2D-NMR spectrum ans exploted to determine the Saupe tensor for each enantiomer. As a control of relative signs of ^{2}H-QDs as well as to avoid ambiguities within the set of assigned lines for each enantiomer in the PBLG-based CLC, the analysis of FCH (with sample composition and temperature) in PBG-based ALC can be useful. The absolute signs of ^{2}H-QDs were obtained by comparison with those of (^{13}C-^{1}H)-RDCs associated with the corresponding C-H direction assuming that the ratio $|\Delta\nu_Q(^2H)/D_{CH}| \approx 11$ - 12. The set of experimental ^{2}H-RQCs for both enantiomers were tabulated as an input for the "MSpin-RQC" program (derived from the "MSpin-RDC" designed by Navarro-Vazquez [**164**], along with the Gaussian 09 file that contains the optimized geometry and computed EFG tensors at nuclear positions. The Saupe tensor parameters were iteratively computed (using a singular value

decomposition (SVD) algorithm) for both enantiomers until the best agreement between experimental and calculated NMR observables was obtained. The schematic principle of the protocol is presented in **Figure 35**. Herein, the so-called Cornilescu's Q-factor,

$$Q = \sqrt{\frac{\sum w_n\left(\mathrm{Obs}_n^{Exptl.} - \mathrm{Obs}_n^{Calc.}\right)^2}{\sum w_n\left(\mathrm{Obs}_n^{Exptl.}\right)^2}}, \qquad \textbf{(10)}$$

is used as quality factor for evaluating the best fit: the smaller the value of Q, the better the agreement [**165**]. In **Eq. 10**, the term, $Obs_n^{Exptl.}$, refers to the NMR anisotropic observable used and related to Saupe parameters experimentally measured without any distinction on their physical origin, *i.e* RCSA, RDC or RQC, and $Obs_n^{Calc.}$ (namely also back-calculated data) are their properly calculated counterpart. Finally, the terms w_n are normalized relative weighting factors allowing the use of three anisotropic observables simultaneously during the best-fit procedure to be combined. When the same experimental data, $\mathrm{Obs}_n^{Exptl.}$, are used in the iterative process, then $w_n = 1$.

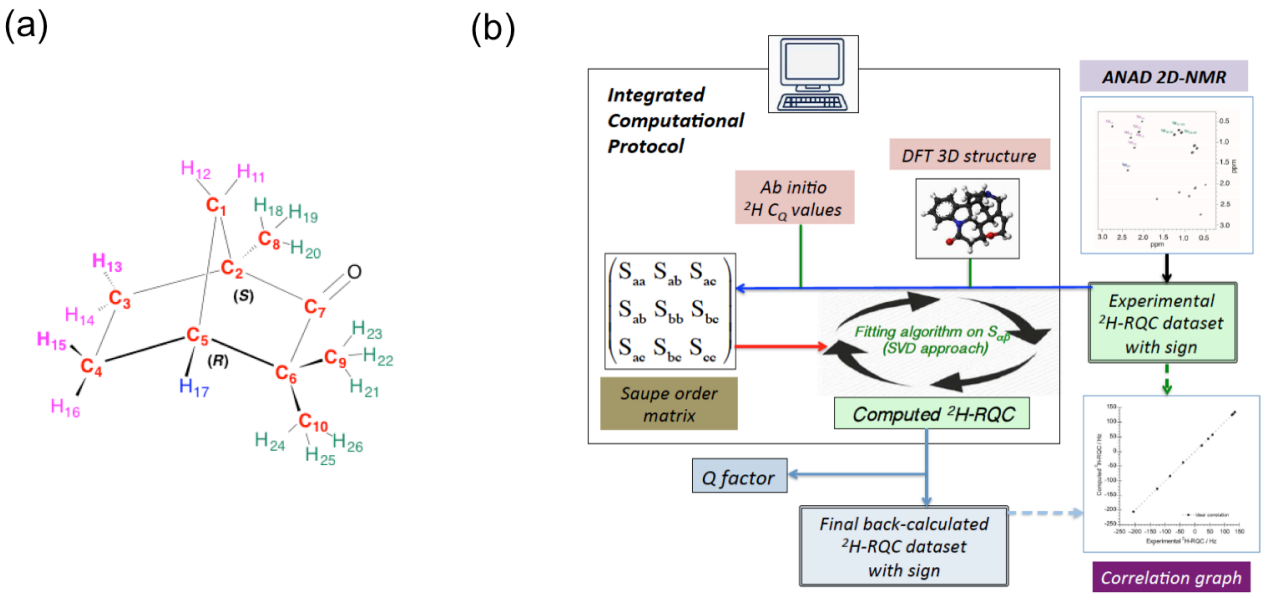

Figure 35 *(a) Molecular structure and numbering of FCH. (b) Simplified flowchart showing the principle of molecular structural analysis using the integrated computational program "MSpin-RQC" from the ^{2}H-RQCs extracted from ANAD 2D-NMR experiments The correlation plot (^{2}H-RQC$^{Calc.}$ vs. ^{2}H-RQC$^{Exptl.}$) simply visualizes the quality of fit of experimental data.* ***Figure from Refs. [2] with permission.***

The Q-factor represents a more general quality factor as entailing all possible experimental data available compared to RMS. In practice, if only one type of data are used, as in the case of **FCH** where only ^{2}H-RQCs were exploited, both parameters are equivalent from numerical point of view (w_n =1). Excellent agreement was found between experimental and back-calculated ^{2}H-RQCs with Q factors equal to 0.007 and 0.013 for (*S*)-FCH and (*R*)-FCH in PBLG, respectively, and 0.008 in PBG. The excellent fit indicates a correct assignment of ^{2}H-QDs for both *R* and *S* isomers. As in the case of norbornene and quadricyclane, as an added value, it was possible to

clearly confirm the spectral assignment performed in 1990 [**166**] and in 2014, [**167**] but was different from the one proposed in 1999, in particular for positions 15 and 16 (relative inverted position) [**168**]. Indeed, exchanging the RDC values for both positions in the bets-fit procedure make the quality factor increases up to 0.4 showing a less best-fit agreement.

Once performed, the MSpin-RQC computational programme displayed all pertinent data relative to the alignment properties of the solute, such as the Saupe matrix elements, asymmetric parameter, as well as, the principal axis system (PAS) of the inertia tensor axis as seen on the graphical interface of the program (see **Figure 36b**). In addition, the Saupe tensor can be represented as a valued 3D surface. All these graphical utilities facilitates the visualization and the comparison the alignment properties reduced to simple vectors or surfaces, particularly in the case of two enantiomers. For illustration, **Figure 36b** shows an example of the graphical screen for enantiomers of FCH, in which the principal axis systems of the Saupe, $S_{x'}$, $S_{y'}$, $S_{z'}$ and inertia tensors $I_{x'}$, $I_{y'}$, $I_{z'}$ are simultaneously displayed.

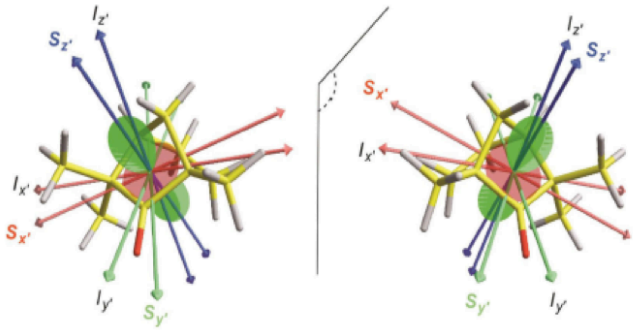

Figure 36 *The principal molecular axis system ($S_{x'}$, $S_{y'}$, $S_{z'}$) of the diagonalized Saupe matrix, the inertia tensor axes, ($I_{x'}$, $I_{y'}$, $I_{z'}$), and the Saupe tensor surface representation (red and green surfaces indicate positive and negative ^{2}H-RQCs, respectively) for (S)-FCH and (R)-FCH oriented in PBLG/$CHCl_3$.* ***Figure adapted from ref. [163] with permission.***

VIII. DETERMINATION OF THE RELATIVE AND ABSOLUTE CONFIGURATION BY ANAD NMR

8.1 | Determination of the relative configuration in bioactive polystereogenic compounds

Determination of the chiral 3D structure (correct relative configuration/preferred conformation) of bioactive complex natural compounds or synthetic molecules containing several sterogenic centers (n > 2) is still an important issue in regard of implications in pharmaceutical sciences **[169]**. It is also a non-trivial analytical task for chemists since single crystal X-ray diffraction spectroscopy is often not applicable in many cases, the analyte of interest failing to produce suitable crystals **[170, 171]**. Anisotropic NMR in weakly aligning media revealed an astonishing ability to solve structural problems of increasingly complex molecules (with a smaller and smaller amount of analyte), from orientational information inherent to anisotropic NMR observables. The reason is that anisotropic data encode valuabes 3D structural information including the molecular relative configuration.

During the last decade, a wide variety of natural substances have been investigated and their structure solved, confirmed or even revisited using (^{13}C-^{1}H)- or (^{1}H-^{1}H)-RDCs data **[172, 173, 174]**, and more recently from ^{13}C-RCSA's data **[175, 176]**. The last frontier of this game has been crossed in 2020 by exploiting the advantages

(simple spectral data, magnitude of RQCs, dilute spins, …), of ^{2}H-RQCs extracted from ANAD NMR 2D spectra, assuming that the sensitivity is nowadays a real drawback [**177**]. The performance of this last tool has been examined for two multi-cyclic chiral, natural compounds of pharmaceutical interest oriented in PBLG-based oriented samples: the strychnine, a poison, and artemisinin, an antimalarial drug used against *Plasmodium falciparum* malaria) as examples. **Figure 37** shows the ANAD *Q*-resolved Fz 2D spectrum of artemisinin recorded within 15 hours with only (50 mg (MW: 282.3), *ie* a molar concentration for each monodeuterated isotopomer of about 35 mmol.l^{-1}) where unambiguous 15 (over 16) ^{2}H-QDs can be experimentally measured and used.

Investigation of polystereogenic rigid molecules requires first the determination of all energetically-reasonable (or possible) structures with a given relative configuration among the 2^{n} possible structures, for n asymmetric carbons. As in the case of small molecules (see above), it is possible to determine the relative configuration by comparing the experimental signed ^{2}H-RQC data and the back-calculated from order matrix with the help of the Cornilescu's *Q*-factor in the frame of an hyphenated computational protocol (using SVD algorithm). The selection of the most probable configuration corresponds to the smallest *Q*-value (with $Q < 0.05$), in combination with the best set of smaller RDs between ^{2}H-RQC$^{Calc.}$ and ^{2}H-RQC$^{Exptl.}$ values. ^{2}H-Finally the selection of the right stereoisomers is obtained unambigously when a large difference between the first and the second smallest *Q* exists. The schematic procedure is schematically depicted in **Figure 38**.

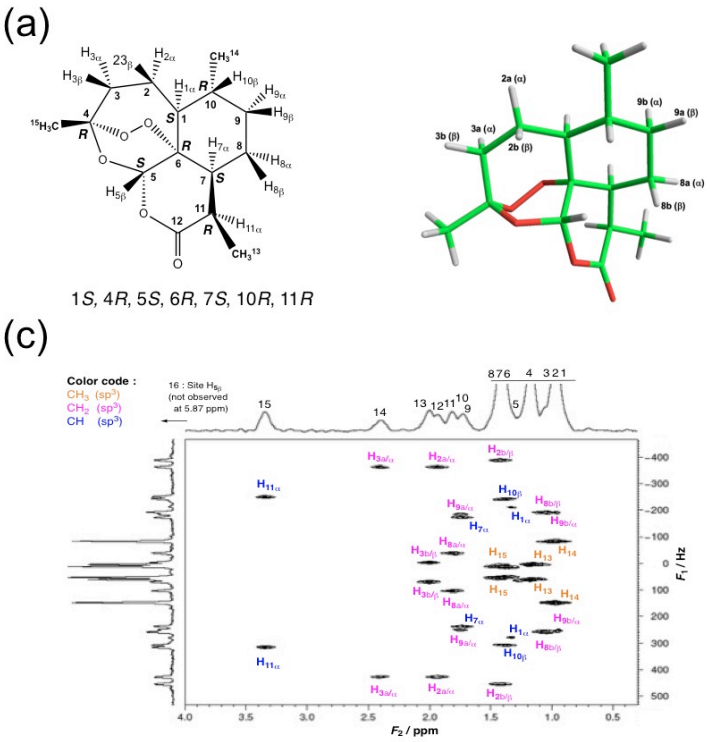

Figure 37 *(a) Molecular structure, atomic labels and R/S descriptors of artemisinin associated with the (known) absolute configuration. (b) DFT-optimized 3D structures labeling the α/β (a/b) positions of diastereotopic protons/deuterons. (c) Part of the 92.1 MHz NAD-{*^{1}*H} Q-resolved Fz map (tilted and then symmetrized).* ***Figure adapted from ref. [177] with permission.***

In case of artemisinin, the smallest *Q*-factor was below 0.02, with a very small of RD average below 4 %. This result has been obtained with the stereoisomer of absolute configuration 1*S*, 4*R*, 5*S*, 6*R*, 7*S*, 10*R*, 11*R*, namely the known absolute configuration. These results have therefore demonstrated that the 3D structure/relative configuration of complex bioactive molecules could be unambiguously determined using ^{2}H-RQCs, being in this case at ^{2}H natural abundance.

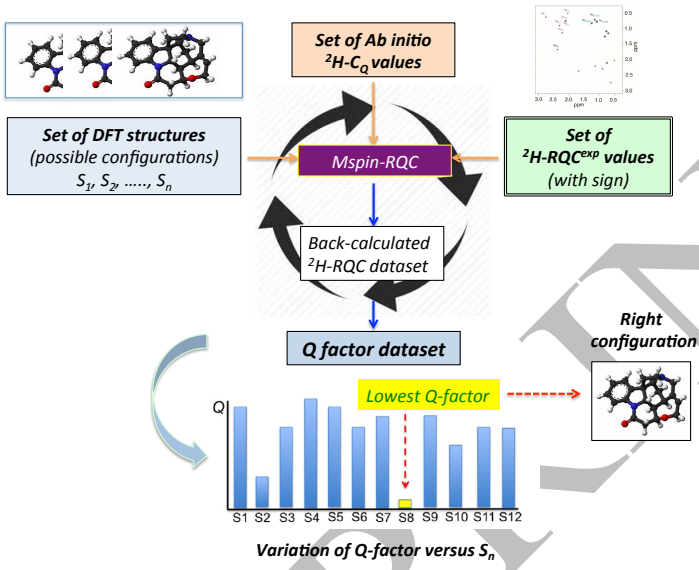

Figure 38** Simplified principle of fitting of experimental ^{2}H-RQC dataset to a possible set of possible structures.* ***Figure adapted from ref. [177] with permission.

Noteworty is that the Cornilescu's *Q*-factor does allow to consider any type of anisotropic observables related to Saupe matrix, both separately or in conjunction, One should be aware that not all anisotropic NMR measurables are equally sensitive to orientational orders as already stated in previous **Section II**, hence the possibility and necessity of weighting them during the best-fit procedure. Interestingly, recent work has shown that it is possible to successfully combine RDC and ^{13}C-RCSA data, extracted from the same molecule **[178]**. This combination can be useful when the number of RDCs or RCSAs are not sufficient one their own. For memory, five anisotropic data (at least) are requested for a C_1-symmetry molecule. Such approach allows also to testing different combinations of data in order to improve the selection of a correct structure when the *Q*-factor is weakly discriminating. This strategy was tested in 2001 by the Orsay's group, combining ^{2}H-RQCs and (^{1}H-^{1}H)-RDCs as independent input data when ^{2}H-RQCs data were not enough to determine the orientational order by their own [**174**]. In this case, the computational program "SHAPE" initially developed by P. Diehl et *al*. **[179]** was suitably modified to handle both types of input data.

8.2 | The problem of the absolute configuration

In contrast to the relative configuration determination problem, assign the absolute configuration (AC) of enantiomers signals (*R*/*S*, *M*/*P*, *Δ*/*Λ*) with a single stereogenic center as well as enantiotopic elements (pro-*R*/pro-*S*) in prochiral molecules using anisotropic NMR in CLCs alone remains an unresolved issue since a no direct

experimental methods exist to do so **[180]**. In fact, as the enantiodiscrimination process originates from a difference in orientational ordering of enantiomers or enantiotopic elements, the a *priori* assignment of AC of a given signal can be only envisaged *via ab initio* methods (as Molecular Dynamic (MD) computational simulations) able to predict molecular alignment and ordering differences from the evaluation of interactions between a given analyte and a helically chiral system **[180, 181, 182, 183, 184, 185, 186]**. Although some achievements were obtained for predicting orientation behavior of analytes interacting with achiral, nematic orienting solvents **[187, 189]**, or even polypeptide-based achiral systems (PBG) **[75]**, the case of two enantiomers interacting with helical-polymer based CLCs remains still problematic despite some recent progresses **[180, 181, 182, 183, 184, 185, 186]**. We can, however, mention the attractive description of a mean torque potential sensitive to the *M/P* chirality of helical solutes aligned in helical-particles based anisotropic media leading to the absolute enantiorecognition, when combined with simulation of order parameters using Monte-Carlo methods **[190, 191, 192]**. So far, a MD simulation involving PBLG using MD are rare in literature, and the results obtained are rather fragile in particular because the MD can be performed with a sufficient long time to correctly evaluate the effect of conformational dynamic of all side chains along the a-helix on the enantiodiscriminating mechanisms. This prerequisite needs a formidable calculation power, even for a small number of units considered.

Nevertheless, an empirical approach combining NAD 2D-NMR and a PBLG-based mesophase was proposed for assigning the AC of small chiral molecules **[193]**. The key idea of this approach lies on the fact that recognition phenomena of molecular shape play an important role in global ordering/differentiation mechanisms. As a consequence, the relative magnitude of molecular ordering for each enantiomer, and their, is expected to be similar for a series of iso-structural chiral compounds dissolved in a given CLC, assuming the same experimental conditions (concentration and *T*). The strategy comprises three steps: i) the optimization of spectral enantiodiscriminations for the compound X1, ii) the analysis of NAD QUOSY 2D spectra for a series of n (enantio-enriched) mixtures (X2, X3, ... , Xn) of isostructural chiral molecules for which the AC of the major enantiomer is known, and iii) the assignment of the absolute stereochemistry of NAD signals of X1 from the analysis of NAD 2D spectra of reference molecules.

This empirical strategy was first explored to determine the AC (unknown by chemists) of the major enantiomer in a prepared enantio-enriched mixture of 1,1,1-trifluoromethyl-2,3-epoxypropane (X1) synthesized in both racemic and enantiopure series. As depicted in **Figure 39,** the analysis of spectral 2D fingerprints of enantio-enriched mixtures shows that the correlation between the fingerprints and enantiomeric shapes is the same for the various mixtures tested while the relative position (inner/outer) of ^{2}H-QDs can be correlated to the major/minor enantiomer (namely the higher/lower peak intensity) for the three ^{2}H sites (2-4). Based on these repetitive spectral patterns it has been possible to conclude that the mixture X1 is most probably enriched in the *R* enantiomer, according to the Cahn-Ingold-Prelog (CIP) rules.

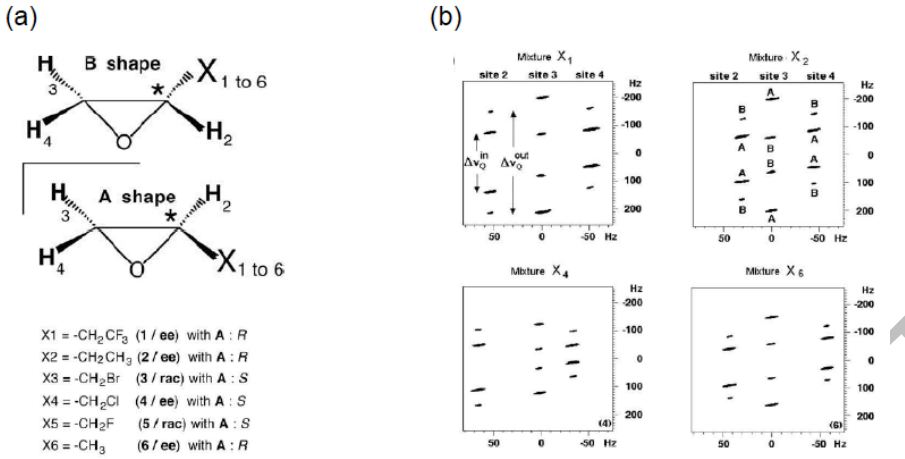

Figure 39 *(a) Structure of enantiomeric shapes denoted A and B and nature of substituents (X_1 to X_6) on the epoxyde ring. The correspondence between the A shape and the stereodescriptors R/S is given. (b) Four examples of 92.1 MHz NAD spectral 2D fingerprints associated with the three epoxyde ring deuteron sites in compounds 1, 2, 4 and 6 (ee = 33%).* ***Figures adapted from ref. [193] with permission.***

IX. STUDIES OF DYNAMIC SYSTEMS: A QUALITATIVE APPROACH

9.1 | The case of tetrahydrofuran

Fast exchange regime conditions on the NMR timescale lead to a fast exchange between conformations along the conformational pathway of a given molecule, meaning that the activation energy of this process is low compared to the thermal energy **[194, 195]**. From the qualitative point of view, the NMR picture is blurried and allows to interpret the experimental data using a fictious molecular structure. This phenomenon is well known when dealing with the ^{1}H signal of methyl rotors for instance as all three constitutive protons usually appear with the same chemical shift due to fast conformational motion between them, or with cyclohexane where a ^{13}C single line (accounting for six carbon atoms) is found on the proton decoupled carbon-13 NMR spectra. In these two examples, the ^{1}H and ^{13}C nuclei are "dynamically" isochronous, although instantaneously they are (partly) anisochronous. In CLCs, same dynamic situation may occur and modulates the instantaneous spectrum one might record and individuate for each confrmation if NMR would be infinitely fast respect to conformtaional motion.

As an illustrative example to evidence the effect of pseudorotation in a five-membered ring on the NMR timescale can be found with tetrahydrofuran (**THF**) **[196]**. Common representation of **THF** is that represented on **Figure 40a**, which is however quite unlikely, according to twell-established thermodynamical rules of stability 5-membered rings. Following its conformational pathway, this high-energy C_{2v}-symmetry representation of **THF** might actually results from a fast motionally averaged equilibrium of two low-energy C_s-symmetry conformers (see **Figure 40b**) or alternatively from the pseudorotation conformational equilibrium shown in **Figure 40c**.

The conformations of C_{2v}-symmetry and the C_s-symmetry (depicted in **Figure 40a,b**) allow to understand the chemical equivalence between hydrogen (deuterium) atoms located on α and β positions of oxygen, that are expected in an isotropic solvent as well as in an ALC. Thus, in the C_s-symmetry structure, sites α_1 and α_4 (resp. β_1

and β_4) as well sites α_2 and α_3 (resp. β_2 and β_3) refer to enantiotopic positions of **THF**, while in the C_{2v}-symmetry structure, all four hydrogen atoms (positions I and II) on each α and β site are isochronous. Therefore in any achiral environment, it is not possible to distinguish between both symmetries. The situation is, however, different when **THF** is dissolved in a CLC. If C_s-symmetry conformers would have been observed in CLCs, two quadrupolar doublets for the couple α_1 and α_4 positions in the A conformer, equivalent to α_2 and α_3 positions in the B conformer by symmetry, centered on quite the same chemical shift δ_α would have been observed on NAD NMR. For the same reason, two ^{2}H-QDs for β_1 and β_4 positions in the *A* conformer, equals to β_2 and β_3 positions in the *B* conformer, all centered on quite the same chemical shift δ_β would have been observed.

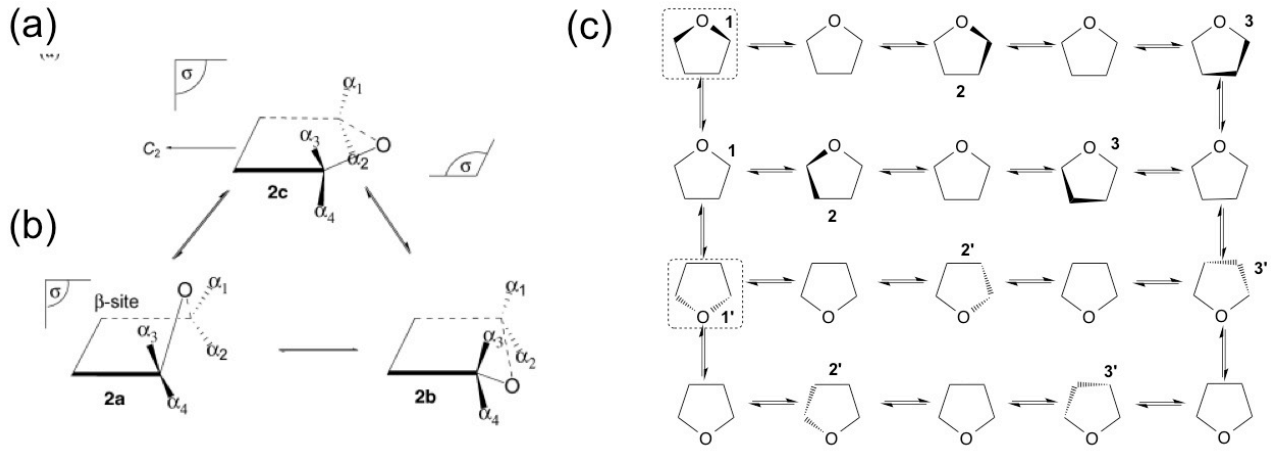

Figure 40 *(a) High-energy C_{2v}-symmetry conformation of **THF** and associated atoms numbering. (b) C_s-symmetry conformation of **THF**. (c) Schematic description of the pseudorotation conformational pathway of **THF**.* ***Figure partially adapted from ref. [196] with permission.***

Experimental ANAD 2D spectrum in the CLC shows only two pairs of ^{2}H-QDs, the centered on δ_α and δ_β (see **Figure 41**). These results are only consistent with the C_{2v}-symmetry structure observed on the NMR timescale and confirmed by the disappearing of doubling of ^{2}H-QDs in the ALC while their splitting for the α and β sites is equal to the average value measured in the chiral mesophase. Both outcomes unambiguously insure that the high-energy level conformation of C_{2v} symmetry explain satisfactorily the experimental data observed due to the thermal conformational motion, too fast on the NMR timescale compared to conformational equilibrium, although this usual C_{2v}-symmetry do not thermodynamically exists. For **THF**, according to the literature, the activation energy barrier is small (*ca* 9 kJ/mol) **[197]**, and so the conformational exchange cannot be slow down enough to increase the contribution of the C_s-symmetry conformers, when decreasing the sample temperature even at very low values; only the pseudorotation conformational pathway has to be retained.

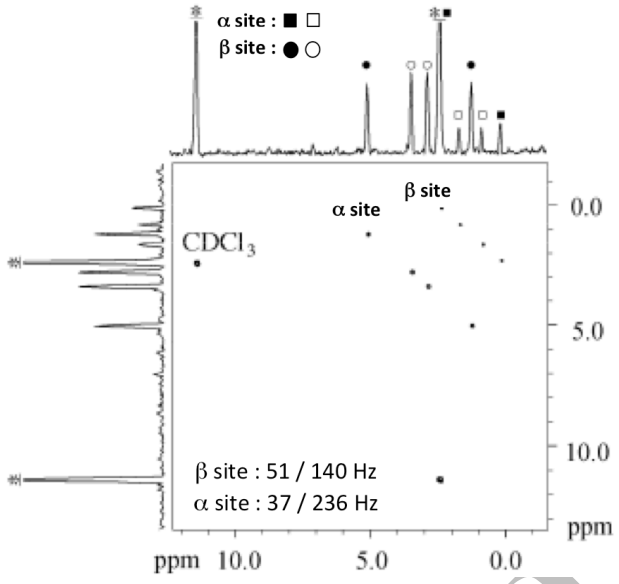

Figure 41 *61.4 MHz NAD Q-COSY 2D spectrum of* ***THF*** *dissolved in a PBLG/$CDCl_3$ solvent recorded at room temperature.* ***Figure adapted from ref. [196] with permission***

9.2 | The *cis*-decalin

In the world of apolar hydrocarbons, the *cis*-decalin (**CDC**) (see **Figure 42a**) is a special issue because this molecule can be described as chiral without any stereogenic center and possesses a two-fold rotational symmetry axis. Interestingly, this molecule is submitted to an interconversion between two limit conformers that constitutes a pair of C_2-symmetry enantiomers. As a consequence, its orientational behavior in a CLC is highly dependent on the temperature used for the measure, while different structures are involved to interpret the experimental data qualitatively according to T.

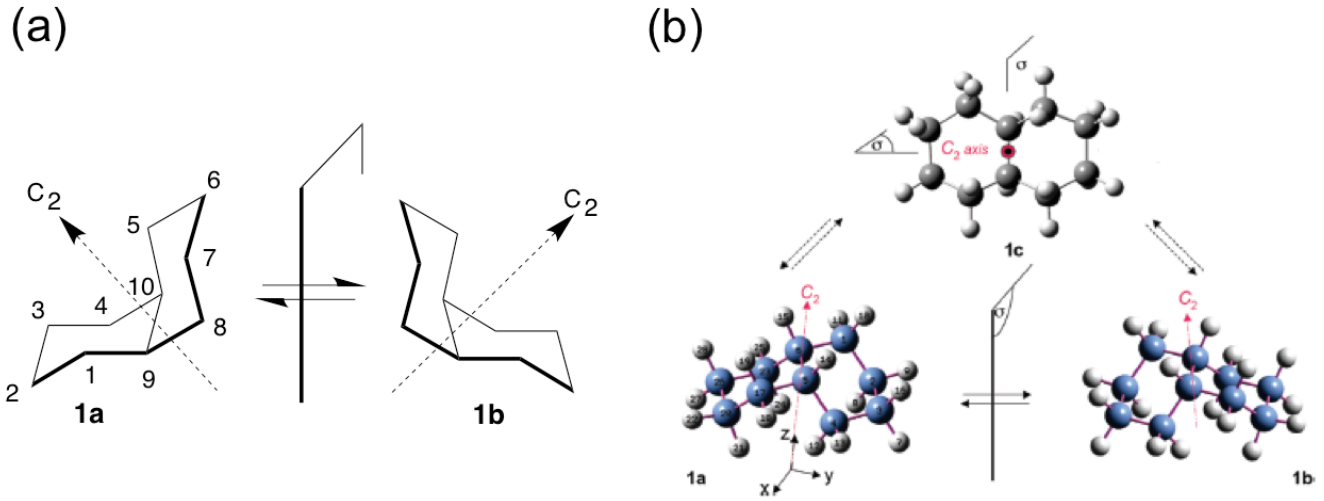

Figure 42 *(a) C_2-symmetry conformers of cis-decalin and associated position numbering; (b) C_{2v}-symmetry high-energy conformation of cis-decalin.* ***Figure adapted from ref. [196] and [198] with permission.***

Experimentally, **CDC** was studied at different temperatures using deuterium (perdeuterated compound) as well as proton-decoupled carbon-13 NMR in anisotropic phase **[196, 198]**. In each case, the NMR spectra obtained result from averaged NMR observables along the conformational pathway. However, in the fast exchange regime, a high- or low-energy specific conformation may be involved to describe qualitatively all experimental anisotropic NMR results.

In **Figure 43** is presented the variation of ^{2}H spectrum of **CDC** in a PBLG phase as a function of temperature between 230 and 360 K. The coalescence is obtained at 300 K. As expected, the presence of a single high-resolution ^{2}H-QD at 300 K originates from deuterium sites 9 and 10 on the bridgehead because, whatever the temperature, they exhibit no kinetic averaging between the enantiomeric conformational forms 1a and 1b **[196]**.

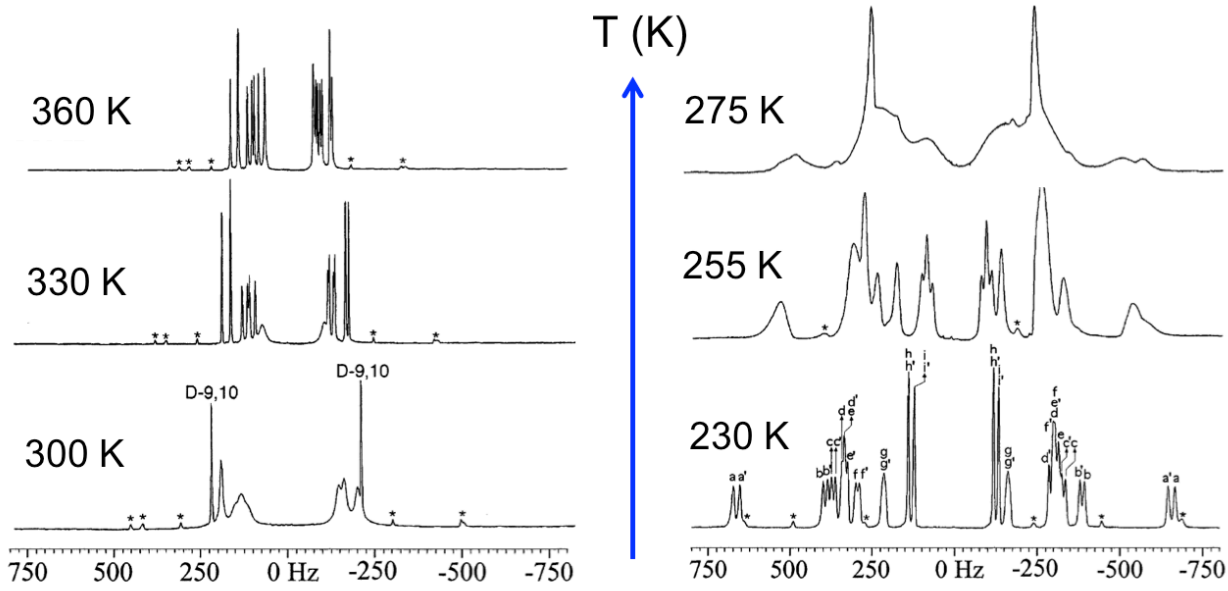

Figure 43 *61.4 MHz NAD NMR spectra of cis-decalin recorded at various temperatures. At 300 K, he single high-resolution doublet can be safely assigned to the deuterons 9 and 10 on the bridgehead because, whatever the temperature, they exhibit no kinetic averaging between the conformational forms.* ***Figure adapted from ref. [196] with permission.***

As seen in **Figures 43** and **44**, the analysis and the interpretation of ^{2}H and ^{13}C 1D and 2D NMR spectra at high temperature (360 K) are coherent with a high-energy, C_{2v}-symmetry conformation, while at low temperature (270 K), chiral differentiation between the C_2-symmetry invertomers are observed by ^{2}H NMR. The analysis of **CDC** oriented in the PBLG-based ALC properly confirms the interpration of results in the CLC as shown in **Figure 44b**, where the spectral discrimination of enantiotopic directions vanished in the racemic phase. Thus from ^{13}C NMR (see **Figures 44c,d**), one single line for each homotopic pair and enantiotopic carbon atom in ALC are expected, meaning one for C-9 et C-10, one for C-5, C-1, C-8, C-4 and one for C-6, C-2, C-7, C-3, whereas in CLC are expected five single lines at maximum, still one for C-9 et C-10, but one for C-5 et C-1 different from the one associated with C-6 et C-2, and one for C-7 et C-3 different from the one associated with C-8 et C-4. For same reasons, a maximum of five ^{2}H-QDs are expected in ^{2}H NMR in the CLC, D-9/D-10, D-5, D-4, D-1, D-8,

D-5', D-4', D-1', D-8', D-6, D-2, D-7, D-3, D-6', D-2', D-7', D-3, and nine of ^{2}H-QDs in CLCs, two for each enantiotopic pairs and one for the homotopic pair D-9/D-10.

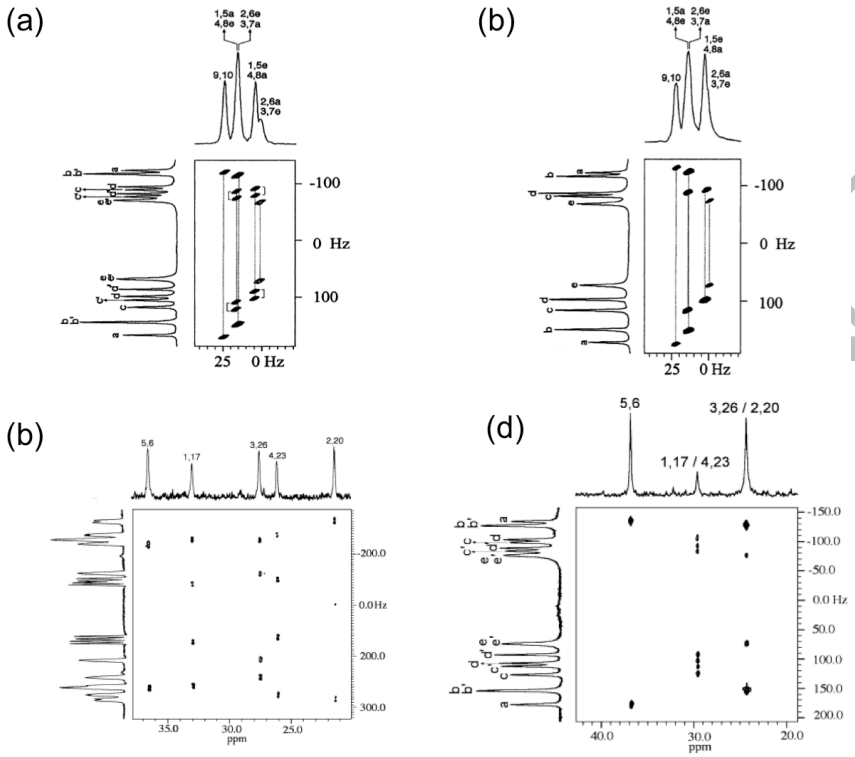

Figure 44 *(a and b) 61.5 MHz NAD NMR tilted Q-COSY 2D spectra of* ***CDC*** *in PBLG/$CHCl_3$ and racemic PBG/$CHCl_3$ at 360 K. (c and d) 9.4T ^{2}H-^{13}C HETCOR correlation spectra of CDC at 243 and 356 K.* ***Figure adapted from refs. [196] and [198] with permission.***

9.3| Determination of the activation barrier energy by anisotropic ^{2}H NMR

Any molecular dynamic processes modulate the experimental anisotropic NMR spectra as the function of the sample temperature **[195, 196, 197]**. Thus, the analysis of NMR data (versus T) allows understand the molecular internal motions as well as access experimentally to dynamic parameters such as exchange or interconversion rate constants, which themselves depend on the magnitude of the barrier to interconversion, $\Delta H^{\ddagger}$ **[195, 196, 198]**.

The dependence of the exchange/interconversion rate constant, k, on temperature is described by Eyring's equation as **[196, 198, 199, 200]**:

$$k = \frac{RT}{N_A h}\exp\left(-\frac{\Delta G^{\ddagger}}{RT}\right) \text{with } \Delta G^{\ddagger} = \Delta H^{\ddagger} - T\Delta S^{\ddagger}, \qquad (11)$$

where R is the gaz constant, N_A is the Avogadro constant, h is Planck constant and T is the absolute temperature expressed in K.

For such investigations, ^{2}H-{^{1}H} NMR studies of (deuterated) molecules dissolved in aligned solvents is very efficient because it presents three advantages: i) simple high-resolution 1D spectra dominated by the ^{2}H quadrupolar interaction are obtained, ii) the coalescence phenomenon is clearly identified on spectra, iii) the

spectral separations between exchanging ^{2}H anisotropic signals can be much larger than those observed in isotropic ^{2}H or ^{13}C NMR, thus allowing a much wider dynamic process range to be studied and iv) when the aligned solvent is chiral, it becomes possible to study the various conformational dynamic phenomena involving enantiomeric molecular forms or enantiotopic elements in prochiral molecules, spectrally undistinguished in ALCs **[201, 202]**.

To illustrate our purpose, here is presented the case of (±)-1-bromo-2-methyl-3-deuterio-5-(1'-naphthyl)benzene (**BMNB**), a chiral atropoisomer orthosubstituted biaryl (see **Figure 45a**). This monodeuterated aromatic compound has been investigated by ^{2}H-{^{1}H} 1D NMR in PBLG/$CHCl_3$ as a function of temperature. The spectral variation versus T is shown in **Figure 45b**; note the coalescence at 250 K. From data measured in simulated NMR spectra and the analysis of the Eyring plot, namely the natural logarithm of kN_Ah/RT against $1/T$ above and below the coalescence temperature **[201, 202]**, the activation parameters $\Delta H^{\ddagger}$, $\Delta S^{\ddagger}$, and subsequently $\Delta G^{\ddagger}$ (T), can be extracted from the slope ($-\Delta H^{\ddagger}/R$) and the y-intercept of plot ($\Delta S^{\ddagger}/R$).

Noteworty is the rate constant, k, and the free energy of activation, $\Delta G^{\ddagger}$, at the spectral coalescence temperature, T_c, (denoted herefater $\Delta G^{\ddagger}(T_c)$) can easily be deduced from the measurement of the half-difference of quadrupolar splittings, $|\Delta\Delta\nu_Q| = |\Delta\nu_Q^A - \Delta\nu_Q^B|/2$, in the ^{2}H spectrum below T_C **[190]**. Indeed, at this particular temperature, assuming identical time constant (T_2^*) for the FID decay of both exchanging deuterons, we can write:

$$k = \pi \times \left|\frac{\Delta\nu_Q^A}{2} - \frac{\Delta\nu_Q^B}{2}\right| \qquad (12)$$

and

$$\Delta G^{\ddagger}(T_c) = RT_c \times \ln\left(\frac{RT}{N_A h} \times \frac{2\sqrt{2}}{|\Delta\nu_Q^A - \Delta\nu_Q^B|}\right) \qquad (13)$$

In practice, the anisotropic ^{2}H-{^{1}H} / NAD-{^{1}H} spectra measured at T_C can be very different depending on the signs of $\Delta\nu_Q$ for deuterons A and B as well as the magnitude of $|\Delta\nu_Q^A - \Delta\nu_Q^B|$ compared to $\Delta\nu_Q^A$ and $\Delta\nu_Q^B$ **[192]**. In the case of BMNB, the value of k is equal to 3.2×10^2 s^{-1} while the activation parameters were found to be equal to $\Delta H^{\ddagger} = 44.7 \pm 0.5$ kJ.mol^{-1} and $\Delta S^{\ddagger} = -18 \pm 2$ J.mol^{-1}.K^{-1}.

9.4 | Monitoring enzymatic reaction in DNA-based oriented solvents

From the study of norbonene in PBLG in which both prostereogenic faces of this prochiral molecule are spectrally distinguished and each atomic site belonging to the same face individuated **[139]**, it was established that ^{2}H-{^{1}H} NMR in CLC may provide a key analytical tool to follow/examine, for instance, the specific approach of an enzyme toward a preferential site or face of a ligand **[141]**. This information is very useful for understanding the enzymatic racemization mechanism that is a crucial step for designing possible inhibitors of associated enzyme **[203]**. To provide an alternative analytical method to well-established methods (circular dichroism (CD) or UV

spectroscopy) or more advanced tools (chiral capillary electrophoresis) **[204, 207, 206]**, in 2013 has been demonstrated the ability the ^{2}H-{^{1}H} NMR in CLC to follow simultaneously, *in situ* and in real-time, the concentrations of a couple of enantiomers in presence of an enzyme *versus* time, in order to determine kinetic parameters and in a second step to study the effect of possible inhibitors **[207]**.

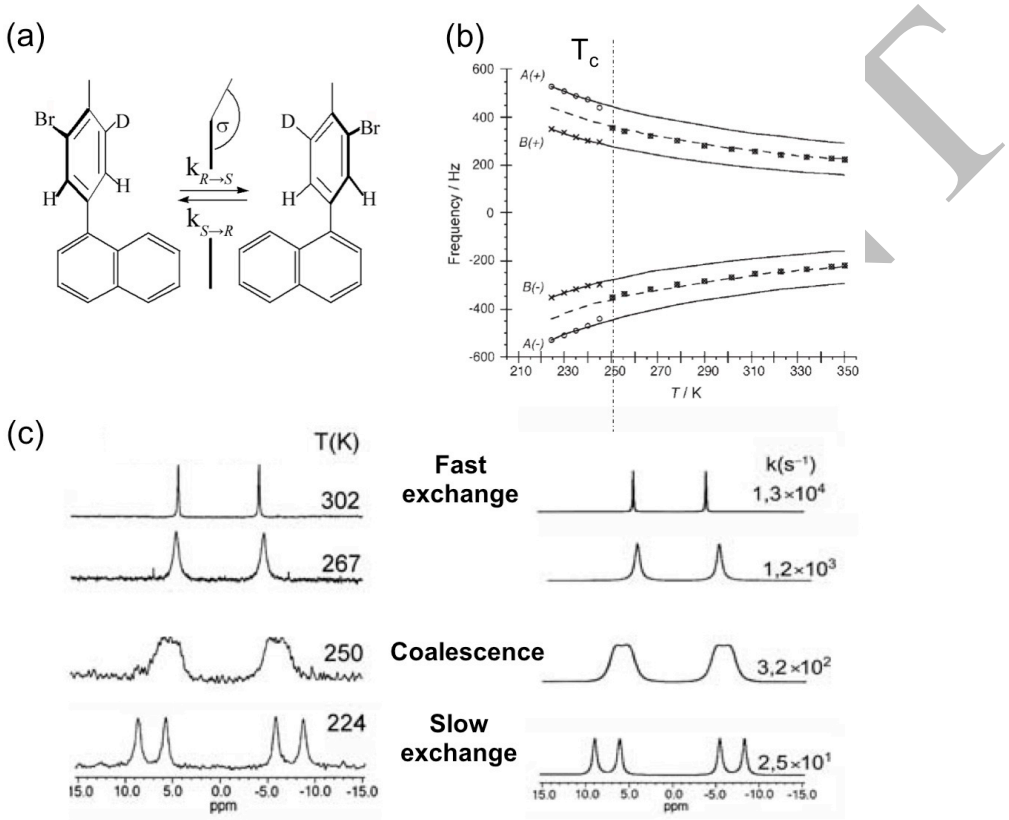

Figure 45 *(a) Enantiomeric conformers associated with the (±)-1-bromo-2-methyl-3-deuterio-5-(1'-naphthyl) benzene. (b) Experimental ^{2}H-{^{1}H} 1D-NMR spectra (61.4 MHz) in PBLG versus five temperatures and showing the coalescence.* ***Figure adapted from Ref. [202] with permission.***

The basic idea is to follow the distinct ^{2}H NMR signals of both deuterated enantiomers dissolved in the CLC in the presence of an active enzyme, and calculate the turnover numbers (k_{catL} and k_{catD}) of the enzyme without the requirement of any chemical transformations of the substrate as needed for current analytical tools, excepted prior deuteration (see **Figure 46**). The proof of principle has been first reported in the case of the alanine racemase (**AR**) which recognizes a chiral substrate, such as *L*-Alanine (***L*-ALA**) and reversibly converts it into its enantiomer, *i.e. D*-Alanine (*D*-ALA) or *vice versa*. In this example, as alanine racemase (**AR**) is only water-compatible, chiral oriented lyotopic solutions of **DNA** fragments in water has been used as discriminating aligning medium **[99, 207]**, while (*D*/*L*)-alanine was selectively deuterated on the methyl group in order to benefit of the quarupolar interaction as well as minimize the acquisition time of ^{2}H spectra during the reaction monitoring. **Figure 46a** presents the variation of ^{2}H-QDs of *L*- and *D*-Alanine-d_3 at different times after the introduction of the enzyme. Careful deconvolution of ^{2}H spectral lines allows to follow the concentration of *D* and *L*-isomers and their quantitative interconversion. **Figure 46b** shows the time-dependent concentrations, showing clearly the

interconversion kinetic until racemisation. Using these data, evaluations of k_{catL} and k_{catD} were performed assuming a reversible Michaelis-Menten model, the Michaelis constants K_M and $K_{M'}$ being determined independently **[207]**. The values of k_{catL} and k_{catD} determined at pH = 7.5 are consistent with previous values obtained at pH = 6.9 and 8.9 by CD technique, thus showing the interest and robustness of the method proposed.

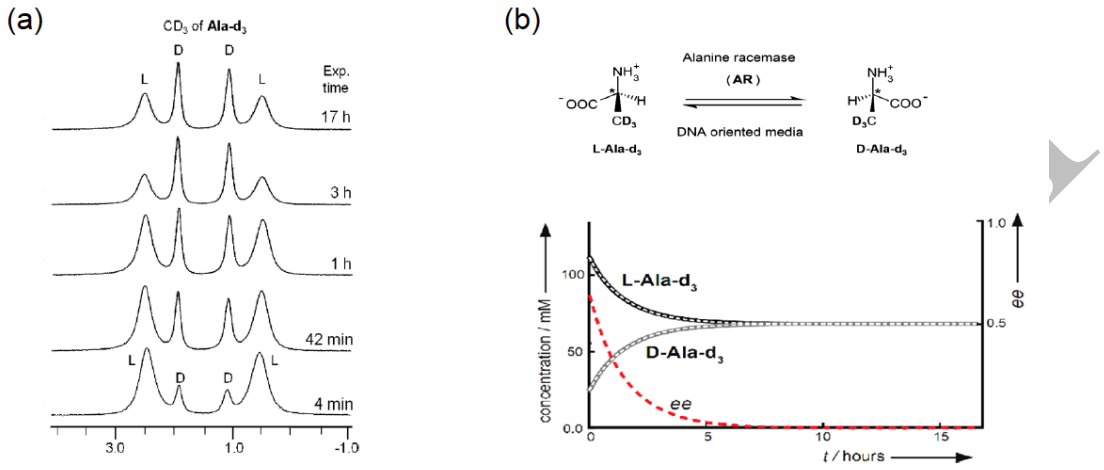

Figure 46 *(a) Evolution of ^{2}H-{^{1}H} 1D signals (same scale) of (L)- and (D)-**ALA**-d_3 recorded at different time intervals after the introduction of **AR** in the DNA-based mesophase. (b) Variation of ee (red dashed line) and experimental (black and grey continuous lines) and fitted (white dashed lines) concentrations (in mM) of (L)- and (D)-**ALA**-d_3 as a function of reaction time.* ***Figure from Ref. [207] with permission.***

Finally, in the framework of *in-situ* reaction monitoring combining weakly orienting solvents and ^{2}H NMR, several anisotropic ^{2}H ultrafast 2D-NMR experiments (denoted "ADUF" spectroscopy) have been designed to follow extremely fast and/or multiple (cascade) chemical transformations for which the fast identification and reliable quantification of ^{2}H signals of chiral (or not) products (reactants, (un)stable intermediates, products, …) could be required. These particular homonuclear experiments replace the usual time encoding by a spatial encoding in QUOSY-like sequences (*Q*-COSY, *Q*-resolved and *Q*-DQ) allow recording anisotropic ^{2}H spectra in sub-second experimental times, allowing to enlarge the usefulness of the proposed technique **[208, 210]**.

X. CONFORMATIONAL ANALYSIS IN ORIENTED SYSTEMS

10.1 | Views on the conformational distribution

The presence of conformational degrees of freedom in flexible molecules, meaning large, low frequency torsional molecular motions, may strongly complicates the interpretation of the anisotropic NMR data compared to the case of rigid compounds **[210, 211]**. Indeed, in the case of flexible analytes one has to deal with the effect of two simultaneous motional averagings: the averaging process due to the tumbling motion of the compound (as for rigid compounds) and the averaging process due to conformational flexibility, implying the existence of large number of different rotamers and conformations, each with its own potential energy and stability. Any flexible molecule therefore exists in more than one conformation each with its own probability and its own Saupe ordering

matrix. If the conformer interconversion rate is in the slow exchange NMR limit, a separate spectrum is expected for each conformer. The analysis of these NMR spectra yields separated conformer geometries and order tensors, while conformer probabilities are obtained from relative integrated intensities. This case is therefore as in conventional isotropic solvents quite easy to be dealt with. Most cases of interest, however, are in the fast exchange NMR limit, and a single, statistically averaged spectrum is measured in that situation.

In previous sections, we have presented various qualitative interpretations of experimental results obtained with dynamical molecules, but that was intimely connected to the conditions of fast or slow exchange regime. To go further, we describe in this last section of this review a quantitative approach developed in the latest decade and used on pharmaceutical targets. Indeed, the spatial arrangement adopted by bioactive flexible compounds affects the interactions they create with endogenous ligands as well as specific systems for the controlled delivery of active agents, influencing hence their biological activity, pharmacokinetic properties and metabolic degradation pathways **[212, 213, 214]**. The elucidation of 3D structures and conformational equilibrium is a preliminary step for rationalizing the relationship between conformation and drug activity and can help for drug design, screening processes and pharmaceutical formulation development.

NMR investigations made in liquid environments are interesting since it is the state of matter where molecules generally interact with endogeneous ligands and, if bioactive, play their role in the living organism. Over the years, *J*-couplings and nOe measurements have provided key clues about the conformation the drug can adopt in solution **[215]**. However, these NMR parameters are quintessentially short range, thus these methods have limitations for obtaining connectivity information between atoms which are far apart and they are often insufficient for an unequivocal structural or conformational determination, in particular when these measurements average over two conformers or more **[94, 216, 217]**.

As an alternative and/or complementary strategy, the combination of NMR using liquid-crystalline solvents and the AP-DPD approach (see below) has been developed and exploited to analyze molecules of pharmaceutical interest and possessing single and multirotors. Two families of drugs were investigated: i) the profens (from flurbiprofen to naproxen), ii) the salycilates (phenylsalicylic acid to diflunisal). As illustrations, the AP-DPD approach combined to NMR in CLC will be only examplified on the case of diflunisal, a single rotor molecule, the case of naproxen possessing two independent rotors and finally the (*S*)-ibuprofen as model for coupled multi-rotors molecules (see **Figure 47**).

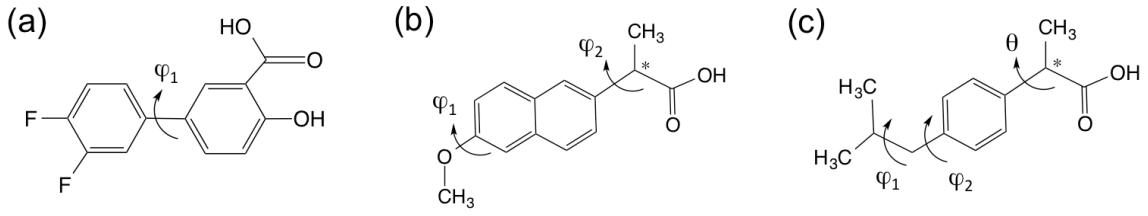

Figure 47 *Molecular structures of (a) diflunisal, (b) (S)-naproxen and (c) (S)-ibuprofen along with the various rotors (φ_I or θ) shown.*

To explicitely consider both the orientational overall motion and the internal rotation motion, it is possible to define a singlet orientational-conformational distribution function, $P_{\mathrm{LC}}(\Omega,\{\phi\})$, assuming as generally done, the conformational probability of a molecule is independent on the probability of its neighbours. Here, for a sake of clarity and simplicity, the conformational problem will be only examplified for the specific case of the dipolar interaction. In an uniaxial liquid-crystalline medium where the director aligns along the $\mathbf{B_0}$ axis (see **Figure 2**), the experimental RDC between the *i*th and *j*th nuclei of a flexible molecule, $D_{\mathrm{ij}}^{\mathrm{obs}}$, can be written as **[218]**:

$$D_{\mathrm{ij}}^{\mathrm{obs}} \propto \int P_{\mathrm{LC}}(\Omega,\{\phi\})\, D_{\mathrm{ij}}(\Omega,\{\phi\})\mathrm{d}\Omega\mathrm{d}\{\phi\} \qquad (\mathbf{14})$$

where the function $P_{\mathrm{LC}}(\Omega,\{\phi\})$ describes the properly normalised orientational-conformational probability distribution function of the solute in the partially ordered environment. In other words, it represents the probability of finding the mesophase director Ω-oriented in the solute-fixed frame when the probe-molecule is in its $\{\phi\}$-conformation in the aligned solution.

Following **Eq. 14,** $D_{\mathrm{ij}}(\Omega,\{\phi\})$ is the RDC between *i* and *j* nuclei within the solute for a given conformation, $\{\phi\}$, submitted to its own orientation Ω respect to the director, **n**, of the mesophase. The quantity $P_{LC}(\Omega,\{\phi\})$ can be related to the total singlet orientational energy, $U_{\mathrm{LC}}(\Omega,\{\phi\})$, $P_{\mathrm{LC}}(\Omega,\{\phi\}) \propto exp\left[-\frac{\mathrm{U}_{LC}(\Omega,\{\phi\})}{k_B T}\right]$, with T the absolute temperature and k_B the Boltzmann constant. In an anisotropic phase, the probability of finding a molecule with a particular conformation $\{\phi\}$ independent of its orientation, $P_{\mathrm{LC}}(\{\phi\})$, is determined by summing over all the orientations $P_{\mathrm{LC}}(\{\phi\}) = \int P_{\mathrm{LC}}(\Omega,\{\phi\})\, d\Omega$.

The mean-field approach allows to be built the term, $U_{\mathrm{LC}}(\Omega,\{\phi\})$, as a "mean-torque" potential by summing two contributions: $U_{\mathrm{ext}}(\Omega,\{\phi\})$ and $U_{\mathrm{int}}(\{\phi\})$. Identically null in isotropic solvent $U_{ext}(\Omega,\{\phi\})$ is an intermolecular potential which depends on both orientational and internal angles, hence contains the conformation/orientation coupling. $U_{\mathrm{int}}(\{\phi\})$ is the internal rotational potential independent of orientation of the molecule: it depends only on the conformational state, and hence the bond rotational potentials. Following $P_{\mathrm{LC}}(\Omega,\{\phi\})$ is expressed as:

$$P_{\mathrm{LC}}(\Omega,\{\phi\}) \propto P_{\mathrm{iso}}(\{\phi\}) \times exp\left[-\frac{U_{\mathrm{ext}}(\Omega,\{\phi\})}{k_{\mathrm{B}}T}\right], \qquad (\mathbf{15})$$

where the distribution function $P_{\mathrm{iso}}(\{\phi\}) \propto exp\left[\frac{-U_{\mathrm{int}}(\{\phi\})}{k_{\mathrm{B}}T}\right]$ represents the target of any conformational study in liquids. $\mathrm{P_{iso}}(\{\phi\})$ is free from any possible conformational effects induced by the orientational ordering of LC, and describes the conformational distribution of the solute in a "virtual" solvent possessing the same physical chemistry properties as the oriented solvent used, with the exclusion of its ability to induce an orientational order. Note that $P_{\mathrm{iso}}(\{\phi\})$ and $P_{\mathrm{LC}}(\{\phi\})$ are fundamentally not expected to be identical, and are in general not equal, with a difference between them increasing as the orientational order increases.

In order to simplify the treatment data, it is quite usual to assume that internal vibrations and overall reorientational (tumbling) motions of the molecule are decoupled, because the dependence of $S(\Omega)$ on the vibrational state of the molecule is believed to be small enough to be neglected. It would be tempting to assume that the dependence of Saupe order parameters on $\{\phi\}$ can also be neglected, as often done when dipolar couplings are used to study protein structures; it is however likely to lead to major errors in the function $P_{\mathrm{LC}}(\{\phi\})$ and the structures derived when there is an appreciable degree of intramolecular motion present in the molecule.

The experimental observables involve products of conformational probabilities and orientational factors and so they cannot be determined individually. Therefore, either the Saupe order matrix $S_{\alpha\beta}$ (one for each conformer) or the conformer populations should be known. Without any reliable equation relating the $S_{\alpha\beta}$ elements of different conformers, models has to be tested in order to treat the interdependent conformational-orientational problem and extract useful information from the experimental data. These models allow: i) to shape the conformational distribution function, i.e introduce a set of potential/probability parameters, ii) to describe, in some way, the conformational dependence of the order parameters. Even so, the number of unknowns *versus* the number of independent variables is often critical and a huge amount of experimental data would be necessary to describe all degrees of freedom.

10.2 | Theoretical approaches describing the interdependent conformational-orientational problem.

Several such approaches have been considered. The simplest possible model, the Rotational Isomeric State (RIS) model assumes that only a restricted set of minimum-energy structures is populated **[219]**. For instance, the free rotation of methyl groups are described by the three statistically weighted staggered conformers. More realistic models allow for continuous bond rotations. Two main approaches, alone or combined, have been proposed in the past **[220]**: i) the Additive Potential (AP) method, an "approximate" approach whose aim is to reduce latest equations to manageable expressions by using some physically justifiable approximations **[221]**, ii) the Maximum Entropy (ME) method, an "unbiased" method based on Information Theory **[222, 223]**. In the last decade, was developed a hydrid approach, combining the AP method and a direct probability distribution, DPD, for describing directly the internal potential as sum of Gaussians **[224]**. Here will be however only introduced and discussed the AP and DPD approaches useful for describing $P_{\mathrm{LC}}(\Omega,\{\phi\})$ in the attempts done in CLCs, as schematically overviewed in **Figure 48**. A more detailed description of this approach is available in references **225** and **226**.

The AP methods for modelling $U_{\mathrm{ext}}(\Omega,\{\phi\})$. Several ways of modeling $U_{\mathrm{ext}}(\Omega,\{\phi\})$ have been proposed; here is discussed only the so-called AP-Independent Fragment model the most commonly used approach to model $U_{\mathrm{ext}}(\Omega,\{\phi\})$, originally introduced by Marčelja and subsequently modified by Emsley *et al*. **[221, 227]**. According to this approach, the $U_{\mathrm{ext}}(\Omega,\{\phi\})$ is written as:

$$U_{\text{ext}}(\Omega,\{\phi\}) = -\sum_{L=2;\text{m}=0,\pm2} \varepsilon_{\text{L,m}}(\{\phi\}) C_{\text{L,m}}(\Omega), \quad (16)$$

where $C_{2,\text{m}}(\Omega)$ are modified spherical harmonics, $\varepsilon_{\text{L,m}}(\{\phi\})$ are elements of a suitable conformation-dependent solute-solvent interaction tensor expressed with respect to the principal axes for each conformation $\{\phi\}$. Their chemical meaning is related to the strength of the interaction between the molecular mean field and the molecule in its conformation $\{\phi\}$.

The peculiar feature of the AP method is that these conformationally dependent interaction tensors $\varepsilon_{L,m}(\{\phi\})$ can be written as a sum of conformationally independent contributions from each rigid fragment *j* in the molecule, $\varepsilon_{2,m}(\{\phi\}) = \sum_p \sum_j \varepsilon_{2,\text{p}}^{\text{j}} D_{\text{p,m}}^2\left(\left\{\Omega_{\phi}^{\text{j}}\right\}\right)$. Here, *j* runs on the number of fragments and $\left\{\Omega_{\phi}^{\text{j}}\right\}$ is the set of Euler angles that describes the orientation of the *j*-fragment in the molecule with respect to fixed axes in a rigid fragment of the molecule, *via* the Wigner rotation matrix $D_{\text{p,m}}^2\left(\left\{\Omega_{\phi}^{\text{j}}\right\}\right)$. In this way, with $\varepsilon_{2,\text{p}}^{\text{j}}$ as adjustable terms, it is possible to express the continuous dependence of the order parameters on the set of internal coordinates. The number of unknowns, $\varepsilon_{2,\text{p}}^{\text{j}}$, is strongly reduced when chosen according to the local symmetry of the fragments within the molecule. There will be for instance only one contribution, $\varepsilon_{2,0}^{\text{j}}$, for a fragment with cylindrical symmetry and two, $\varepsilon_{2,0}^{\text{j}}$ and $\varepsilon_{2,2}^{\text{j}}$, from a fragment with lower symmetry, provided that the principal axes for $\varepsilon_{2,\text{p}}^{\text{j}}$ are known.

Description of $U_{\text{int}}(\{\phi\})$ and DPD approach. To fully describe $P_{\text{LC}}(\{\phi\})$ and $\text{P}_{\text{iso}}(\{\phi\})$, the conventional way is to set an appropriate model for $U_{\text{int}}(\{\phi\})$. Models for $U_{\text{int}}(\{\phi\})$ may vary, and are often specific to the molecule under consideration and the amount of experimental data available from which they may be characterized. An alternative approach is based on the Direct Probability Description (DPD) of the conformational distribution **[224]**. In this case, $P_{\text{LC}}(\{\phi\})$ is modelled without any assumptions on $U_{\text{int}}(\{\phi\})$. According to this model, $P_{\text{LC}}(\{\phi\})$ is written as a sum (for interdependent conformations) or a product (for independent states) of Gaussian functions whose related parameters can then be varied independently, but with the constraint that $P_{\text{LC}}(\{\phi\})$ is normalized.

Knowing $P_{\text{LC}}(\{\phi\})$, it becomes straightforward to determine $P_{\text{iso}}(\{\phi\})$. Compared with the conventional Fourier expansion approach, the DPD method has particular advantages: i) a smaller number of parameters is useful to give a correct description of the probability function, ii) each parameter in the expansion influences only one peculiar aspect of the probability distribution (positions, width and height of maxima), and iii) conformational parameters are usually less correlated. This makes very easy to describe even complicated conformational probability density functions (even those needed to deal with cooperative motions). Usually, a good starting approximation for the shape of $P_{\text{iso}}(\{\phi\})$ is obtained from *in silico* calculations using any appropriate theoretical calculations software and method.

Technically speaking, the determination of structure, order and conformational distribution of the molecule is obtained by fitting a set of calculated dipolar couplings (obtained by a trial set of orientational, geometrical and conformational parameters) against the experimental data, while iterating on a set of unknown parameters till their optimized values. Such unknowns can be collected into three categories: i) the geometrical parameters (distances and angles), ii) the orientational parameters, whose number varies with the molecule and the model used to fit the data, and iii) the potential parameters, including those parameters required to shape the internal potential. Dipolar couplings are iteratively calculated for each selected conformation, averaged on the whole distribution, and then fitted against their experimental counterpart, until their best agreement (see **Figure 49**). Using weakly orienting polypeptide mesophases, vibrational effects do not affect the values of ^{1}H-^{1}H or ^{1}H-^{13}C dipolar couplings, and hence, the computation of vibrational corrections is rarely considered **[228, 229]**.

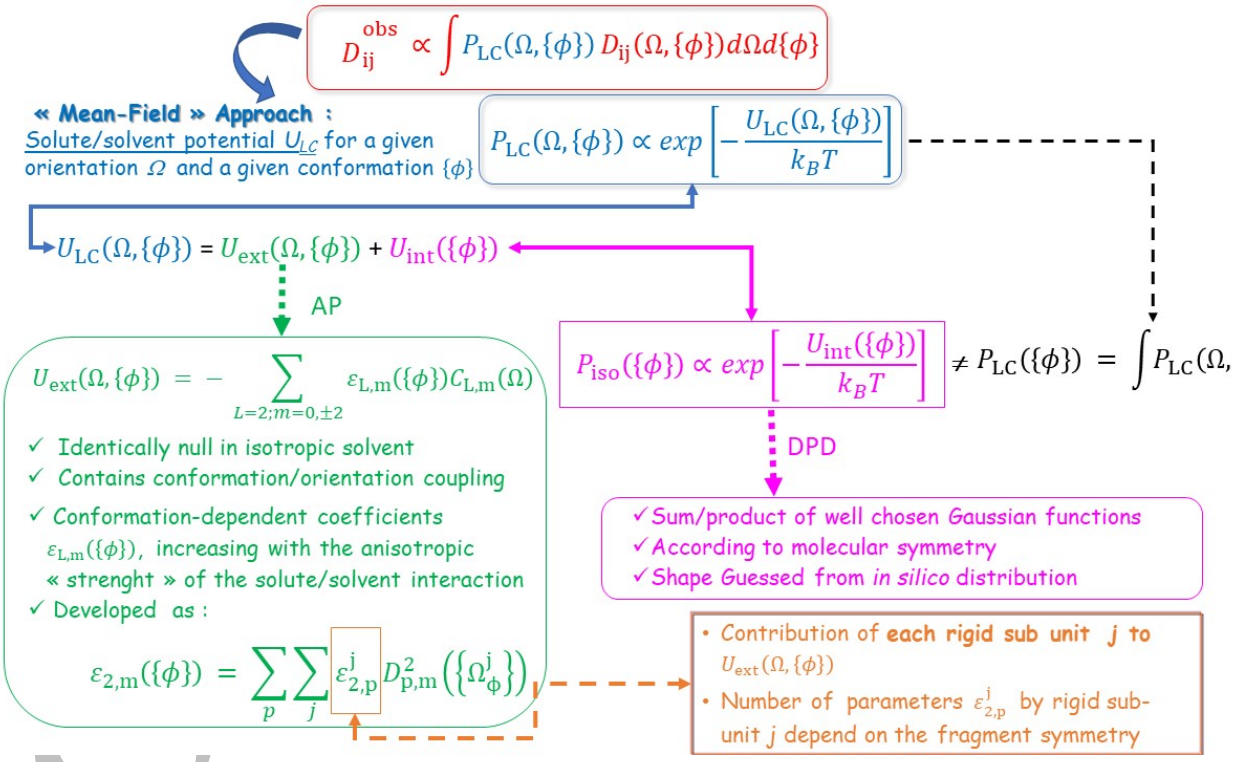

Figure 48 *Schematic overview of the analytical strategy used describing the conformational distribution of flexibles solutes, involving the AP-DPD approach. The final target is* $P_{iso}(\{\phi\})$.

10.3 | Single-rotor molecules: the case of diflunisal

The AP-DPD approach was first examplified on the case of diflunisal (**DFL**) (see **Figure 50a**) dissolved in a PBLG phase **[230]**. For this compound, it is important to establish the geometry of the most stable conformers and a good estimate of the potential energy surface (PES) from molecular modelling calculations. Density functional theory (DFT) approach with the functional B3LYP and the basis set 6-31++G**, using the Gaussian09 software package, was chosen **[231]**.

For **DFL** the presence of a hydrogen bond between -C=O and -O-H reduces to one the degree of flexibility of the molecule. This means that $P_{\mathrm{iso}}(\{\phi\})$ equals to $P_{\mathrm{iso}}(\varphi)$, the torsional probability distribution around the single inter-ring torsion angle φ = C_4-C_5-C_7-C_8. First, structures and locations of the lowest minimum energy conformers were evaluated *in vacuo*. In order to exclude significant solvent effects, geometry optimization calculations were also performed taking into account tetrahydrofuran as medium, by means of the Polarizable Continuum Model (PCM) implemented in the Gaussian package **[231]**. No significant difference in terms of structure and relative energies of the most stable conformers emerged between the gas and liquid state. Then, assuming the bond lengths and angles are, to a good approximation, independent on the conformational state, the minimum energy structures found for an isolated molecule were used to perform *in vacuo* a rigid PES scan for the torsion angle φ between the two rings over the 0° - 360° range with a 5°-step sampling **[230]**. This hypothesis of weak correlation between geometrical data and conformational distribution was carefully tested and validated in the case of **DFL**. Indeed, no significant difference was observed on the structures and proportions of conformers obtained by allowing a geometry optimization at each step of the conformational sampling, and by the rigid PES scan described. Following the solute symmetry, a couple of two non-equally probable conformers is found (see **Figure 50**).

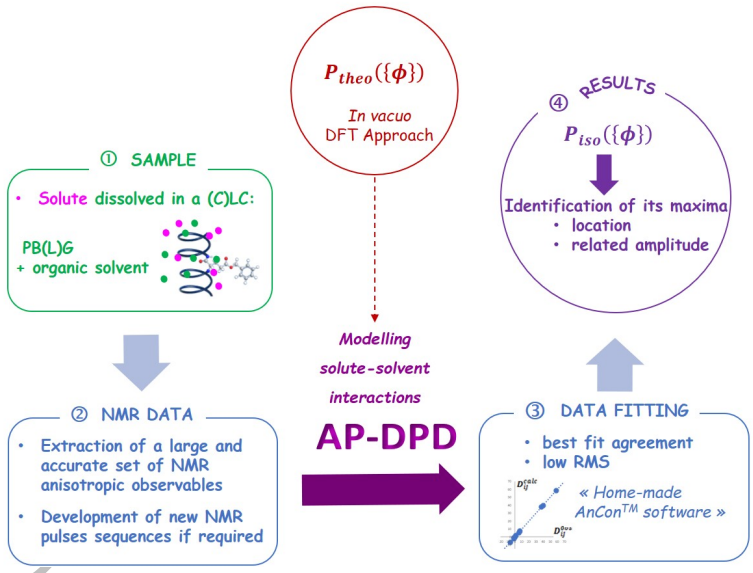

***Figure 49**. Schematic description of the conformational analysis in a PBLG mesophase using the AP-DPD model: from the sample preparation (step 1) to the determination of the isotropic conformational distribution of the flexible solute studied (step 4).*

Starting from the shape of conformational distribution found *in vacuo*, $P_{\mathrm{iso}}(\varphi)$ can be directly modelled as a sum of four Gaussian functions by the DPD, namely:

$$P_{\mathrm{iso}}(\varphi) \propto \left\{\frac{A_1}{2}\cdot exp\left[-\frac{(\varphi-\varphi_1^{max})^2}{2h_1^2}\right] + \frac{A_1}{2}\cdot exp\left[-\frac{(\varphi-\pi+\varphi_1^{max})^2}{2h_1^2}\right]\right. \quad (17)$$

$$+ \frac{A_2}{2} \cdot exp\left[-\frac{\left(\varphi-\frac{\pi}{2}+\varphi_2^{max}\right)^2}{2h_2^2}\right] + \frac{A_2}{2} \cdot exp\left[-\frac{\left(\varphi-\frac{\pi}{2}-\varphi_2^{max}\right)^2}{2h_2^2}\right]\Bigg\},$$

where φ_1^{max} and φ_2^{max} are the most probable values of the torsion angle, $A_1$and $A_2 = 1 - A_1$ are the relative weights of the two couples and, finally, h_1 and h_2 give the width at half maximum height of each Gaussian.

Within the AP model, for the specific case of **DFL**, the description of orientational interaction energy requires six fragment tensors $\varepsilon_{2,p}^{j}$, as follows: i) $\varepsilon_{2,0}^{ring\ A}$ and $\varepsilon_{2,2}^{ring\ A}$ for the biaxial C_{2v}-symmetry fluorinated ring (ring A), ii) $\varepsilon_{2,0}^{ring\ B}$ and $\varepsilon_{2,2}^{ring\ B}$, for the biaxial C_{2v}-symmetry salicylic ring (ring B), iii) $\varepsilon_{2,0}^{C-F}$ for the monoaxial component along the C-F bond direction, iv) $\varepsilon_{2,0}^{C-C}$, for the monoaxial component along the C-C(OOH) bond direction (see **Figure 44a**).

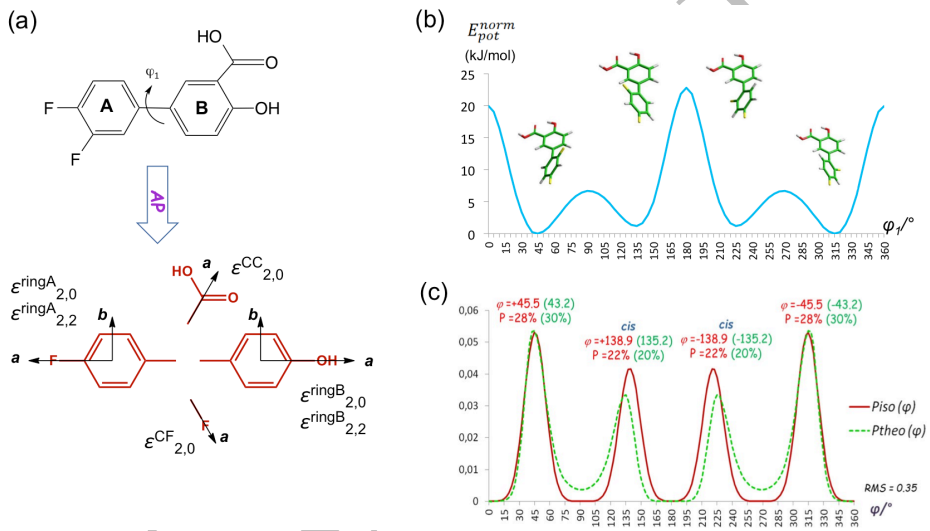

Figure 50 *(a) AP modelisation of $U_{ext}(\Omega,\{\phi\})$ applied to diflusional. (b) Variation of normalized potential energy as a function of φ_1 obtained from B3LYP/6-31++G** calculations in vacuo. (c) Modelisation of $P_{iso}(\varphi)$ of* ***DFL*** *compared to its in vacuo theoretical torsional curve $P_{theo}(\varphi)$.* ***Figure adapted from Ref. [230] with permission.***

In the case of **DFL**, ten unknowns (six $\varepsilon_{2,p}^{j}$ and four potential terms) have to be determined using forty independent D_{ij}^{obs} (twenty one for the fluorinated ring, nine for the salicylic ring, 10 between the two rings). In this peculiar case, NMR methodology was performed in order to properly be able to measure and individuate couplings involving fluorine nuclei **[230]**. After optimization, a good agreement between D_{ij}^{obs} and D_{ij}^{calc} has been obtained.

10.4 | Conformational distribution of multi-rotors molecules

Analysis of (*S*)-naproxen. (*S*)-naproxen is a commonly used as non-steroidal anti-inflammatory drugs (NSAIDs) belonging to the family of profens. From the NMR point of view, this chiral molecule is a 14-spin system constituted by two non-coupled torsional degrees of freedom (φ and θ) and three fragments interconnected, denoted "M" (methoxy-group), "N" (naphtalenyl group), and "P" (profenic group) were denoted

for the conformational analysis, as shown in the **Figure 51a**. As for single-rotor molecules, the AP-DPD method combined to anisotropic NMR data (PBLG) allows to determine the molecular conformational distribution **[232]**. In the case of independent rotors (here two), as previously stated, it is quite trivial to define $P_{\mathrm{iso}}(\theta,\varphi) = P_{\mathrm{iso}}(\theta) \times P_{\mathrm{iso}}(\varphi)$ once the isotropic single rotor probability function determined by analog processing described for diflunisal preceedingly.

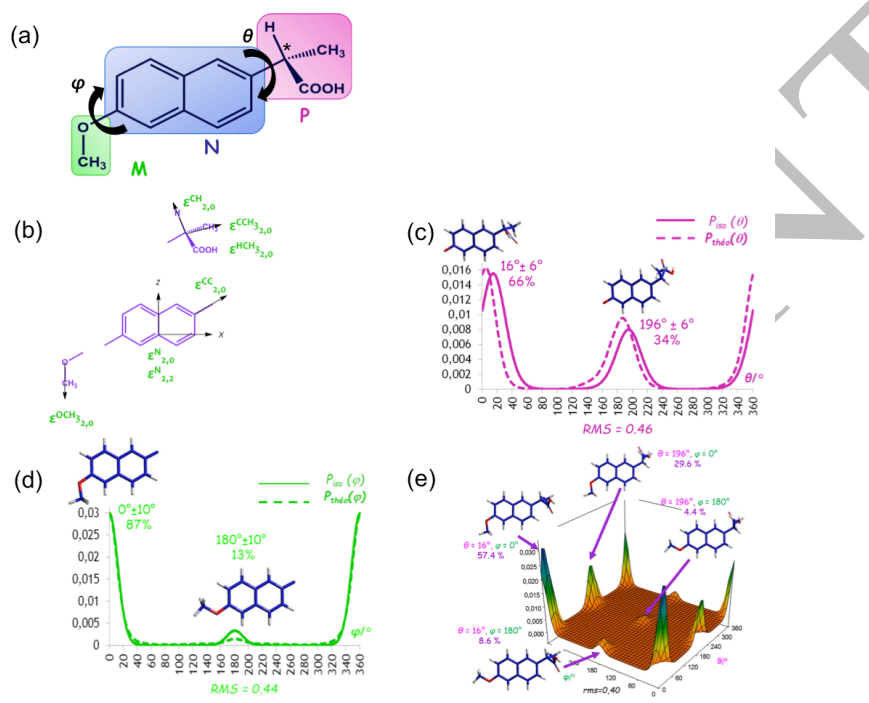

Figure 51 *(a and b) Decomposition of (S)-naproxen into three fragments and AP modelisation applied. (c and d) Shapes of functions $P_{iso}(\theta)$ and $P_{iso}(\varphi)$, respectively, compared to their in vacuo theoretical torsional curves couterparts. (e) Plot of $P_{iso}(\theta,\varphi)$ resulting from AP-DPD approach in the case of (S)-naproxen.* ***Figure adapted from Ref. [232] with permission.***

Analysis of (*S*)-ibuprofen (*S*)-ibuprofen is a three-rotor chiral molecule whose the conformational surface can be described according to the three dihedral angles (φ_1, φ_2 and θ) as displayed in **Figure 52 [233]**. For this solute, the torsional degrees of freedom φ_1 and φ_2 are coupled while θ is independent. Compared to previous cases, this last system is more complex to handle and request a larger number of anisotropic data. In order to increase this number, two PBLG-based anisotropic samples with different concentrations in polypetide were prepared (9.0 and 11.7 wt%) and data were combined. As for the others cases, 3D structure of ibuprofen was first investigated using DFT calculations with the widely employed hybrid method functional B3LYP and the basis set 6-31++G**. Assuming the independence of the rotations of the two *para*-substituents, rigid and relaxed PES scans were performed separately for the torsion angle θ for the propanoic acid fragment, over the 0° − 360° range with a 3°-step sampling, and for the torsion angles φ_1 and φ_2, for the isobutyl chain, over the 0° − 360° range with a 20°-step sampling, allowing to obtain the in *vacuo* theoretical conformational distributions $P_{\mathrm{theo}}(\theta)$ and $P_{\mathrm{theo}}(\varphi_1,\varphi_2)$, respectively **[232]**. Concerning the dihedral angle θ, it was possible to extract 24 independent

dipolar couplings to characterize $P_{\mathrm{iso}}(\theta)$: they were reproduced with a good agreement and a satisfactory RMS error of 0.37 Hz, and two equally populated maxima at 13° ± 1° (conformation I) and 193° ± 1° (conformation II), indicating the quasiplanarity of the hydrogen atom directly bound to the stereogenic carbon atom were found. Concerning both cooperative motions defined by φ_1 and φ_2, a good fitting of the experimental data of each sample could be achieved considering an equilibrium between four predominant *gauche* conformers (23.25% each in terms of relative population) and two barely populated *trans* structures (3.5% each). The corresponding torsional probability distribution $P_{\mathrm{iso}}(\varphi_1, \varphi_2)$ is reported in **Figure 52d**. It shows a significant qualitative agreement with the theoretical probability distribution $\mathrm{P}_{theo}(\varphi_1, \varphi_2)$ calculated from the potential energy values obtained by DFT calculations (see **Figure 52d)** as well as theoretical data found in the literature although an upper shift of about $10° - 15°$ can be noticed by comparing the φ_2 value for gauche conformers. As a consequence of the symmetry of the whole molecular system, the twelve conformers obtained combining the spatial arrangement for the propionic fragment (I and II) and for the isobutyl chain (g_1, g_1*, g_2, g_2*, t and t*) end up overlapping, so that only six independent minimum-energy structures are needed to describe exhaustively the conformational flexibility of *S*-ibuprofen (see **Figure 52e**).

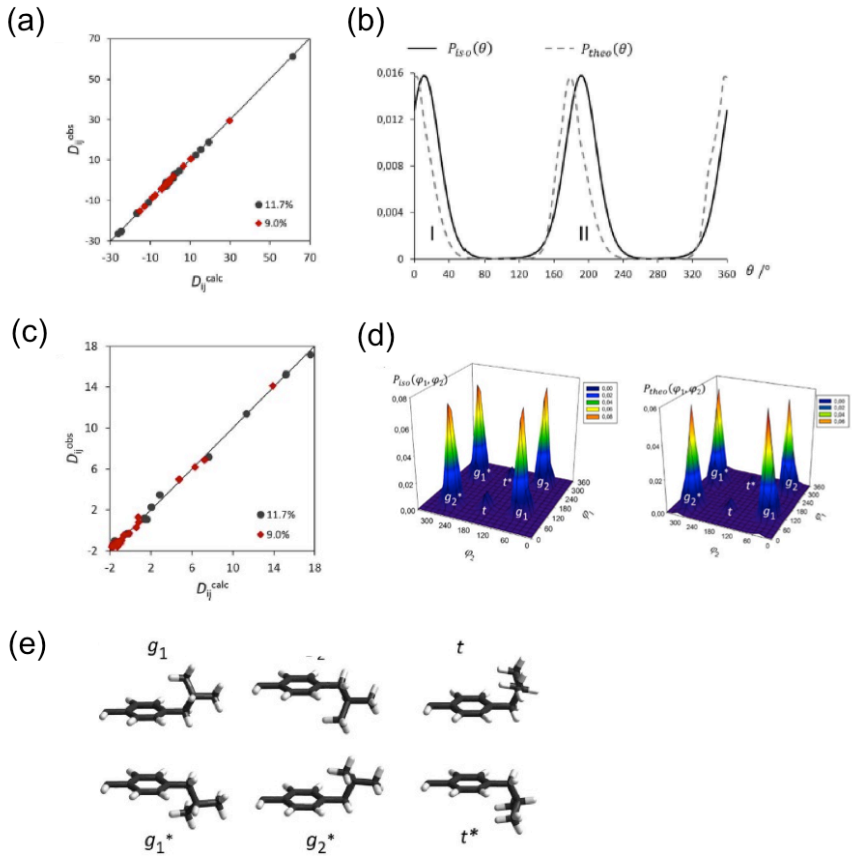

Figure 52 *(a) Description of best fit agreement between experimental and calculated dipolar couplings of (S)-ibuprofen allowing to characterize the function* $P_{iso}(\theta)$ *shown in (b). (c) Description of best fit agreement between experimental and calculated dipolar couplings allowing to characterize* $P_{iso}(\varphi_1, \varphi_2)$ *shown in graphs (d). (e) Representation of the six conformers of (S)-ibuprofen.* ***Figure adapted from Ref. [233] with permission.***

Finally, for the sake of completness, it is noteworthy to stress out a promising alternative approach combining MD simulations and RDC-based orientational tensorial constraints (MDOC) in order to overcome the use of theoretical models. Latest developments were successfully obtained, in particular, on **DFL**, based on the experimental data reported in Ref. **183**. Although a promising tool for the investigation of torsional angle distributions in flexible molecules, this approach requires quite high level/CPU time-consuming data computing and the use of the specific software (COSMOS) **[183]**.

XI. CONCLUSION AND PROSPECTS

Proposing tools to reveal the complexity of molecular stereogenicity concept is a fascinating investigation field and a continuous challenging task for spectroscopists. Many new aspects and original approaches have been explored and applied in France, but also in other international research groups, with the intensive work or remarkable achievements of G. Celebre, G. De Luca, R.R. Gil, C. Griesinger, B. Luy, G.E. Martin, A. Navarro-Vázquez, C.M. Thiele, M. Reggelin, R.T. Williamson, for instance, (non-exhaustive, alphabetic list), and all their collaborators.

Based on the detection of residual order-dependent intramolecular NMR interactions (RCSA, RDC, RQC), multinuclear NMR of magnetically oriented-samples (weaking oriented CLCs) provides original, efficient, flexible and versatile analytical tools to extract a wide variety of global or local molecular information on solutes, thus covering all the aspects of enantiomorphism (enantiomerism and enantiotopism). Advantageously, the advent of routine high magnetic fields has made possible the observation of nuclei with very low sensitivity with acceptable S/N ratios such as deuterium at the natural abundance level.

In this comprehensive compendium, we have shown, through illustrative examples, the various possibilities to probe chirality and prochirality based on the same concept, namely the induction of diastereomorphic interactions inside an enantiopur oriented environments. The key advantage of this methodology is therefore the astonishing ability of polypeptide helices to interact enantioselectively with almost type of enantio-objects (whatever their chemical nature and their structure) to give sufficiently large orientational differences exploitable in various analytical domains: 3D structure, configuration and conformational analysis, internal dynamics, natural isotopic distribution determination, and finally the molecular stereochemistry if the alignment system is chiral and enantiopur.

For almost all of the NMR methods designed, enantiodifferentiation and quantitative determination of enantiomeric purity is experimentally possible even if each of them possesses both advantages and drawbacks in terms of spectral complexity, signal sensitivity, quality of enantiodiscrimination and accuracy in measurements of *ee* values. Selecting the most adequate anisotropic NMR tool and spy nucleus for a given compound will depend on both the chemical and NMR features but also the available amount of material. This choice, however, does not exclude the examination of other nuclei of the molecule when the first results obtained are not convincing.

Finally, the valuable advantage lies on the labelling or any chemical modification of the chiral material is

needed and the NMR requirements are not different compared to those for other isotropic methods.

Pioneered from 1967, the efficient development of anisotropic enantiodiscrimination NMR tools really start with the use of weaking weakly oriented system made of polymeric-based, as PBLG, leading continuous new methods demonstrating the vitality of this exciting approach to solve new analytical problems.

Numerous research axes exploiting the enantiodisciminating potential of NMR in CLC are still open, both from a methodological and application point of view. In particular, the recent developments of the dissolution dynamic nuclear polarization (DNP) that could potentially be applied in anisotropic media to improve the sensitivity of low-abundance nuclei such as ^{13}C or ^{2}H when analyzing natural products with sub-ten milligram quantities, seems to be a formidable challenge.

An active work on the conformational analysis of flexible enantiomers in PBLG phase remains to do, in particular with the analysis a mixture of enantiomers (in as single sample) and the comparison of their respective in-solution conformational distribution. This important aspect of topics is under investigation and a complete work will be reported soon.

Also, as already mentionned above, important developments remain to perform concerning the computational predition of solute orientational orders (in polypeptide based system as PBLG) based on molecular dynamics approaches. Several papers have been reported on the subject, so far **[75, 180, 181, 182, 183, 184, 185, 186]**. However contrasted results were obtained depending on the model/parameter used, and authors remain more or less cautious about the relevance of predicted results. The difficulty for fine-grained predictions originates in particular from the complexity of the conformational dynamics of the polymer side and the subsequent elaboration of a robust model keeping physically and chemically significant. Additionnally, in the case of flexible molecules, it is far from trivial to take into account also to a good approximation the whole solute conformational space interacting into (at least) a three-bodies system in case of lyotropic media (solute, polymer, co-solvent) **[180]**.

Finally, the ultimate challenge (and probably the most difficult one) will be the promotion of this methodology to the large community of chemists (non-expert NMR users) and the demonstration of the advantages of anisotropic NMR compared to isotropic NMR methods used in routine.

XII. ACKNOWLEDGMENTS

Authors would like to warmly thank Prof. Jacques Courtieu who initiated the first developments of NMR spectroscopy on CLCs in France, Prof. Marcello Longeri for fruitful scientific discussions and finally Profs. Aahron Loewenstein, James W. Emsley and Zeev Luz, for their active contributions over two decades.

Also thank you to all international (Brazil, Canada, England, Finland, Germany, India, Israel, Italy, Poland, USA, …) scientific partners, all national (CEA, ENSCP, ICSN, Universities of Lille, Nantes,

Paris VI, Paris VII, Orléans, Rennes, Strasbourg, …) collaborators and ICMMO's colleagues who successfully contributed to all the work done, with the help of all students and visitors of our laboratory who also participated, as well.

XIII. REFERENCES

1. Emsley JW, Feeney J. Milestones in the first fifty years of NMR. *Prog Nucl Magn Reson Spectrosc*. **1995**; 28: 1-9.

2. Eliel EL, Wilen SH in Stereochemistry of organic compounds, John Wiley & Sons, New York, (**1994**).

3. Emsley JW in NMR in anisotropic systems, theory. Encyclopedia of Spectroscopy and Spectrometry, *Eds.* Lindon JC, and GE, Koppenaal DW, Elsevier / Academic Press. Vol. 3: 134-139, (**2017**).

4. Lesot P, Aroulanda C, Berdagué P, Meddour A, Merlet D, Farjon J, Giraud N, Lafon, O. Three fertile decades of methodological developments and analytical challenges. *Prog Nucl Magn Reson Spectrosc*. **2020**; 116: 85-154.

5. Lesot P, Aroulanda C, Zimmermann H, Luz Z. Enantiotopic discrimination in the NMR spectrum of prochiral solutes in chiral liquid crystals. *Chem Soc Rev.* **2015**; 44: 230-275.

6. Sarfati M, Lesot P, Merlet D, Courtieu J. Theoretical and experimental aspects of enantiomeric differentiation using natural abundance multinuclear NMR spectroscopy in polypeptide liquid crystals. *Chem Commun*, **2000**; 2069-2081.

7. Parker D. NMR determination of enantiomeric purity, *Chem Rev.* **1991**; 91: 1441-1457.

8. To find information, an entire issue of Chemical Review was devoted to cyclodextrins: *Chem Rev.* **1998**; 98: 1751-2076.

9. Wenzel TJ, Wilcox JD. Chiral reagents for the determination of enantiomeric excess and absolute configuration using NMR spectroscopy, *Chirality*. **2003**; 15: 256-270.

10. Wenzel TJ in Discrimination of chiral compounds using NMR spectroscopy, John Wiley & Sons, INC. New Jersey, **(2007**).

11. Saupe A, Englert G. High-resolution nuclear magnetic resonance spectra of orientated molecules *Phys Rev Lett.* **1963**; 11: 462-464.

12. Emsley JW, Lindon JC in NMR spectroscopy using liquid crystal solvents, Pergamon, Oxford, (**1975**).

13. Veracini CA in Nuclear magnetic resonance of liquid crystals, NATO ASI Series C, (**1985**).

14. Dong RY (Ed) in Nuclear magnetic resonance spectroscopy of liquid crystals, World Scientific, Singapore, (**2010**).

15. Zannoni C in Quantitative description of orientational order: rigid molecules, nuclear magnetic resonance of liquid crystals, edited by J.W. Emsley, Reidel, Dordrecht, pp. 1-34, (**1985**).

16. Merlet D, Emsley JW, Lesot P, Courtieu J. The relationship between molecular symmetry and second-rank orientational order parameters for molecules in chiral liquid crystalline solvents. *J Chem Phys.* **1999**; 111: 6890-6896.

17. Sackmann E, Meiboom S, Snyder LC. Nuclear magnetic resonance spectra of enantiomers in optically active liquid crystals, *J Am Chem Soc.* **1968**; 90: 2183-2184.

18. Brevard C in Handbook of high-resolution multinuclear NMR, New York, Wiley-Interscience, (**1981**).

19. Lesot P, Merlet D, Meddour A, Courtieu J, Loewenstein A. Visualization of enantiomers in a polypeptide liquid-crystal solvent through carbon-13 NMR spectroscopy. *J Chem Soc, Faraday Trans.* **1995**; 91: 1371-1375.

20. A. Meddour A, Berdagué P, Hedli A, Courtieu J, Lesot P. Proton-decoupled carbon-13 NMR spectroscopy in a lyotropic chiral nematic solvent as an analytical tool for the measurement of the enantiomeric excess, *J. Am Chem Soc.* **1997**; 119: 4502-4508.

21. Lesot P, Sarfati M, Courtieu J. Natural abundance deuterium NMR spectroscopy in polypeptide liquid crystals as a new and incisive means for enantiodifferentiation of chiral hydrocarbons. *Chem Eur J.* **2003**; 9: 1724-1745.

22. Lesot P, Courtieu J. Natural abundance deuterium NMR spectroscopy: developments and analytical applications in liquids, liquid crystals and solid phase. *Prog Nucl Magn Reson Spectrosc.* **2009**; 55: 128-159.

23. Lesot P, Lafon O. Natural abundance ^{2}H NMR spectroscopy, in Encyclopedia of Spectroscopy and Spectrometry. *Eds.* Lindon J, Tranter GE and Kopenaal DW, Elsevier, Vol. 3: 1-14, (**2017**).

24. Graf E, Graff R, Hosseini W, Huguenard C, Taulelle F. Probing peristatic chirality of alkaline cations: NMR study of alkaline borocryptates, Chem. Commun. **1997**; 1459-1460.

25. Jakubcova M, Péchiné J-M, Baklouti A, Courtieu J. Measurement of the optical purity of fluorinated compounds using proton decoupled ^{19}F-NMR spectroscopy in a chiral liquid crystal solvent, *J. Fluorine Chem.* **1997**; 86: 149-153.

26. Madiot V, Grée D, Grée R, Lesot P, J. Courtieu. Highly enantioselective propargylic monofluorination established by carbon-13 and fluorine-19 NMR in chiral liquid crystals. *Chem. Commun*. **2000**; 169-170.

27. Phillips AR, Sharman GJ. The measurement of high enantiomeric excesses in chiral liquid crystals using ^{19}F NMR and exchangeable protons in ^{2}H NMR. *Chem. Commun*. **2004**; 1330-1331.

28. Berdagué P, Herbert-Pucheta J-E, Jha V, Panossian A, Leroux F, Lesot P. Multi-nuclear NMR of axially chiral biaryls in polypeptide orienting solvents: spectral discriminations and enantiorecognition mechanisms. *New J Chem*. **2015**; 39: 9504-9517.

29. Giraud N, Farjon J. Analyses of enantiomeric mixtures using chiral liquid crystals. *Current Opinion in Colloid & Interface Science*. **2018**; 33: 1-8.

30. Prabhu UR, Suryaprakash N. Application of z-COSY experiment and its variant for accurate chiral discrimination by ^{1}H NMR. *J Magn Reson.* **2010**; 202: 217-222.

31. Prabhu UR, Suryaprakash N. Band selective small flip angle COSY: A simple experiment for the analyses of ^{1}H NMR spectra of small chiral molecules. *J Magn Reson.* **2008**; 195: 145-152.

32. Ziani L, Courtieu J, Merlet D. Visualisation of enantiomers via insertion of a BIRD module in X-H correlation experiments in chiral liquid crystal solvent. *J Magn Reson*. **2006**; 183: 60-67.

33. Farjon J, Baltaze J-P, Lesot P. Merlet D, Courtieu J. Heteronuclear selective refocusing 2D NMR experiments for the spectral analysis of enantiomers in chiral oriented solvents. *Magn Reson Chem.* **2004**; 42: 594-599.

34. Nath N, Suryaprakash N. Enantiodiscrimination and extraction of short and long-range homo- and hetero-nuclear residual dipolar couplings by a spin selective correlation experiment. *Chem Phys Lett.* **2010**; 496: 175-182.

35. Nath N, Suryaprakash N. Selective detection of single-enantiomer spectrum of chiral molecules aligned in the polypeptide liquid crystalline solvent: transition selective one-dimensional ^{1}H-^{1}H COSY. *J Magn Reson*. **2010**; 202: 34-37.

36. Giraud N, Beguin L, Courtieu J, Merlet D. Nuclear magnetic resonance using a spatial frequency encoding: application to J-edited spectroscopy along the sample. *Angew. Chem., Int. Ed.* **2010**; 49: 3481-3484.

37. Farjon J, Merlet D. SERF-filtered experiments: New enantio-selective tools for deciphering complex spectra of racemic mixtures dissolved in chiral oriented media. *J. Magn. Reson.* **2011**; 210: 24-30.

38. Merlet D, Ancian B, Courtieu J, Lesot P. Two-dimensional deuterium NMR spectroscopy of chiral molecules oriented in a polypeptide liquid crystal: application for the enantiomeric analysis through natural abundance deuterium NMR. *J Am Chem Soc.* **1999**; 121: 5249-5258.

39. Merlet D, Sarfati M, Ancian B, Courtieu J, Lesot P. Description of natural abundance deuterium 2D NMR experiments in weakly ordered liquid crystalline solvents using a tailored cartesian spin-operator formalism. *Phys Chem Chem Phys*. **2000**; 2: 2283-2290.

40. Lesot P, M. Sarfati M., Merlet D, Ancian B, Emsley JW, Timimi BA, 2D-NMR strategy dedicated to the analysis of weakly ordered, fully deuterated enantiomers in chiral liquid crystals. *J Am Chem Soc*. **2003**; 125: 7689-7695.

41. Lafon O, Lesot P, Merlet D, Courtieu J. Modified z-gradient filtering as a new mean to obtain phased deuterium autocorrelation 2D NMR spectra in oriented solvents. *J Magn Reson.* **2004**; 171: 135-142.

42. Lafon O, Lesot P. Deuterium three-dimensional NMR experiments for analysing weakly aligned, isotopically enriched molecules. *Chem Phys Lett.* **2005**; 404: 90-94.

43. Lesot P, O. Lafon O. Enantiomeric analysis using natural abundance deuterium 3D NMR spectroscopy in polypeptide chiral oriented media. *Chem Phys Lett.* **2008**; 458: 219-222.

44. K., O. Lafon, H. Zimmermann, E. Guittet, P. Lesot. Homo- and heteronuclear 2D NMR approaches to analyse a mixture of deuterated unlike/like compounds using weakly ordering chiral liquid crystals. *J Magn Reson.* **2007**; 87: 205-215.

45. Lesot P, Lafon O. Experimental detection of achiral and chiral naturally abundant ^{13}C-^{2}H isotopomers by 2D-NMR in liquids and chiral oriented solvents. *Anal Chem.* **2012**; 84: 4569-4573.

46. Kovacs H, Moskau D, Spraul M. Cryogenically cooled probes, a leap in NMR technology. *Prog Nucl Magn Reson Spectrosc.* **2005**; 45: 131-155.

47. Lafon O, Hu B, Amoureux J-P, Lesot P. Fast and high-resolution stereochemical analysis by non-uniform sampling and covariance processing of anisotropic natural abundance 2D ^{2}H-NMR datasets. *Chem Eur J.* **2011**; 17: 6716-6724.

48. Kazmierczuk K, Lafon O, Lesot P. Criteria for sensitivity enhancement by compressed sensing: practical application to anisotropic NAD 2D-NMR spectroscopy. *Analyst* **2014**; 139: 2702-2713.

49. Lesot P, K. Kazimierczuk K., Trebosc J., Amoureux J-P, Lafon O. Fast acquisition of multidimensional NMR spectra of solids and mesophases using alternative sampling methods. *Magn Reson Chem*. **2015**; 53: 927-939.

50. Laughlin RG in: The aqueous phase behaviour of surfactants. London: Academic Press, (**1996**), ISBN 0-12-437760-2.

51. IUPAC of Chemical Terminology, 2nd Ed. (the "Gold Book"). Compiled by McNaught AD and Wilkinson A. Blackwell Scientific Publications, Oxford (**1997**). Online version (2019-) created by Chalk SJ, ISBN 0-9678550-9-8, DOI: 10.1351/goldbook.

52. Lafontaine E, Pechiné J-M, Courtieu J, Maine CL. Visualization of enantiomers in cholesteric solvents through deuterium NMR. *Liq. Crystals.* **1990**; 7: 293-298.

53. Canet I, Lovschall J, Courtieu J. Visualization of enantiomers through deuterium NMR in cholesterics optimization of the chiral liquid-crystal solvent. *Liq. Crystals.* **1994**; 16: 405-412.

54. Bayle J-P, Courtieu J, Gabetty E, Loewenstein A, Péchiné J. Enantiomeric analysis in a polypeptide lyotropic liquid-crystal through proton decoupled deuterium NMR. *New J Chem.* **1992**; 16: 837-838.

55. Tjandra N, Bax A, Direct measurem*ent of distances and angles in biomolecules by NMR in a dilute liquid crystalline medium*. *Science* **1997**; 278: 1111-1114.

56. Panar M, W. D. Phillips WD. Magnetic ordering of poly(*γ*-benzyl-*L*-glutamate) solutions. *J Am Chem Soc*. **1968**; 90: 3880-3882.

57. Guha C, Hines WA, Samulski ET, Polypeptide liquid crystals: magnetic susceptibily, twist elastic constant, rotational viscosity coefficient, and PBLG sidechain conformation. *J Chem Phys.* **1974**; 91: 947-953.

58. Czarniecka K, Samulski ET, Polypeptide liquid crystals: a deuterium NMR study, *Mol Cryst Liq Cryst.* **1981**; 63: 205-214.

59. Poliks MD, Park YW, Samulski ET. Poly-*γ*-benzyl-L-glutamate: order parameter, oriented gel, and novel derivatives. *Mol Cryst Liq Cryst.* **1987**; 153: 321-345.

60. Aroulanda C, Sarfati M, Courtieu J, Lesot P. Investigation of enantioselectivity of three polypeptide liquid-crystalline solvents using NMR spectroscopy. *Enantiomer.* 2**001**; 6: 281-287.

61. Thiele CM, Simultaneous assignment of all diastereotopic protons in strychnine using RDCs: PELG as alignment medium for organic molecules. *J Org Chem.* **2004**; 69: 7403-7413.

62. Hansmann S; Larem T, Thiele CM. Enantiodifferentiating properties of the alignment media PELG and PBLG - a comparison. Eur. *J Org Chem.* **2016**; 7: 1324-1329.

63. Schwab M, Herold D, Thiele CM. Polyaspartates as thermoresponsive enantiodifferentiating helically chiral alignment media for anisotropic NMR spectroscopy. *Chem Eur J.* **2017**; 23: 14576-14584.

64. Hirschmann M, Schwab M, Thiele CM. Molecular weights: the key of lyotropic liquid crystalline of poly-*β*-benzyl-*L*-aspartate. *Macromolecules.* **2019**; 52: 6025-6034.

65. Jeziorowski S, Thiele CM. Poly-*γ*-p-biphenylmethyl-glutamate as enantiodifferentiating alignment medium for NMR spectroscopy with temperature-tunable properties. *Chem Eur J.* **2018**; 24: 15631-15637.

66. Hansmann S, Schmidts V, Thiele CM. Synthesis of poly-*γ*-*S*-2-methylbutyl-*L*-glutamate and poly-*γ*-*S*-2-methylbutyl-*D*-glutamate and their use as enantiodiscriminating alignment media in NMR spectroscopy. *Chem Eur J.* **2017**, 23: 9114-9121.

67. Schwab M, Schmidts V, Thiele CM. Thermoresponsive alignment media in NMR spectroscopy: helix reversal of a co-polyaspartate at ambient temperatures. *Chem Eur J.* **2018**; 24: 14373-14377.

68. Canlet C, Merlet D, Lesot P, Meddour A, Loewenstein L, Courtieu J. Deuterium NMR stereochemical analysis of threo-erythro isomers bearing remote chiral centres in racemic and non-racemic liquid crystalline solvents. *Tetrahedron: Asymmetry.* **2000**; 11: 1911-1918.

69. Courtieu J, Aroulanda C, Lesot P, A, Merlet D. Evolution of the Saupe order parameters of enantiomers from a non-chiral to a chiral liquid crystal solvent: an original light on the absolute configuration problem. *Liq Crystals.* **2010**; 37: 903-912.

70. Lesot P, O. Lafon O, Aroulanda C, Dong R. ^{2}H NMR studies of two-homopolypeptide lyotropic mesophases: toward the quantification of solute-fiber interactions. *Chem. Eur. J.* **2008**; 14: 4082-4092.

71. Serhan Z, Aroulanda C, Lesot P. Investigation of solute-fiber affinity and orientational ordering of norbornadiene interacting with two-polypeptide chiral liquid crystalline solvents by NAD NMR. *J Phys Chem. A.* **2016**; 120: 6076-6088.

72. Texier-Bonniot T, Berdagué P, Robins RJ, Remaud G, Lesot P. Analytical contribution of deutrium 2D-NMR in oriented solvents to ^{2}H/^{1}H isotopic characterization: the case of vanillin. *Flavour Fragance J.* **2018**; 34: 217-229.

73. Solgadi A. Jean L, Lasne MC, Rouden J, Courtieu J, Meddour A. NMR in chiral polypeptide liquid crystals: the problem of amines, *Tetrahedron: Asymmetry.* **2007**; 18: 1511-1516.

74. Lesot P, Serhan Z, Billault I. Recent advances in the analysis of the site-specific isotopic fractionation of metabolites such as fatty acids using anisotropic natural abundance ^{2}H NMR spectroscopy: application on conjugated linolenic methyl esters. *Anal Bioanal Chem.* **2011**; 399: 1187-1200.

75. Serhan Z, Billault I, Borgogno A, Ferrarini A, Lesot P. Analysis of NAD 2D-NMR spectra of saturated fatty acids in polypeptide aligning media by experimental and modeling approaches. *Chem Eur J.* **2012**; 18: 117-126.

76. Marx A, Boettcher B, Thiele CM. Enhancing the orienting properties of poly(γ-benzyl-*L*-glutamate) by means of additives, *Chem Eur J.* **2010**; 16: 1656-1660.

77. Thiele CM, Pomerantz WC, Abbott NL, Gellman SH. Lyotropic liquid crystalline phases from helical β-peptides as alignment media. *Chem Commun.* **2011**; 47: 502-504.

78. Arnold L, Marx A, Thiele CM, Reggelin M. Polyguanidines as chiral orienting media for organic compounds. *Chem Eur J.* **2010**; 16: 10342-10346.

79. Dama M, Berger S. Polyisocyanides as a new alignment medium to measure residual dipolar couplings for small organic molecules. *Org Lett.* **2012**; 14: 241-243.

80. Meyer NC, Krupp A, Schmidts V, Thiele CM, Reggelin M. Polyacetylenes as alignment enantiodifferentiating alignment media. *Angew Chem, Int Ed.* **2012**; 51: 8334-8338.

81. Krupp A, Reggelin M. Phenylalanine-based polyarylacetylenes as enantiomer-differentiating alignment media. *Magn Reson Chem.* **2012**; 50: S45-S52.

82. Dama M, Berger S, Polyacetylenes as a new alignment medium to measure residual dipolar couplings for chiral organic molecules. *Tetrahedron: Letters.* **2012**; 53: 6439-6442.

83. Li GW, Cao JM, Zong W, Hu L, Hu ML, Lei X, Sun H, Tan RX. Helical polyisocyanopeptides as lyotropic liquid crystals for measuring residual dipolar couplings. *Chem Eur J.* **2017**; 23: 7653-7656.

84. Kobza K, Kessler KH, Luy B. Stretched gelatin gels as chiral alignment media for the discrimination of enantiomers by NMR spectroscopy. *Angew Chem, Int Ed*. **2005**; 44: 3145-3147.

85. C. Naumann, W.A. Bubb, B.E. Chapman. P.W. Kuchel, Tunable-alignment chiral system based on gelatin for NMR spectroscopy, *J Am Chem Soc*, **2007**; 129: 5340-5341.

86. Gayathri C, Tsarevsky NV, Gil RR. Residual dipolar couplings (RDCs) analysis of small molecules made easy: fast and tuneable alignment by reversible compression/relaxation of reusable PMMA gels. *Chem Eur J.* **2010**; 16: 362-3626.

87. Tracey A, Diehl P. The interaction of *D* and *L*-alanine with an optically active model membrane system, *FEBS Lett*. **1975**; 59: 131-132.

88. Tracey AS, Radley K. Effects of composition on cholesteric behavior in the lyotropic mesophase system of potassium N-dodecanoyl-l-alaninate, *J Phys Chem.* **1984**; 88: 6044-6048.

89. Solgadi A, Meddour A, Courtieu J. Enantiomeric discrimination of water-soluble compounds using deuterium NMR in a glucopon/buffered water/*n*-hexanol chiral lyotropic liquid crystal. *Tetrahedron: Asymmetry.* **2004**; 15: 315-1318.

90. Baczko K, Larpent C, Lesot P. New amino acid based on anionic surfactants and their use as enantiodiscriminating lyotropic liquid crystalline NMR solvent. *Tetrahedron: Asymmetry*. **2004**; 15: 971-982.

91. Tjandra N, Grzeisek S, Bax A, Magnetic field dependence of nitrogen−proton *J* splittings in ^{15}N-enriched human ubiquitin resulting from relaxation interference and residual dipolar coupling. *J. Am. Chem. Soc.* **1996**; 18; 6264-6272.

92. Clore GM, Starich MR, Gronenborn AM. Measurement of residual dipolar couplings of macromolecules aligned in the nematic phase of a colloidal suspension of rod-shaped viruses. *J Am Chem Soc.***1998**; 120: 10571-105782.

93. Ottiger M, Bax A. Characterization of magnetically oriented phospholipid micelles for measurement of dipolar couplings in macromolecules. *J Biomol NMR*. **1998**; 12: 361-372.

94. de Alba E, Tjandra N. NMR dipolar couplings for the structure determination of biopolymers in solution, *Prog Nucl Magn Reson Spectrosc.* **2002**; 40: 175-197.

95. Prestegard JH, Bougault CM, Kishore AI. Residual dipolar couplings in structure determination of biomolecules. *Chem Rev.* **2004**; 104: 3519-3540.

96. Lorieau J, Yao L Bax A. Liquid cystalline phase of G-tetrad DNA for NMR study of detergent-solubilized proteins. *J Am Chem Soc.* **2008**; 30: 7536-7537.

97. Sau SP, Ramanathan KV.Visualization of enantiomers in the liquid-crystalline phase of a fragmented DNA solution. *J Phys Chem. B.* **2009**; 113: 1530-1535.

98. Brandes R, Kearns DR. Biochemistry, Magnetic ordering of DNA liquid crystals. *Biochemistry*. **1986**; 25: 5890-5885.

99. Lesot P, Venkateswara Reddy U, Suryaprakash NS. Exploring the enantiodiscrimination potentialities of DNA-based orienting media using deuterium NMR spectroscopy. *Chem Commun*. **2011**; 47: 11736-11738.

100. Zangger K. Pure shift NMR. *Prog Nucl Magn Reson*, **2015**; 86-87: 1-20.

101. Marx A, Thiele C-M, Orientational properties of poly-γ-benzyl-*L*-glutamate: influence of molecular weight and solvent on order parameters of the solute, *Chem Eur J*. **2009**; 15: 254-260.

102. Dirat O, Kouklovsky C, Langlois Y, Lesot P, Courtieu J. Double diastereoselection in asymmetric [2+3] cycloadditions reactions of chiral oxazoline n-oxides and application to the kinetic resolution of a racemic α,β-unsaturated δ-lactone. *Tetrahedron: Asymmetry.* **1999**; 10: 3197-3207.

103. Queffelec C, Boeda F, Pouilhès A, Meddour A, Kouklovsky C, Hannedouche J, Collin J, Schulz E. Enantioselective intramolecular hydroamination of secondary amines catalyzed by easily accessible ate and neutral rare-earth complexes. *ChemCatChem.* **2011**; 3: 122-126.

104. Didier D, Meddour A, Bezzenine-Lafollée S, Collin J. Samarium iodobinaphtholate: an efficient catalyst for enantioselective aza-michael additions of O-benzylhydroxylamine to N-alkenoyloxazolidinones. *Eur J Org Chem.* **2011**; 14: 2678-2684.

105. Rivard M, Guillen F, Fiaud J-C, Aroulanda, C, Lesot P. Efficient enantiodiscrimination of chiral monophosphine oxides and boranes by phosphorus coupled carbon-13 NMR spectroscopy in the presence of chiral ordering agents. *Tetrahedron: Asymmetry.* **2003**; 14: 1141-1152.

106. Prevost S, Gauthier S, Caño De Andrade MC, Mordant C, Touati AR, Lesot P, Savignac P, Ayad T, Phansavath P, Ratovelomanana-Vidal V, Genet JP. Dynamic kinetic resolution of α-chloro β-keto esters and phosphonates: hemisynthesis of taxotere® through Ru-difluorphos asymmetric hydrogenation. *Tetrahedron: Asymmetry*. **2010**; 21: 1436-1446.

107. Lafon O, Lesot P, Rivard, Chavarot M, Rose-Munch F, Rose E. Enantiomeric aalysis of planar chiral (η^6-arene) chromium tricarbonyl complexes using NMR in oriented solvents. *Organometallics*, **2005**; 24: 4021-4028.

108. Eloi A, Rose-Munch F, Rose E, Pillet A, Lesot P, Herson P. Cationic planar chiral (η^6-arene)$Mn(CO)_3^+$ complexes: resolution, NMR study in chiral oriented solvents and applications to the enantioselective syntheses of 4-substituted cyclohexenones and of (η^6-phosphinoarene)$Mn(CO)_3^+$ complexes. *Organometallics*, **2010**; 29: 3876-3886.

109. Lesot, P, Merlet D, Courtieu J, Emsley JW. Discrimination and analysis of the NMR spectra of enantiomers dissolved in chiral liquid crystal solvents through 2D correlation spectroscopy. *Liq. Crystals.* **1996**; 21: 427-435.

110. Geen H, Freeman R. Band-selective radiofrequency pulses. *J Magn Reson.* **1991**; 93: 93-14.

111. Liu Y, Cohen RD, Martin GE, Williamson RT. A practical strategy for the accurate measurement of residual dipolar couplings in strongly aligned small molecules. J Magn Reson. **2018**; 291: 63-72.

112. Enthart A, Freudenberger JC, Furrer J, Kessler H, Luy B, The CLIP/CLAP-HSQC: Pure absorptive spectra for the measurement of one-bond couplings. *J. Magn. Reson.* 2008; **192**: 314-322.

113. Krabbe HJ, Heggemeir H, Schrader B, Korte EH. Determination of the absolute-configuration of chiral molecules from the infrared rotatory-dispersion of their liquid-crystalline solutions. *J Chem Res* (S). **1978**; 238-238.

114. Canet J-L, Fadel A, Salaün J, Canet-Fresse I, Courtieu J. Enantiomeric excess analysis of sesquiterpene precursors through proton-decoupled deuterium NMR in cholesteric lyotropic liquid crystal. *Tetrahedron: Asymmetry.* **1993**; 4; 31-34.

115. Meddour A, Canet I, Loewenstein A, Péchiné J-M, Courtieu J. Observation of enantiomers, chiral by virtue of isotopic substitution, through deuterium NMR in a polypeptide liquid crystal. *J Am Chem Soc.* **1994**; 116: 9652-9656.

116. Canet I, Courtieu J, Loewenstein A, Meddour A, Péchiné J-M. Enantiomeric analysis in a polypeptide lyotropic liquid crystal by deuterium NMR. *J Am Chem Soc*. **1995**; 117: 6520-6526.

117. Canet J-L, Canet I, Coutieu J, Da Silva S, Gelas J, Troin Y. Acetyl-d_3 chloride: a convenient non chiral derivatizing agent (NCDA) for a facile enantiomeric excess determination of amines through deuterium NMR. *J Org Chem*. **1996**; 61: 9035-9037.

118. Meddour A, Atkinson D, Loewenstein A, Courtieu J. Enantiomeric analysis of homologous series of secondary alcohols by deuterium NMR spectroscopy in a chiral nematic liquid crystal: influence of molecular geometry on chiral discrimination. *Chem. Eur. J*. **1998**; 4: 1142-1147.

119. Meddour A, Courtieu J. Achiral deuterated derivatizing agent for enantiomeric analysis of carboxylic acids by NMR in a chiral liquid crystalline solvent. *Tetrahedron: Asymmetry*. **2000**; 11: 3635-3644.

120. Tavasli M, Courtieu J, Goss RJM, Meddour A, O'Hagan D. Extreme enantiomeric discrimination of fluoroalkanes using deuterium NMR in chiral liquid crystalline media. *Chem Commun*. **2002**; 844-845.

121. Palomino M, Khudr H, Courtieu J, Merlet D, Meddour A, The use of exchangeable nuclei to observe enantiomers through deuterium NMR in chiral liquid crystalline solvents. *Magn Reson Chem.* **2012**; 50: S12-S16.

122. Lafon O, Berdagué P, Lesot P. Use of two-dimensional correlation between ^{2}H quadrupolar splittings and ^{13}C-CSA's for assignment of NMR spectra in chiral nematics. *Phys Chem Chem Phys*. **2004**; 6: 1080-1084.

123. Lesot P, Merlet D, Loewenstein A, Courtieu J. Enantiomeric visualisation using proton-decoupled naturala abundance deuterium NMR in poly(*γ*-benzyl-L-glutamate) liquid crystalline solutions. *Tetrahedron: Asymmetry.* **199**8; 9: 1871-1881.

124. Parenty A, Campagne J-M, Aroulanda C. Lesot P. Routine use of natural abundance deuterium NMR in a polypeptidic chiral oriented solvent for determination of the enantiomeric composition of chiral building blocks. *Org Lett*. **2002**; 4: 1663-1666.

125. Lemetay A, Bourdeux Y, Lesot P, Farjon J, Beau J-M. Synthesis of a mycobacterium tuberculosis tetra-acylated sulfolipid analogue and characterization of the chiral acyl chains using anisotropic NAD 2D-NMR spectroscopy. *J Org Chem*. **2013**; 78: 7648−7657.

126. M. Sarfati, M Courtieu J, Lesot P. First successful enantiomeric discriminations of chiral alkanes using NMR spectroscopy. *Chem Commun*. 2000; 1113-1114.

127. P. Lesot, Berdagué P, Meddour A, Kreiter A, Noll M, Reggelin M. ^{2}H and ^{13}C NMR-based enantiodetection using polyacetylene *versus* polypeptide aligning media: versatile and complementary tools for chemists. *ChemPlusChem*. **2019**; 84: 144-155.

128. Lesot P in Deuterium NMR of Liquid-crystalline Samples at Natural Abundance. *Encyclopedia of Magnetic Resonance* (eMagRes), *Eds*. Harris RK and Wasylishen RE, Wiley, Chichester, **2013**; 3: 315-334.

129. Smadja W, Auffret S, Berdagué P, Merlet D, Canlet C, Courtieu J, Legros J-Y, Boutros A, Fiaud J-C. Visualisation of axial chirality using ^{2}H-{^{1}H} NMR in poly-*γ*-benzyl-*L*-glutamate, a chiral liquid crystal solvent. *Chem Commun.* **1997**; 2031-2032.

130. Chureau E, Meddour A. Courtier J. Enantiomeric visualization of metallic tris-(acetylacetonate) chiral complexes by NMR in a chiral liquid crystal, Internship report, University of Paris-Sud, (**1999**), unpublished results in the literature.

131. Szalontai G, Kovacs M. Distinction of tris(diimine)ruthenium(II) enantiomers chiral by virtue of helical chirality: Temperature-dependent deuterium NMR spectroscopy in partially oriented phases. *Magn Reson Chem*. **2006**; 44: 1044-1050.

132. 129. Lesot P, Merlet D, Sarfati M, Courtieu J, Zimmermann H, Luz Z. Enantiomeric and enantiotopic analysis of cone-shaped compounds with C_3 and C_{3v} symmetry using NMR spectroscopy in chiral anisotropic solvents, *J Am Chem Soc.* **2002**; 124: 10071-10082.

133. Mislow, K, Bickart P. An espistemological note on Chirality. *Isr J Chem.* **1976**; 15: 1-6.

134. Wynberg H, Hekkert GL, Houbiers JPM, Bosch HW. The optical activity of butylethylhexylpropylmethane. *J Am Chem Soc.* **1965**; 87: 2635-2639.

135. Kawasaki T, Tanak H, Tsutsumi T, Kasahara T, Sato I, Soai K. Discrimination of cryptochiral saturated quaternary and tertiary hydrocarbons by asymmetric autocatalysis. *J Am Chem Soc.* **2006**; 128: 6032-6033.

136. Masarwa A, Oskar L, Loewenstein A, Reisenauer HP, Gerbig D, Lesot P, Schreiner R, I. Marek I. Probing the limits of NMR and VCD spectroscopy in the stereochemical assignment of chiral $^2H_6$-neopentane. *Angew Chem, Int Ed.* **2015**; 54: 13106-13109.

137. de Meijere A, Khlebnikov AF, Kostikov RR, Kozhushkov SI, Schreiner PR, Wittkopp A, Yufit DS. The first enantiomerically pure triangulane (M)-trispiro[2.0.0.2.1.1]nonane s a s-[4]helicene. *Angew Chem, Int Ed. Engl.* **1999**; 38: 3474-3477.

138. Altmann SI. The summary of nonrigid molecules: the Schrödinger supergroup. *Proc Roy Soc.* (London), **1967**; A298: 184-203.

139. Aroulanda C, Merlet D, Courtieu J, Lesot P. NMR experimental evidence of the differentiation of enantiotopic directions in C_s and C_{2v} molecules using partially oriented, chiral media. *J Am Chem Soc.* **2001**; 123: 12059-12066.

140. Merlet D, Loewenstein A, Smadja W, Courtieu J, Lesot P. Quantitative description of the facial discrimination of molecules containing a prochiral group oriented in a chiral liquid crystalline solution. *J Am Chem Soc.* **1998**; 120: 963-969.

141. Fan CA, Ferber B, Kagan HB, Lafon O, Lesot P. Two aspects of the desymmetrization of selected prochiral aromatic or vinylic dihalides: enantioselective halogen-lithium exchange and prochiral recognition in chiral liquid crystals. *Tetrahedron: Asymmetry.* **2008**; 19: 2666-2677.

142. Aroulanda C, Lesot P, Merlet D, Courtieu J. Structural ambiguities in bridged ring systems resolved using natural abundance deuterium NMR in chiral liquid crystals. *J Phys Chem A*. **2003**; 107: 10911-10918.

143. Aroulanda C, Zimmermann H, Luz Z, Lesot P. Enantiotopic discrimination in the deuterium NMR spectrum of solutes with S_4 symmetry in chiral liquid crystals. *J Chem Phys.* **2011**; 134: 134502-1/8.

144. Naumann C, Kuchel PW. NMR (pro)chiral discrimination using polysaccharide gels. *Chem Eur J*. **2009**; 15: 1218-12191.

145. Mislow M, Raban M in Topics in stereochemistry, Vol. 1, *Eds*. N.L. Allinger, E.L. Eliel, Wiley, New York, (**1967**).

146. Fujita S. Chirality fittingness of an orbit governed by a co-set representation. Integration of point-group and permutation-group theories to treat local chirality and prochirality. *J Am Chem Soc*. **1990**; 112: 3390-3397.

147. Fujita S. Promolecules for characterizing stereochemical relationships in non-rigid molecules. *Tetrahedron*. **1991**; 47: 31-46.

148. Fujita S. Systematic characterization of prochirality, prostereogenicity, and stereogenicity by means of the sphericity concep. *Tetrahedron.* **2000**; 56: 735-740.

149. Martin GJ, Martin ML. Deuterium labelling at the natural abundance level as studied by high-field quantitative ^{2}H NMR.*Tetrahedron Letters.* **1981**; 22: 3525-3528.

150. Martin ML, Martin GJ in NMR basic principles and progress, Ed. P. Diehl, Springer-Verlag Vol. 23, pp. 1-61, (**1990**).

151. 148. Martin G, Zhang B-L, Naulet N, Martin M. Deuterium transfer in the bioconversion of glucose to ethanol studied by specific isotope labeling at the natural abundance level. *J Am Chem Soc.* **1986**; 108: 5116-5122

152. Pionnier S, Robins RJ, Zhang B-L, Natural abundance hydrogen isotope affiliation between the reactants and the products in glucose fermentation with yeast. *J Agric Food Chem.* **2003**; 51: 2076-2082.

153. Lesot P, Determination of the natural deuterium distribution of fatty acids by application of ^{2}H 2D-NMR in liquid crystals: fundamentals, progresses, abroad and beyond. *Liq Crystals.* **2020**; 47: 1886-1910.

154. Lesot P, Aroulanda C, Billault I. Exploring the analytical potential of NMR spectroscopy in chiral anisotropic media for the study of the natural abundance deuterium distribution in organic molecules. *Anal Chem.* **2004**; 76: 2827-2835.

155. Baillif V, Robins RJ, Billault I., Lesot P. Assignment of absolute configuration of natural abundance deuterium signals associated with (*R*)- and (*S*)-enantioisotopomers in a fatty acid aligned in a chiral liquid crystal: enantioselective synthesis and NMR Analysis. *J Am Chem Soc.,* **2006**; 128: 11180-11187.

156. Lesot P, V. Baillif I. Billault I. Combined analysis of four C-18 unsaturated fatty acids using natural abundance deuterium 2D NMR spectroscopy in chiral oriented solvents. *Anal Chem*. **2008**; 80: 2963-2972.

157. Serhan Z, Martel L, Billault I, Lesot P. Complete determination of site specific bio-enantiomeric excesses in linoleic acid using natural abundance deuterium 2D NMR in polypeptide mesophase. *Chem Commun.* **2010**; 46: 6599-6601.

158. Baillif V, Robins R, Le Feunten S, Lesot P, Billault I. Investigation of fatty acid elongation and desaturation steps in *Fusarium lateritium* by quantitative two-dimensional deuterium NMR spectroscopy in chiral oriented media. *J Biol Chem.*, **2009**; 284: 10783-10792.

159. Billault I, Ledru A, Ouetrani M, Serhan Z, Lesot P. Robins RJ. Probing substrate-product relationships by natural abundance deuterium 2D NMR spectroscopy in liquid-crystalline solvents: the case of the epoxidation of linoleate to vernoleate by two different plant enzymes. *Anal Bioanal Chem*. **2012**; 402: 2985-2998.

160. Lesot P, Serhan Z, Aroulanda C. Billault I. Analytical contribution of NAD 2D-NMR spectroscopy in polypeptide mesophases to the investigation of triglycerides. *Magn Reson Chem*. **2012**; 50: S2-S11.

161. Villar H, Guibé F, Aroulanda C, Lesot P. Investigation of SmI_2 mediated cyclisation process of δ-iodo-α, β-unsaturated esters by deuterium 2D NMR in oriented solvents. *Tetrahedron: Asymmetry*. **2002**; 13: 1465-1475.

162. Aroulanda C, Boucard V, Guibé E, Courtieu J, Merlet D. Weakly oriented liquid-crystal NMR solvents as a general tool to determine relative configurations. *Chem Eur J.* **2003**; 9: 4536-4539.

163. Navarro-Vazquez A, Berdagué P, Lesot P. Integrated computational protocol for analyzing quadrupolar splittings from natural abundance deuterium NMR spectra in (chiral) oriented media. *ChemPhysChem.* **2017**; 18: 1252-1266.

164. Navarro-Vázquez A. MSpin-RDC. A program for the use of residual dipolar couplings for structure elucidation of small molecules. *Magn Reson Chem.* **2012**; 50: S73-S79.

165. Cornilescu, G, Bax, A. Measurement of proton, nitrogen, and carbonyl chemical shielding anisotropies in a protein dissolved in a dilute liquid-crystalline phase. *J Am Chem Soc*. **2000**; 122: 10143-10154.

166. Kolehmainen E, Laihia K, Korvola J, Kauppinen R, Pitkänen M, Mannila B, Mannila E. Multinuclear NMR study of 1,3,3-trimethylbicyclo[2.2.1]heptan-2-one (fenchone) and its six monochlorinated derivatives. *Magn Reson Chem.* **1990**; 28: 812-816.

167. Nowakowski M, Ejchart A. Complex formation of fenchone with α-cyclodextrin: NMR titrations. *J. Incl. Phenom & Macrocycl Chem.* **2013**; 79: 337-342.

168. Abraham RJ, Ainger NJ. Proton chemical shifts in NMR. Part 13: Proton chemical shifts in ketones and the magnetic anisotropy and electric field effect of the carbonyl group. *J Chem Soc, Perkin Trans. II* **1999**: 441-448.

169. Bifulco G, Dambruoso P, Gomez-Paloma L, Riccio R. Determination of relative configuration in organic compounds by NMR spectroscopy and computational methods. *Chem Rev.* **2007**; 107: 3744-3779.

170. Karki, S, Fábián L, Friscić T, Jones W. Powder X-ray diffraction as an emerging method to structurally characterize organic solids. *Org Lett*. **2007**; 9: 3133-3136.

171. García ME. Pagola S, Navarro-Vazquez A, Phillips DD, Gayathri C, Krakauer H, Stephens PW, Nicotra VE, Gil RR. Stereochemistry determination by powder X-ray diffraction analysis and NMR spectroscopy residual dipolar couplings. *Angew Chem, Int Ed*. **2009**; 48: 5670-5674.

172. Liu Y, Navarro-Vázquez A, Gil RR, Griesinger C, Martin GE, Williamson RT, Application of anisotropic NMR parameters to the confirmation of molecular structure. *Nature Protocol.* **2018**; 14: 217-247.

173. Navarro-Vázquez A, Gil RR., Blinov K. Computer-Assisted 3D structure elucidation (CASE-3D) of natural products combining isotropic and anisotropic NMR parameters. *J Nat Prod.* **2018**; 81: 203-210.

174. Immel S, Köck M, Reggelin M. Configurational analysis by residual dipolar coupling driven floating chirality distance geometry Calculations. *Chem Eur J.* **2018**; 24: 13918-13930.

175. Hallwass F, Schmidt M, Sun H, Mazur A, Kummerlöwe G, Luy B, Navarro-Vázquez A, Griesinger C, Reinscheid UM. Residual chemical shift anisotropy (RCSA): a tool for the analysis of the configuration of small molecules. *Angew Chem, Int Ed.* **2011**; 50: 9487-9490.

176. Gil RR, Hellemann E. New stretching method for aligning gels. Its application to the measurement residual chemical shift anisotropies (RCSAs) without the need for isotropic shift correction. *Chem Eur J.* **2018**; 24: 3689-3693.

177. Lesot P, Gil RR Berdagué P, Navarro-Vazquez A. Residual quadruplar couplings: crossing the current frontiers in the relative configuration analysis of natural products. *J Nat Prod.* **2020**; 833: 141-3148.

178. Unpublished results, **2001**.

179. Diehl, P.; Henrichs, P. M.; Niederberger, W. Mol Phys. A study of the molecular structure and of the barrier to methyl rotation in o-chlorotoluene partially oriented in the nematic phase. **1971**; 1: 139-145.

180. Berger R, Courtieu, J, Gil RR, Griesinger C, Köck M. Lesot P., Luy B, Merlet D, Navarro-Vazquez A, Reggelin M, Reinscheid UM, Thiele C-M, Zweckstetter M. Is the determination of absolute configuration possible by using residual dipolar couplings from chiral-non- racemic alignment media? - A critical assessment. *Angew Chem, Int Ed*. **2012**; 51: 2-5.

181. Helfrich J, Hentschke J, Apel UM. Molecular-dynamics simulation study of poly(γ-benzyl *L*-glutamate) in dimethylformamide. *Macromolecules.* **1994**; 2: 472-482.

182. Frank AO, Freudenberger JC, Shaytan AK, Kessler H, Luy B. Direct prediction of residual dipolar couplings of small molecules in a stretched gel by stochastic molecular dynamics simulations. *Magn Reson Chem.* **2015**; 53: 213-217.

183. Di Pietro ME, Sternberg U, Luy B. Molecular dynamics with orientational tensorial constraints: A New approach to probe the torsional angle distributions of small rotationally flexible molecules. *J Phys Chem B*, **2019**; 123: 8480-8491.

184. Sager E, Tzvetkova P, Gossert AD, Piechon P, Luy B. Determination of configuration and conformation of a reserpine derivative with seven stereogenic centers using molecular dynamics with RDC-derived tensorial constraints. *Chem. Eur. J*. 2020; 26: 14435-14444.

185. Ibanez de Opakua A, Klama F, Ndukwe IE, Martin GE, Williamson T, Zweckstetter M. Determination of complex small-molecule structures using molecular alignment simulation. Angew Chem, Int Ed. **2020**; 59: 6172 -6176

186. Ibanez de Opakua A, Zweckstetter M. Extending the applicability of P3D for structure/ Magn. Reson. **2021**; 2: 105 -116.

187. Alvira E, Breton J, Plata J. Chiral discrimination - a model for the interaction between a helicoidal system and an amino-acid molecule. *Chem Phys*. **1991**; 155: 7-18.

188. Nandi N, Bagchi B. Molecular origin of the intrinsic bending forces for helical morphology observed in chiral amphiphic assemblies: Concentration and size dependence. *J Am Chem Soc*.**1997**; 118: 1343-135.

189. Nandi N. Role of secondary level chiral structure in the process of molecular recognition of ligand: Study of model helical peptide. *J Phys Chem B*. **2004**; 108: 789-797.

190. Celebre G. On the anisotropic intermolecular potential of biaxial apolar solutes in nematic solvents: Monte Carlo predictions and experimental data. *J Chem Phys*. **2001**; 115: 9552-9556.

191. Photinos J. in NMR of ordered liquids, *Eds*. Burnell EE, de Lange CA, Kluwer Academic Publisher, Dordrecht, Chap. 12, (**2003**).

192. Celebre G, De Luca G, D'Urso C, Di Pietro ME. Helical solutes orientationally ordered in anisotropic media composed of helical particles: Formulation of a mean torque potential sensitive to *P* and *M* chirality as a tool for the assignment of the absolute configuration of enantiomers. *J Mol Liquids*, **2019**; 288: 111044 (1-5).

193. Ziani L, Lesot P, Meddour A, Courtieu J. Empirical determination of the absolute configuration of small chiral molecules using natural abundance ^{2}H NMR in chiral liquid crystals. *Chem Commun*. **2007**; 45: 4735-4739.

194. Luz Z, Dynamic of molecular processes by NMR in liquid crystalline solvents. *Israel J. Chem*. **1983**; 23: 305-313.

195. Luz Z in Dynamic NMR in liquid crystals and liquid crystalline solutions, *Eds*. Burnell EE, de Lange CA, Kluwer Academic Publisher, Dordrecht, Chap. 19, (**2003**).

196. Aroulanda C, Lafon O, Lesot P. Enantiodiscrimination of flexible cyclic solutes using deuterium NMR spectroscopy in polypeptide chiral mesophases: investigation of *cis*-decalin and THF. *J Phys Chem B.* **2009**; 113: 10628-10640.

197. Esteban AL, Galache MP, Diez E, San Fabian J, Guilleme J, NMR study of tetrahydrofuran oriented in a nematic phase. *J. Mol. Struc.* **1986**; 142: 375-378.

198. Sarfati M, Aroulanda C, Courtieu J, Lesot P. Enantiomeric recognition of chiral invertomers through NMR in chiral oriented solvents: a study of the *cis*-decalin. *Tetrahedron: Asymmetry*. **2001**; 12: 737-744.

199. Eyring H. Activated Complex in Chemical Reactions. *Chem. Rev.* **1935**; 17: 65-77.

200. Bain AD. Chemical exchange in NMR. *Prog. Nucl. Magn. Reson. Spectrosc*. **2003**; 43: 63-103.

201. Lesot P, Lafon O, Kagan HB, Fan P. Study of molecular rotational isomerism using deuterium NMR in chiral oriented solvents. *Chem. Commun.* **2006**; 389-391.

202. Lafon O, Lesot P, Fan CA, Kagan HB. Analysis of intramolecular dynamic processes in enantiomeric diaryl atropisomers and related derivatives through ^{2}H NMR in polypeptide liquid crystals. *Chem. Eur. J.* **2007**; 13: 3772-3786.

203. Ward JB. Biosynthesis of peptidoglycan: points of attack by wall inhibitors. *Pharmacol Ther*. **1984**; 25: 327-369.

204. Noda M, Matoba Y, Kumagai K, Sugiyama M. A novel assay method for an amino acid racemase reaction based on circular dichroism. *Biochem J*. **2005**; 389: 491-496.

205. Diven WF, Johnston RB, Scholz J. Purification and properties of the alanine racemase from Bacillus subtilis. *Biochim. Biophys Acta.* **1964**; 85: 322-332.

206. Gavina, JMA, White CE, Tulough M, Britz-McKibbin P. Determination of 4-hydroxyproline-2-epimerase activity by capillary electrophoresis: A stereoselective platform for inhibitor screening of amino acid isomerases. *Electrophoresis*. **2010**; 31: 2831-2837.

207. Chan-Huot M, Lesot P, Pelupessy P, Duma L, Duchambon P, Bodenhausen G, Toney MD, Reddy UV, Suryaprakash N, 'On-the-fly' kinetics of enzymatic racemization using deuterium NMR in DNA-based, oriented chiral solvents. *Anal Chem.* **2013**; 85: 4694-4697.

208. Lesot P, Berdagué P, Giraudeau P. Detection of quadrupolar nuclei by ultrafast 2D-NMR: exploring the case of deuterated analytes aligned in chiral oriented solvents. *Chem Commun*. **2016**; 52: 2122-2125.

209. Gouilleux B, Meddour A, Lesot P.^{2}H QUOSY 2D-NMR Experiments in weakly aligning systems: From the conventional to the ultrafast approach. *ChemPhysChem,* **2020**; 21: 1548-1563.

210. Samulski ET. Very flexible solutes: alkyl chains and derivatives, *Eds*. Burnell EE, de Lange CA, Kluwer Academic Publisher, Dordrecht, Chap. 13, (**2003**).

211. Celebre G, Longeri M in NMR studies of solutes in liquid crystals: small flexible molecules, *Eds*. Burnell EE, de Lange CA, Kluwer Academic Publisher, Dordrecht, Chap. 14, (**2003**).

212. Boehr D, Nussinov R, Wright P. The role of dynamic conformational ensembles in biomolecular recognition. *Nat Chem Biol.* **2009**; 5: 789-796.

213. Hilt JZ, Byrne ME. Configurational biomimesis in drug delivery: molecular imprinting of biologically significant molecules. *Adv Drug Delivery Rev*. **2004**; 56: 1599-1620.

214. Fairlie, DP, Tyndall JDA, Reid RC, Wong AK, Abbenante G, Scanlon MJ, March DR, Bergman DA, Chai CLL, Burkett BA. Conformational selection of inhibitors and substrates by proteolytic enzymes: implications for drug design and polypeptide processing. *J. Med. Chem*. **2000**; 43: 1271-1281.

215. Luy B, Frank A, Kessler H, Molecular drug properties. Measurement and prediction; Mannhold R, Ed. Wiley-VCH Verlag: Weinheim, Germany, Chap. 9, pp 207-245, (**2008**).

216. Lipsitz RS, Tjandra N. Residual dipolar couplings in NMR structure analysis. *Ann. Rev Biophys. Biomol. Struct*. **2004**; 33: 387-413.

217. Prestegard JH, Al-Hashimi HM, Tolman JR. NMR structures of biomolecules using field oriented media and residual dipolar couplings. *Quat Rev Biophys*. **2000**; 33: 371-424.

218. Zannoni C in An internal order parameter formalism for non-rigid molecules, in Nuclear Magnetic Resonance of Liquid Crystals, Ed. Emsley JW, Reidel, Dordrecht, Chap. 2, ISBN: 9027718784, (**1985**).

219. Flory PJ, Foundations of rotational isomeric state theory and general methods for generating configurational averages. Macromolecules, **1974**; 7: 381-392.

220. Stevensson B, Sandström D, Maliniak A. Conformational distribution functions extracted from residual dipolar couplings: A hybrid model based on maximum entropy and molecular field theory *J Chem Phys*. **2003**; 119: 2738-2746.

221. Emsley JW, Luckhurst GR, Stockley CP. A theory of orientational ordering in uniaxial liquid crystals composed of molecules with alkyl chains. *Proc. R. Soc. London, Ser. A*. **1982**; 381: 117-138.

222. Di Bari L, Forte C, Veracini CA. Zannoni C, An internal order approach to the investigation of intramolecular rotations in liquid crystals by NMR: 3-Phenyl-thiophene in PCH and phase IV. *Chem Phys Lett.* **1988**; 143: 263-269.

223. Catalano D, Di Bari L, Veracini CA. A maximum-entropy analysis of the problem of the rotameric distribution for substituted biphenyls studied by ^{1}H nuclear magnetic resonance spectroscopy in nematic liquid crystals. *J Chem Phys.* **1991**; 94: 3928-3935.

224. Celebre G, De Luca G, Emsley JW, Foord EK, Longeri M, Lucchesini F, Pileio G. The conformational distribution in diphenylmethane determined by nuclear magnetic resonance spectroscopy of a sample dissolved in a nematic liquid crystalline solvent *J Chem Phys.* **2003**; 118: 6417-6426.

225. Celebre G, De Luca G, Di Pietro ME. Conformational distribution of *trans*-stilbene in solution investigated by liquid crystal NMR spectroscopy and compared with in vacuo theoretical predictions. *J Phys Chem B*. **2012**; 116: 2876-2885.

226. Celebre G, De Luca G, Longeri M. Exploiting the information content of dipolar couplings: determination of the temperature dependence of the inter-ring twist angle of biphenyl dissolved in uniaxial mesophases. *Liq Crystals*. **2010**; 37: 923-933.

227. Marčelja S. The even-odd effects in liquid crystals: a simple model. *J Chem Phys*. **1974**; 60: 2533-2539.

228. Lesot P, Merlet D, Courtieu J, Emsley JW, Rantala TT, Jokisaari J. Calculation of the molecular ordering tensors of (±)-3-butyn-2-ol in an organic solution of poly(g-benzyl-*L*-glutamate). *J Phy. Chem. A*. **1997**; 101: 5719-5724.

229. Kock M, Reggelin M, Immel S. Configurational analysis by residual dipolar couplings: critical assessment of "structural noise" from thermal vibration. *Angew Chem, Int. Ed.* **2020**; 60: 3412-3416.

230. Di Pietro ME, Aroulanda, C, Merlet, D, Celebre G, De Luca G. Conformational investigation in solution of a fluorinated anti-inflammatory drug by NMR spectroscopy in weakly ordering media. *J Phys Chem B*. **2014**; 118: 9007-9016.

231. Frisch MJ, Trucks GW, Schlegel HB, Scuseria GE, Robb MA, Cheeseman JR, Scalman G, Barone V, Mennucci B, Petersson GA et al. Gaussian 09 (Revision A.02); Gaussian: Wallingford, CT, USA, (**2009**).

232. Di Pietro ME, Aroulanda C, Celebre G Merlet, D. De Luca G. The conformational behaviour of naproxen and flurbiprofen in solution by NMR spectroscopy. *New J Chem*. **2015**; 39: 9086-9097.

233. Di Pietro ME, Celebre G, Aroulanda C, Merlet D, De Luca G, Assessing the stable conformations of ibuprofen in solution by means of residual dipolar couplings. *European Journal of Pharmaceutical Sciences* **2017**; 106: 113-121.